Users Manual

Version: 5.11

Prepared by: Dr. Scott R. Runnels
Southern Rockies Consulting

For: The RSI-AAR Railroad Tank Car Safety Research & Test Project

Compiled March 26, 2025

Disclaimer

Southern Rockies Consulting provides this document on an as-is basis with no warranty, and with the understanding that it bears no responsibility for how this document is used.

LICENSE AGREEMENT FOR USE OF AFFTAC FOR WINDOWS SOFTWARE

The purpose of this License Agreement ("Agreement") is to set forth the terms and conditions that shall govern the use of the "AFFTAC 5.11" software ("AFFTAC") by the licensee (the "Licensee") to whom AFFTAC has been distributed without charge through The RSI/AAR Tank Car Safety and Research Project (comprised of The Railway Progress Institute and the Association of American Railroads, collectively "Licensor"). The parties agree as follows:

TERMS

1. LIMITED LICENSE. Licensor hereby grants to the Licensee and the Licensee hereby accepts a non-transferable, non-exclusive limited license to use AFFTAC and any licensed supporting materials ('Licensed Materials'). Notwithstanding the foregoing, the Licensee's right to use AFFTAC is subject to the restrictions set forth in Sections 1(a)-1(e), below.

a. The Licensee may not disassemble, decompile or otherwise reverse-engineer AFFTAC.

b. The Licensee shall not remove or alter any copyright notices and other proprietary rights legends of Licensor or of any other entity contained in, or on, AFFTAC.

c. The Licensee shall not misrepresent to a third party that the Licensee or any party other than Licensor:
(i) has title to AFFTAC; or (ii) is in any way responsible for the creation of the content of AFFTAC.

d. Licensor shall have the right, at its sole discretion and without incurring any liability to the Licensee, to modify AFFTAC or discontinue its development, sale, or support.

e. The Licensee shall not modify AFFTAC or combine AFFTAC with any other software.

2. OWNERSHIP OF INTELLECTUAL PROPERTY. Licensors own all intellectual property rights (including but not limited to all patents, trademarks, copyrights, trade secrets, and data rights) pertaining to AFFTAC, including translations, compilations, partial copies and derivative works thereof, and such rights shall remain in Licensor or its licensors. The Licensee agrees that, except for the limited license granted herein, this Agreement does not grant the Licensee any rights to patents, copyrights, trade secrets, trademarks (whether registered or unregistered), data rights or any other rights or licenses with respect to AFFTAC. AFFTAC may not be sold, leased, or sublicensed, in whole or in part, by the Licensee except with Licensor 's prior written consent. The Licensee acknowledges Licensor 's intellectual property rights in AFFTAC, and agrees that it will not challenge such rights in any way.

a. Derivative Works. The Licensee may not create any derivative works of AFFTAC. In the event that the Licensee creates any derivative works of AFFTAC, the Licensee hereby agrees that such property shall be the sole property of Licensor. The Licensee hereby waives all 'moral rights' and any other ownership rights therein.

b. All Rights Reserved. Licensor reserves all rights not expressly granted to the Licensee. AFFTAC is protected by copyright laws and international copyright treaties, as well as other intellectual property laws and treaties.

3. NO WARRANTIES. SOUTHERN ROCKIES CONSULTING, LLC, LICENSOR AND ITS LICENSORS HEREBY DISCLAIM ALL EXPRESS OR IMPLIED CONDITIONS, REPRESENTATIONS AND WARRANTIES, INCLUDING ANY IMPLIED WARRANTY OF MERCHANTABILITY, FITNESS FOR A PARTICULAR PURPOSE, DATA ACCURACY, QUIET ENJOYMENT OR NON-INFRINGEMENT, EXCEPT TO THE EXTENT THAT SUCH DISCLAIMERS ARE HELD TO BE LEGALLY INVALID. THE LICENSEE AGREES TO HOLD LICENSOR AND ITS LICENSORS HARMLESS FOR ANY CLAIMS OR LIABILITY ARISING FROM The Licensee 'S USE OF OR RELIANCE UPON AFFTAC FOR ANY PURPOSE.

4. TERM AND TERMINATION. This Agreement shall commence on execution of the installation software.

5. ASSIGNMENT AND SUBLICENSE. The Licensee may not assign, sublicense or transfer any of its rights or obligations under this Agreement.

6. GOVERNING LAW. Disputes which cannot be settled amicably will be governed by the laws of the District of Columbia, USA. Choice of law rules of any jurisdiction and the United Nations Convention on Contracts for the

International Sale of Goods will not apply. The venue for litigation will be the appropriate courts located in the District of Columbia.

7. IMPORT AND EXPORT LAWS. AFFTAC may be subject to U.S. and local export laws and may be subject to export or import regulations of other countries. The Licensee agrees to comply strictly with all such laws and regulations and acknowledges that it has the responsibility to obtain such licenses to export, re-export or import as may be required after delivery to the Licensee.

8. ENTIRE AGREEMENT; SEVERABILITY; WAIVER.

This Agreement constitutes the entire agreement between the parties with regard to the subject matter of this Agreement and supersedes all previous communications, whether oral or written, between the parties with respect to such subject matter. No waiver or modification of any of the provisions hereof shall be binding unless in writing and signed by duly authorized representatives of Licensee and Licensor. Any provision of this Agreement that is held to be invalid by a court of competent jurisdiction shall be severed from this Agreement, and the remaining provisions shall remain in full force and effect. Neither the course of conduct between the parties nor trade usage shall modify or alter this Agreement. Failure or delay by either party to enforce compliance with any term or conditions of this Agreement shall not constitute a waiver of such term or condition.

Contents

Chapter 1

Release Notes

1.1 New Capabilities since AFFTAC 4.00

1.1.1 AFFTAC Advisor and Help Bubbles

AFFTAC Advisor is a new built-in help facility that allows the user to see graphics-based, context-sensitive help and advice for nearly every window in AFFTAC. It is accessed through a blue button that appears in the window being accessed by the user; the user's context is therefore known by virtue of that window when AFFTAC Advisor is launched. AFFTAC Advisor also includes context-sensitive links to the on-line User's Manual. When one of those links is clicked by the user, the appropriate section of the on-line User's Manual PDF file is opened and displayed on the screen. AFFTAC 5.11 also comes with "help bubbles" over nearly every entry. These help bubbles appear when the user hovers their mouse over any text/numerical entry, list, or selection ("radio") buttons.

1.1.2 PDF and CSV Output

AFFTAC 5.11 includes the ability to export the output of a simulation to a PDF file. High-level inputs and the bottom-line results of the simulation are presented on the first page. Plots of the results follow on subsequent pages, and after that, more details of the input, including graphical representations of property data. The numerical results are included at the end of the document. AFFTAC 5.11 also includes the ability to export the numerical output of a simulation to a "CSV" (comma-separated values) file, a human-readable file that can be read directly into Excel.

1.1.3 Improved Advanced TPS Interface

This new version of AFFTAC has a completely redesigned user interface for the Advanced TPS Model setup, formerly called the "Generalized TPS Model". The old interface was counterintuitive and difficult to use. The new interface draws semicircles on the screen, one for each layer of the thermal protection system, and allows the user to interact with those semicircles through right-clicks of the mouse (Figure 1.1, top). The new interface also allows the user to drag demarcation symbols (the blue circles in the bottom of Figure 1.1) around the tank to denote different regions of coverage. As a result, TPS defects can now be clearly specified and seen by the user.

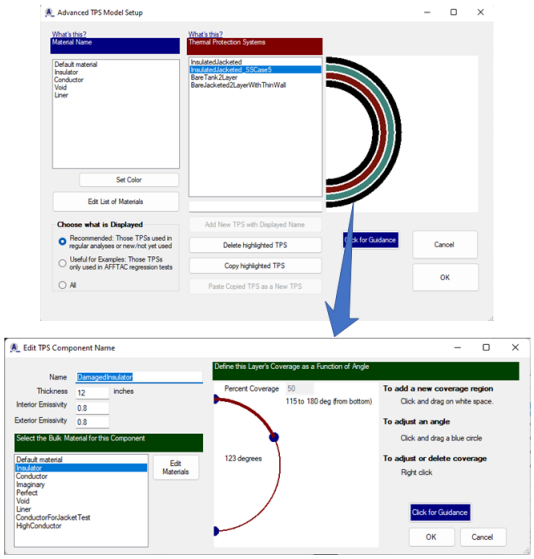

Figure 1.1: Screenshot of the new Advanced TPS Model setup window in AFFTAC 5.11.

1.1.4 Improved Property Entry Window

The "Property Entry" window in AFFTAC is used repeatedly when the user needs to enter a property that is a function of something else, for example, thermal conductivity as a function of temperature. The Property Entry window prior to AFFTAC 5.11 was counterintuitive and difficult to use. These specific changes were made to it:

- Enabled standard cut, copy, paste, and delete capabilities on multiple cells containing the tabular values.
- Added the ability to paste $x - y$ data that is copied from Microsoft Excel.
- Continuous update of the plot as data is entered or altered.
- Added `Ctrl-Z` (undo) capability, which allows the user to quickly undo mistakes.

1.1.5 Improved Error Reporting

AFFTAC's error handling and reporting has been upgraded. The need for this upgrade was identified through difficulties encountered while diagnosing user issues of AFFTAC 5.10 Alpha 01 through 04. The error handling is more hierarchical and always provides a recommended action. Moreover, the user can save the detailed version of the error messages to a file. These detailed messages contain information that helps the developer more quickly pinpoint the problem, whether it be a user error or internal code error.

1.1.6 Single Input File Format

AFFTAC 5.11 reads and writes a single input file, called a "unified database file" or "udb" file, instead of working with multiple database files. In other words, files such as `Ladings.db`, `TPS.db`, `Insulations.db`, `Strength.db`, and `PRD.db`, which have resided in a user's `Documents` folder, will be replaced by a single input file. Moreover, multiple versions of that single input file may exist. In other words, AFFTAC 5.11 adopts a single-file input methodology similar to other standard MS-Windows applications, with standard File-Open, File-Save, File-Save As, File-Close capabilities. Users moving from previous versions of AFFTAC can make use of AFFTAC 5.11's conversion capability, which is included in the Main Window menu, to convert their db files into a single udb file (more in next sub-section).

1.1.7 Flexible db to udb File Conversion

AFFTAC 5.11 automatically detects the presence of pre-AFFTAC 5.11 db files and prompts the user to convert those files to a single input (udb) file (see previous section). If the user accepts that prompt, those db files are moved to a backup location. If the user does not accept the prompt, they can still operate on the db files, but cannot save their changes to those db files.

In addition, AFFTAC 5.11 provides a menu option in the Main Window that allows the user to navigate to any set of db files, move them to a backup location, and convert them to a udb file in one step. And the user can execute that procedure as many times as necesary.

1.1.8 Multi-User Capability

New in AFFTAC 5.11 is the ability to accommodate the possibility that multiple users might try to run in the same shared network directory and also might desire to use the same input file. Various issues arise with that scenario. For example, AFFTAC writes multiple intermediate files during simulations, usually unseen by the user, that could be corrupted when multiple users are running in the same directory. And, of course, two users trying to open, modify, and save the same udb input file could result in work being overwriiten.

To accommodate this new scenario, a “lock-out” technology has been introduced in AFFTAC 5.11 that creates “lock files”, which tell AFFTAC that another user is either trying to access the same file or that they are working in the same directory. AFFTAC then uses that information to prevent the user from proceeding until the situation is rectified.

Issues with the lock-out technology could arise when AFFTAC exits ungracefully, for example if the network goes down while AFFTAC has a file open across that network, a laptop battery dies, or AFFTAC itself crashes. In these cases, lock-out files might be left behind, disabling a user from either opening their input file or running a simulation. To handle this possibility, AFFTAC provides guidance for the user, which includes ignoring the problem, contacting the other user, terminating other AFFTAC sessions, or navigating to a new Main Menu item where they can see and remove the lock-out files that are preventing their progress.

Note that this is a new capability that was not present in the AFFTAC 5.11 Alpha versions or Alpha testing. The need for it was identified during Alpha testing, and is associated with the new flexibility that has arisen through AFFTAC’s single (udb) file input approach.

1.1.9 Customizable PRV Open-Close Model

A new PRV model is included in AFFTAC 5.11 that allows users to construct customized open-close paths, with multiple segments. [1]

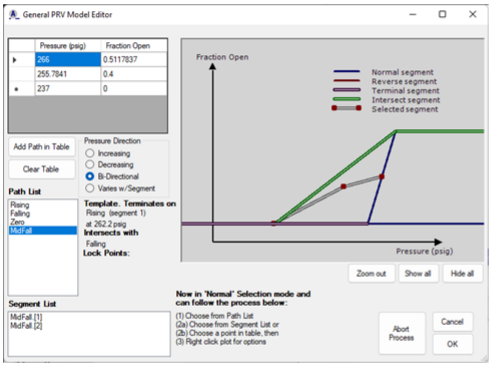

Figure 1.2: Screenshot of the new customizable PRV Open-Close Model setup window in AFFTAC 5.11.

1.1.10 Adjustable Solver Parameters

The user is now allowed to adjust two nonlinear solver parameters that are used in the Generalized TPS Model. These parameters are adjusted in the same window used to change the name of the particular TPS setup in the Generalized TPS Model editing window.

1.2 Documentation Changes

1.2.1 Improved Guidance in the User’s Manual

The AFFTAC 5.11 User’s Manual includes new text that provides advice to the user regarding high-level modeling choices, e.g., which approach they should use for strength modeling, or whether or not they should use the Advanced PRV Open-Close model. Among other parts of the User’s Manual, these sections are hot-linked to the user’s context through AFFTAC Advisor, which also provides advice on these and other topics. The User’s Manual also provides

[1] This capability was introduced in the Beta versions of 5.00.

new guidance on how to compute the percent coverage of defective insulation as a function of angle, and the impact of defects on the end caps. The impact of certain modeling assumptions are also provided, including the thermal implications of venting and of non-circumferential heat conduction.

1.2.2 Terminology Change

Starting with AFFTAC 5.11, the terms “Legacy Model” and “Generalized Model”, are replaced with “Basic Model” and “Advanced Model” to more properly account for the passage of time and the implications of those terms. Thus, for example, what was once called the “Legacy TPS Model” is now called the “Basic TPS Model” and what was once called the “Generalized TPS Model” is now called the “Advanced TPS Model”.

All inputs for a simulation that are not individual in nature but are, instead, representing collections of individual inputs are referred to as a “Resource”. For example, each lading is a collection of tables that represent quantities such as specific heat as a function of temperature. Typically, the user does not enter their own individual values in those tables. Rather, they select a lading, e.g., “Propane”, that contains multiple tables. The same is true for the Advanced Strength Model and the Advanced PRD Model. These types of inputs are all referred to as “Resources” in AFFTAC 5.11.

1.3 Installation Notes

At the time of this release, it had been found that some new computers come with a fresh Windows 10 installation that includes software called “.NET 5.0”, which skipped all the service packages previous to that version. Programs such as AFFTAC that are created and compiled for previous versions, such as “.Net 3.0”, may be incompatible with “.NET 5.0”. To remedy this situation, the user must reinstall the previous .NET version, version 3.5. [2]

[2] Thanks to Tony Sisto for working through this.

Chapter 2

Introduction

2.1 History

The AFFTAC computer program was originally developed by Dr. Milton Johnson at IITRI circa 1984 under funding from the United States Federal Railroad Administration to predict the effects of fire on railroad tank cars. It makes predictions of key state variables such as the lading temperature, temperature of the tank wall, pressure inside the tank, flow through the pressure relief device, and failure (if relevant) of the tank wall. In the years following its initial development, AFFTAC was expanded to provide more information and handle more types of vents, as well as be more accessible to users. Eventually in 1992, it was ported to the PC.

Beginning in 2000, AFFTAC entered a new phase of development with Dr. Scott Runnels as its custodian. The first task undertaken in this new phase was the development of a graphical user interface (GUI) to assist the user in managing data and analysis. A third phase of development began circa 2008 with multiple new efforts. The first was a new, more general thermal protection system model. After that, an effort was undertaken to use AFFTAC to validate model parameters for liquid/two-phase flow through pressure relief devices. A fourth phase of development added a new creep and failure model along with significant advances in testing, software quality assurance, and usabiity. Over time, a regression test system and database of over 130 regression tests have been established; many of those tests are carefully designed verification tests. All of the regression tests and the recent validation work are described in separate companion documents entitled *AFFTAC Verification and Validation Testing* and *Programmer's Guide to the Computational Module Unit Tests*. As of this release, those documents, along with this manual, are updated with each AFFTAC formal release. However, the testing documents are proprietary to the RSI-AAR Tank Car Safety Research & Test Project and must be obtained through it.

2.2 Software Components: GUI, Computational Module, and Databases

An overview of how the AFFTAC software package components interact is shown in Figure 2.1. The user interacts with the GUI, which operates from a single input file that can be opened, modified, and then saved using the GUI. In addition to opening, modifying, and saving the user's input file, the GUI manages the execution of the Computational Module and the displaying of the results from its computations. The Computational Module ("CM") is a stand-alone computer program. The GUI writes input files for it, executes it, reads its output files, and then displays the results for the user.

Inside the user's input file are multiple collections of inputs that, together, represent multiple Analyses and multiple setups for different ladings, tank wall strengths, pressure relief devices, etc. The results of an Analysis is not stored in the input file, but most Analyses run very quickly in AFFTAC and so storage of the results is not necessary. The inputs for each Analysis are broken into two types: (1) Individual values, such as tank volume tank wall thickness, etc., and (2) Collections of input values that are grouped together to represent a single entity, such as a type of lading,

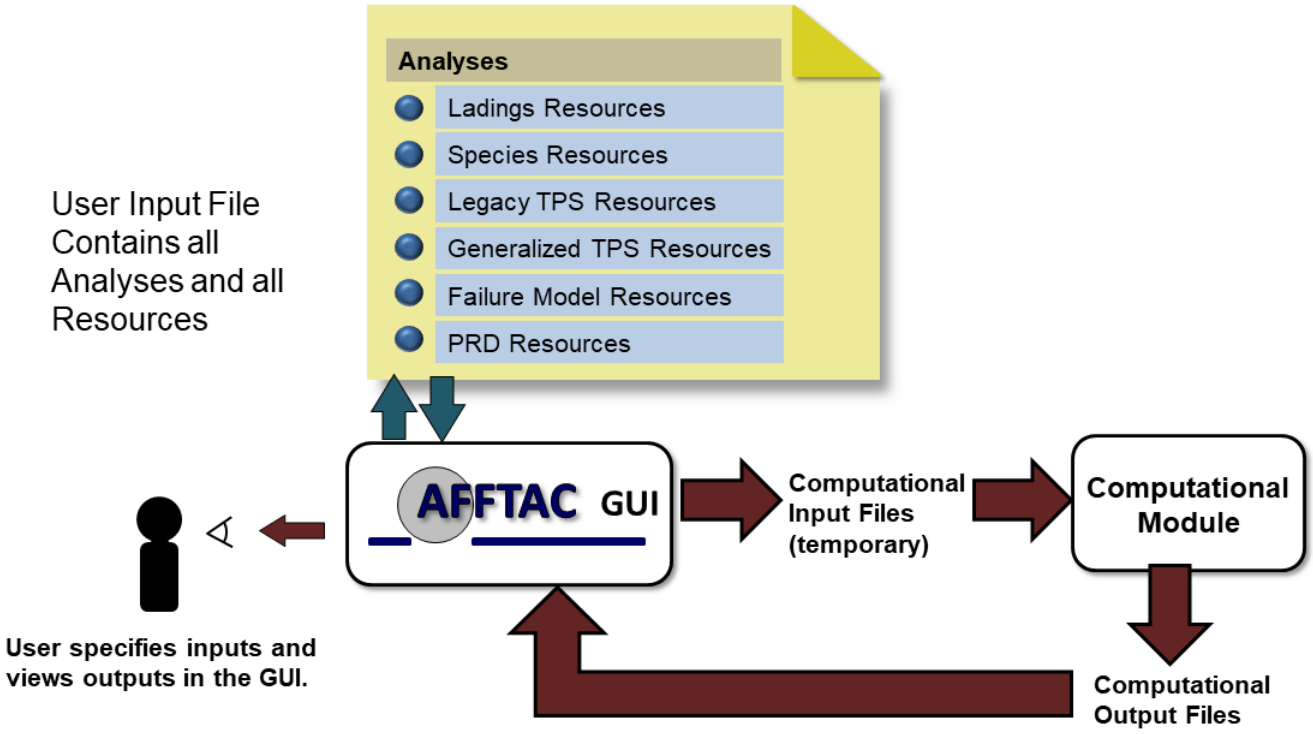

Figure 2.1: Overview of AFFTAC operations and components

a pressure relief valve, a thermal protection system, etc. These collections of input values are called "Resources" inside the GUI. The complete list of Resources are shown in Figure 2.1. These Resources are described in more detail later. For now, a brief summary is provided below.

Ladings Resources: The "Ladings Resources" are a collection of inputs representing different types of ladings, e.g., Propane, Butane, etc. The inputs for each lading are comprised of all the thermodynamic properties needed to represent that lading, e.g., specific heat, vapor pressure, etc. The lading model can be used for pure substances or binary solutions.

Basic TPS Model Resources and **Advanced TPS Model Resources**: The "Basic TPS Resources" and "Advanced TPS Resources" are setups for thermal protection systems using AFFTAC's Basic TPS Model or Advanced TPS Model, respectively. Each entry in either of these two Resources is comprised of multiple values that represent the multiple layers existing in a thermal protection system (TPS). Every Analysis must identify a TPS from one of these two Resources. Even a bare tank is considered a TPS in AFFTAC, despite it being perhaps the most rudimentary form of such, and so even bare tank analyses must select a TPS entry. The Basic TPS Model was implemented by Dr. Milt Johnson decades ago. It has undergone some revision since 2000, but remains largely unchanged. Because it is simpler than the Advanced TPS Model and so well tested, the Basic TPS Model provides an important resource for comparison. Also it contains one capability not exactly represented in the Advanced TPS model. [1]

Advanced PRD Model Resources: The "Advanced Pressure Relief Device (PRD) Resource" is a collection of setups, each representing a type of pressure relief device in AFFTAC's Advanced PRD Model. The Advanced PRD Model in AFFTAC can model frangible disks as well as pressure relief valves (PRVs). It also can handle

[1] That being time-dependent deterioration of insulations. The Advanced Model uses a temperature-dependent deterioration model.

PRVs that have much more customized open-close behavior than can be represented using AFFTAC's Basic PRD Model, which is very restrictive by comparison and consists of so few inputs that they are not broken out as a Resource. Rather, they are simply lumped in with the other individual inputs in an Analysis. Use of the Advanced PRD Resources gives you access to pre-established PRV setups calibrated in an extensive validation exercise, which is discussed in the *AFFTAC Verification and Validation Testing* document. It also gives you more freedom in how you specify PRD performance. The Basic PRD Model, which again is more restrictive, is in some ways faster to set up, especially if you want to vary a PRD parameter in a study.

Advanced Strength Model Resources: The "Advanced Strength Model Resources" is a collection of setups, each representing a type of tank wall material for AFFTAC's Advanced Strength Model. The Advanced Strength Model in AFFTAC allows the user to enter values for the Larson-Miller parameter as a function of temperature, ultimate tensile strength as a function of temperature, and creep strain at failure as a function of temperature. The first two represent two different methods of computing the burst strength of the tank, and they can be run together until one predicts failure, or just one can be chosen. The creep strain at failure data can be used as an auxiliary model to augment the computation changes to the tank volume as creep occurs. The Advanced Strength Model stands in contrast to AFFTAC's Basic Strength Model in which the user simply selects a material identification from a pull-down menu, causing AFFTAC to use hard-coded ultimate tensile strength formulae to compute the tank's burst pressure. Like the Basic PRV Model, when the Basic Strength Model is selected by the user, that material selection is integrated with the rest of the Analysis' individual inputs, i.e., a "Resource" is not required for the tank wall strength.

2.3 Installation, System Requirements, and Technical Assistance

AFFTAC 5.11 is designed for systems running MS-Windows 10 operating systems. The AFFTAC 5.11 graphical user interface was developed in Microsoft Visual Studio 2012. Assistance can be obtained from:

Dr. Scott R. Runnels
Southern Rockies Consulting, LLC
505-695-9241
SRunnels@SRConsult.com
www.srconsult.com

2.4 Acknowledgements

Special thanks go to John Sbragia whose careful testing of AFFTAC has revealed multiple deficiencies that, once fixed, improved the reliability and robustness of the code. Also, thanks go to Todd Treichel for his skillful management of the AFFTAC project.

The original development of AFFTAC for Windows and the initial three databases were funded by the RSI-AAR Railroad Tank Car Safety Research & Test Project and was performed under Southwest Research Institute project number 18-6965. Development past 2000 was continued under the same funding source by Scott Runnels Consulting, which became Southern Rockies Consulting, LLC in 2014.

Thanks go to Tom Dalrymple for his advice during the designing of the graphical user interface and suggesting the use of databases in the original AFFTAC for Windows, as well as the overall project management during 2000-2002. Thanks also to those who tested the earlier versions, including Bill Bitting, Al Henzi, Thomas Petrunich, and Andy Rohrich.

The late Dr. Milton Johnson's contributions to the earlier versions of this manual are gratefully acknowledged. Much of his contributions remain in this revision, in particular the "Aside" comments in Appendix B and elsewhere. Likewise, Mr. Joe Cardinal at Southwest Research Institute also provided helpful input on earlier versions of this manual.

Chapter 3

The Scope and Interaction of AFFTAC's Models

AFFTAC is a simulator combining the effects of several physical phenomena that, together, comprise a complex nonlinear system. In this chapter, the scope and interaction of those multiple physics models are described.

AFFTAC is best thought of as a transient, quasi-two-dimensional model. The heat transfer through the tank wall is one-dimensional. However, some models in AFFTAC support variation in the insulation properties as a function of angle around the tank. Conversely, the liquid and vapor are at a uniform temperature at any point in time and in that sense AFFTAC is a zero-dimensional model. Yet, the tank may be modeled as rolled over, meaning the location of the liquid surface and its interaction with the location of the pressure relief device is accommodated. In short, separate assumptions regarding dimensionality are made for individual models. The individual models are then combined in a consistent way.

An Important Note Regarding Theory in this Manual

It is important to point out that while AFFTAC carries out the computations described in this manual, there are also multiple heuristics and other subtle details to the AFFTAC calculations that are not described here. The discussions of AFFTAC's theory in this manual are best thought of as high-level descriptions. Some but not all of the heuristics and subtleties are described more fully in the *Programmer's Guide to the Computational Module's Unit Tests*, which is proprietary and must be obtained through the RSI-AAR Railroad Tank Car Safety Research & Test Project.

3.1 Physics Aspects of a Typical Simulation

Heat is added to the tank car and lading system on the outside of the tank car through heat exchange with the fire. This heat is transported to the inside of the tank through the tank wall and thermal protection system, eventually reaching the lading. The heat is transported to the lading by contact with the tank wall and by radiation and convection through and with the vapor from the tank wall's interior surfaces. The lading responds by heating up; the liquid thermally expands and the vapor pressure increases. If the tank is in a shell full condition, i.e., when it is completely full of liquid, the liquid's thermal expansion results in an increase in pressure inside the tank. Conversely, when vapor is present, the pressure also increases but is due instead to the vapor pressure. Either way, when the pressure inside the tank reaches a sufficient level, the tank's pressure relief device opens and allows lading to be released. Models for the pressure relief device are provided as part of the AFFTAC simulator. Flow of vapor, liquid, or a mixture of the two, depending on the rollover condition and the amount of liquid present, is accommodated by these models.

The simulation is carried out starting at time = 0 and, under normal circumstances, ending at a user-specified time. However, as the simulation proceeds, the lading could eventually be completely expelled, causing the simulation to end earlier. Another possibility for early termination occurs when the pressure relief device is not able to

accommodate the expulsion of lading quickly enough. In that case, the pressure inside the tank car can build up to become high enough to rupture the tank.

In addition to the models for the pressure relief device and the flow through it, AFFTAC has other supporting models that play key roles in the simulation. There are models for how the insulating layers of the tank wall change with time and temperature. There are also auxiliary models, including elastic strain, permanent creep, and thermal expansion in the tank wall, which are used to compute the change in the tank volume. Finally, there is a temperature-dependent and temperature- and pressure- dependent failure model for the tank wall as a structural layer.

An overview of the AFFTAC simulation is shown in Figure 3.1 and a summary of the models is shown in Figure 3.2. As shown in Figure 3.1, each of the models are linked and executed in a time-marching loop that proceeds through the simulation in small time increments. The equations describing these models are all linked and, in principle, must be solved simultaneously at each point in time. In practice, however, they are separated and solved in an alternating fashion where some values from the previous time step are used to update other values. Then, those newly updated values are used to update the first set of values. In reality, there are more than just two groups that operate in this way. At multiple steps in the calculations, a mixture of old values and newly updated values are used to propagate the calculation forward. At the end of each time step, all variables will have been updated. This method is often referred to as “nonlinear lagging”. This aspect of the calculations is very important to understand when delving into the theoretical descriptions in the chapters that follow. In all of the chapters, you will notice that some values, which you know to be transient and part of the overall solution, will be assumed known for that part of the theory. By considering all parts of the theory together, you will see how all values are eventually updated.

3.2 Heat Transfer Assumptions

Heat transfer is a primary driver in AFFTAC. Consequently, the heat transfer model is the core, driving model. It has multiple aspects that are addressed in multiple places in this manual. Here, some of the key overarching assumptions and approaches are described.

First, the fire is modeled as a surface, some arbitrary distance from the tank, held at a fixed temperature during the simulation, e.g., 1,500 deg-F. In a “pool fire” simulation, this surface surrounds the tank entirely. The lading inside the tank is assumed to be well mixed and at a uniform temperature. The liquid and vapor phases are assumed to be in thermodynamic equilibrium with each other and thus are at the same temperature. Note that this assumption relies upon the assumption that venting occurs. Specifically, venting results in cooling of the vapor through mechanical work, as well as the intermixing of the liquid’s lower thermal energy with the vapor’s higher thermal energy due to evaporation of the liquid into the vapor.

Second, the tank car’s innermost surface is considered to have two different temperature regions, one for the segment of the tank adjacent to the liquid lading and one for the segment adjacent to the vapor. This division is established because it is assumed that the liquid has a great thermal mass and is in intimate contact with the tank wall’s innermost surface. Thus the tank wall in contact with the liquid is assumed to be at the same temperature as the lading. In contrast, the tank wall adjacent to the vapor does not have intimate contact, nor does the vapor have any appreciable thermal mass. Therefore, the tank wall’s innermost surface temperature can be very different from the vapor temperature. In fact, the temperature of the tank wall adjacent to the vapor is among the most important state variables, for it is that temperature that often impacts the strength and ultimate life of the tank wall.

Third, a variety of models can be chosen for computing the heat transfer between the tank’s innermost surface, outermost surface, and the fire. These are the “thermal protection system” or “TPS” models. When the TPS model is invoked at any time during the simulation, it is given the current temperature of the interior surface of the tank wall and the temperature of the flame. Using those two boundary conditions, it computes the temperature of the tank’s outermost surface and the heat flux through the TPS. The TPS model is invoked at least twice, once for the segment of the tank wall adjacent to the liquid, and again for that adjacent to the vapor. In simulations where the TPS is specified to have angular dependence, it is invoked multiple times, one for each angular segment you specify.

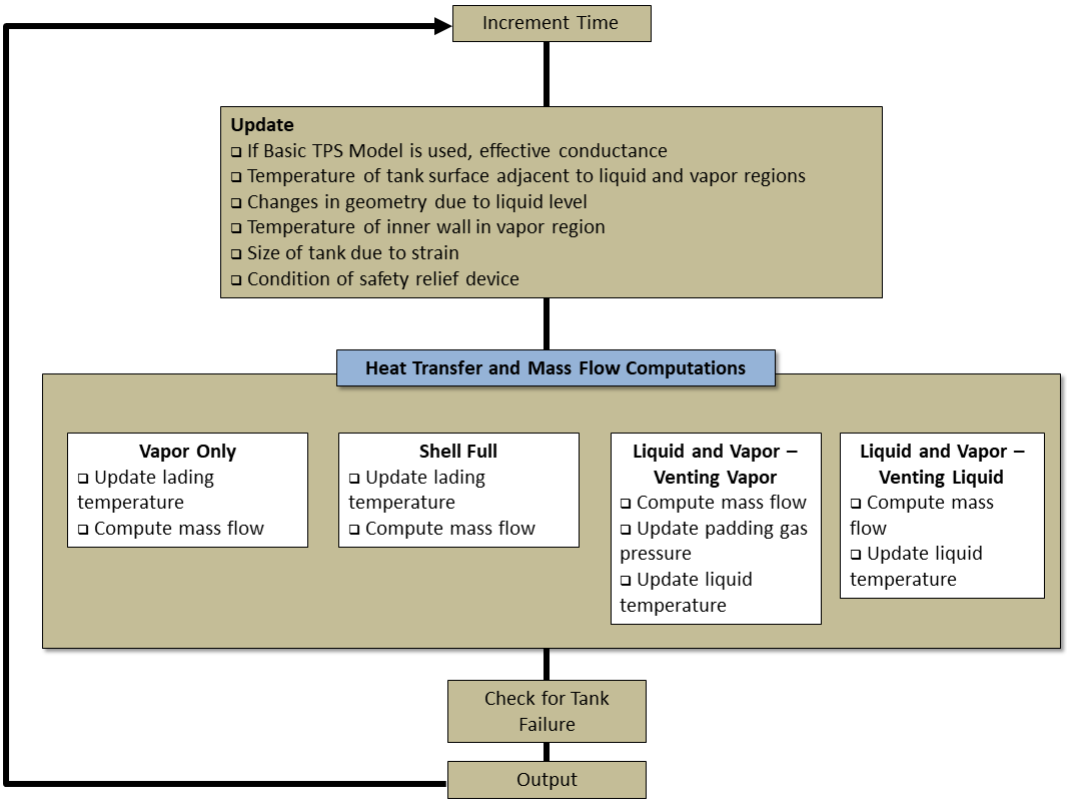

Figure 3.1: Conceptual flow chart of the AFFTAC model computations

Note that the TPS models are set up and used by AFFTAC in a circular cross section of the tank. They do not, therefore, represent the bidirectional heating that occurs at the intersection of the end cap and the main body of the tank. In a simulation where a large defect is present at the end cap, it is recommended that the TPS defect be exaggerated in the circular cross section setup to help compensate for that aspect of the model. Note also that AFFTAC does not model circumferential heat conduction around the tank wall, including between the liquid-adjacent and vapor-adjacent tank wall regions or from regions where there are TPS defects. Thus, for example, if the vapor-adjacent tank wall is much hotter than the liquid-adjacent tank wall, the liquid-adjacent tank wall is not allowed to provide any relief, even though it would in a real-life situation. AFFTAC not including circumferential heat conduction is therefore a conservative assumption in that way, and is considered to be conservative in most [1] if not all applications.

Fourth, in addition to the conduction of heat into the lading, heat is transferred into the lading through the heat radiated and convected from the inner surface of the tank wall. The radiation occurs between the tank's innermost surface adjacent to the vapor and the top surface of the liquid while the convection is between the tank's innermost surface and the vapor. Either way, whether exchanged with the vapor or liquid phase, the heat is considered to be exchanged with the lading as a whole, which again is at one uniform temperature at each point in time. Other heat-related mechanisms include thermodynamic work associated with discharging lading through the pressure relief device and the associated heat of vaporization that cools the liquid when it evaporates to replace the vapor lading

[1] It is possible to contrive a situation in which the disallowance of circumferential heat conduction could be ever so slightly non-conservative. In particular, if a very large TPS defect is aligned perfectly with the liquid surface that never moves, it is possible that the lack of circumferential heat conduction could cause the liquid temperature to be underestimated by AFFTAC, leading to an underestimate of vapor pressure.

that is expelled.

Fifth, a heat balance on the innermost tank wall is used to determine the temperature of the tank wall for the portion of the tank over the vapor region.

3.3 Pressure Relief Device Modeling

AFFTAC accommodates pressure relief devices (PRDs) that, under appropriate conditions, allow lading to be discharged. Depending on the amount of liquid lading present and the angle of tank rollover, the discharge may be purely liquid, purely vapor, or a mix. The details of how the pressure relief device's opening and closing action are modeled as well as the fluid flow through it are described in a separate chapter.

One important note to make here, however, is that you have two ways of entering specifications for the PRD. One is to specify them directly as numerical entries as part of an analysis. Another way is to choose from a list of PRDs that are contained in what we call the "Advacned PRD Modeling Resources", which you can also edit. In this second mode, you have the ability to enter a much more general, customized relationship between pressure and fraction open.

3.4 Tank Failure Modeling

The strength of the tank is a very important model in AFFTAC. It provides a determination regarding whether the tank will burst during the simulation.

There is more than one strength model from which to choose in AFFTAC. The Basic Strength Model only requires the current, highest temperature of the tank wall. From that temperature and knowledge of the material from which the tank wall is constructed, the Basic Strength Model computes a current value for the tank's ultimate tensile strength. That value is compared to the stress required to contain the pressure inside the tank. If it is insufficient, the tank bursts.

In addition to the Basic Strength Model, AFFTAC also offers an Advanced Strength Model, which includes a Larson-Miller creep and failure model that has been validated against more recently acquired data. Instead of only using the current temperature to determine the tank material's strength, the Larson-Miller model computes the damage accumulated at the microscopic level as the tank material is heated and stretched. As this accumulated damage is computed, it is used to compute the amount of "life", so to speak, of the tank wall that has been depleted. Once all of the life has been depleted, the tank is said to have burst. The Advanced Strength Model can also simultaneously compare against ultimate tensile strength data to test for failure. Lasty, the Advanced Strength Model can include creep strain in the volume calculation for the tank. Because there are so many inputs into the Advanced Strength Model, each setup is collected into an individual entry in the "Advanced Strength Model Resource", and is given a name to represent a single tank wall material.

The tank strength model interacts with AFFTAC's thermal model in fairly intricate ways. If the Basic TPS model is used, then the highest temperature experienced by the tank wall is that adjacent to the vapor and that temperature is used as input into relatively straightforward algebraic equations to compute an ultimate tensile strength. In contrast to this, the Advanced Strength Model's Larson-Miller option operates differently because it depends on the history of each point around the tank. In the Larson-Miller model, 180 points are established around the tank, at one degree intervals, and those "tracking points" are used to track the temperature-pressure-life-remaining metrics at their respective locations. Thus, when the Basic TPS Model is used, the Larson-Miller tracking points are fed either the tank wall temperature adjacent to the liquid or the vapor, depending on their location. As the liquid level rises or falls, the temperature fed into each Larson-Miller tracking point may change.

If the Advacned TPS Model is invoked, and significant angular dependence to the insulation is specified, the interactions are more complex. For the Basic Strength Model, a search must be made through the TPS segments for the

highest temperature, and that temperature is fed to the algebraic equations mentioned above. But for the (Advanced) Larson-Miller model, each of its 180 tracking points uses the temperatures in their respective TPS segments.

Thus, one can imagine a variety of complex scenarios arising, depending on the type of simulation carried out. For example, consider a setup using the Advanced TPS Model with angular dependence such that significant defects in the insulation exist around the liquid level. As the liquid expands or lading is discharged, there may be significant changes into the input of the strength model for those points. This type of complexity testifies to the need for a computer model to understand it and also to the need for careful use and understanding of the model.

3.5 Material Expansion Modeling

Both the liquid lading and the tank itself can expand during a simulation. The liquid lading may expand due to heating. The tank may expand due to heating, as well as elastic stress and permanent creep. The interaction of these expansions is very important when the tank is completely full of liquid, i.e., the "shell full" condition. In that case, further expansion of the liquid can lead to tremendous stresses in the tank wall that can result in failure. Thus there is an important interaction between the models computing the expansion of the liquid, its possible release through the PRD, the expansion of the tank wall due to heat and stress, and the tank failure model.

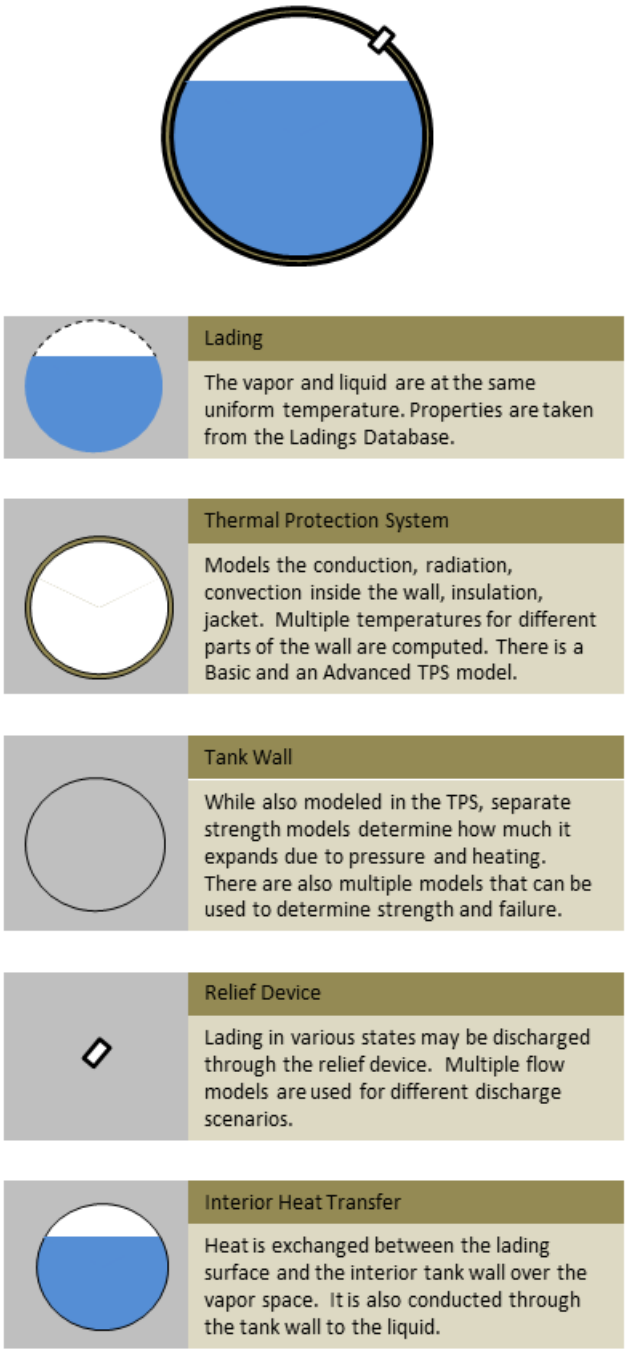

Figure 3.2: Overview of AFFTAC's primary models

Chapter 4

Creating and Running AFFTAC Simulations

4.1 Setting up an Analysis

Each Analysis in AFFTAC is comprised of individual values, e.g., tank volume, tank wall thickness, and *names* of more complex inputs, i.e., collections of values that, together, represent something more complex, such as a lading. Each of these "named" values are referred to in AFFTAC as "Resources". A setup for a lading, which consists of multiple thermodynamic values, is referred to as a "Lading Resource", for example. All data used by AFFTAC, including the Analyses and all the Resources, are stored in your input (.udb) file. The Analyses are central to AFFTAC and are displayed in AFFTAC's **Main Window**, as in Figure 4.1. To create a new analysis from scratch using default values, click on the **New** button in the **Main Window**. To create a new analysis that is based on an existing one, highlight the existing one, click **Copy** and then click **Paste**. When you do, a new analysis will be created that is identical to the one you copied except for its title and its administration information, which you will eventually specify. You may edit that analysis by highlighting it and clicking **Edit Analysis**.

As mentioned above, each of your analyses will contain two kinds of entries:

1. **Numerical and Logical Data:** These are straightforward entries having to do with direct data about the simulation. For example, the length of the simulation is a numerical entry that is part of an analysis.

2. **References to other "Resources":** These are names of collections of inputs that represent complex parts of the simulation, such as ladings, thermal protection systems, and pressure relief devices (PRDs). If you select "Butane" for the lading, that name is used to pull thermodynamic properties from the Ladings Resources under the name "Butane" and provide them to the Computational Module for the simulation. Thus the single entry "Butane" in the analysis specification contains a great deal of information, including multiple tables of data. Other examples include the TPS setup, the tank material, and can also include the pressure relief device.

The process of setting up a simulation is divided into four steps which are conducted using four sequential windows: **Edit Analysis Conditions**, **Edit Tank Car Properties**, **Select TPS Model**, and **Setup Lading**. These four windows are shown in Figure 4.2.

4.1.1 Edit Analysis Conditions Window

In this window, you may set basic analysis conditions, including the flame type and the length of the simulation. From this window you can launch a sub-window that allows you to set the time step and the frequency of printouts. An important decision in this window is the type of simulation to be run. A Standard Simulation engulfs the tank fully by a flame at 1,500 deg-F. A Special Conditions simulation allows you to modify the flame temperature and the amount of engulfment. Higher flame temperatures and more engulfment produce shorter survival times. Thus, you should not

lower either of those two values from the Standard Simulation values unless you are confident about the values you will be entering.

The **Timing Details** button opens an additional window that allows you to adjust the "time step" for the simulation. AFFTAC uses numerical algorithms to solve the various physics equations representing the tank exposed to fire. Those equations are transient in nature, and so a "time stepping" algorithm is used to "march" through time, gradually accommodating all of the transient effects as it goes. The smaller the time step, the more accurate the simulation. But smaller time steps take longer, so there is a trade-off. On critical simulations, you should lower the time step a few times and look for significant changes in your results. Be mindful of the second input in the Timing Details window, that of the frequency of output. As you lower the time step, the output will be more volumous unless you keep this value constant. On the other hand, if you do not decrease it along with the time step, you might miss seeing some features of the simulation, for instance, oscillations in the PRV opening and closing, which can occur at relatively high frequences under some modeling conditions.

It is always important to examine the plot of burst pressure and tank internal pressure, which is the upper right plot shown when you click the **Plot Displayed Results** button in the **Main Window**. When those two pressure plots touch, the tank fails. In some simulations, there can be near misses, where the internal pressure approaches the burst pressure but does not cross it because the PRV opens just in time. You should be mindful of those "near miss" situations when making any adjustments to the inputs of your simulation, for example the time step.

4.1.2 Edit Tank Car Properties Window

In this window, you set up the properties of the tank car, including the material from which the tank is made and the safety relief device properties. Both the material setup and the PRD setup may be handled in two ways. You may choose to use the basic models and setup methods by making choices directly in this window. Or you may choose to use the Advanced PRD Model, which uses more complex inputs and is therefore gathered together as a Resource. Likewise you may choose which of the Basic Strength Models to use or may switch to using one of the Advanced Strength Model Resources. Guidance for which PRD model to choose is provided in subsection 4.6.2, and the models are discussed in greater detail in subsequent chapters. Likewise, guidance for which strength modeling approach to choose is provided in subsection 4.6.3, and the models are discussed in greater detail in subsequent chapters.

Another choice to be made in this window relates to the shell full condition. AFFTAC's Basic Model, described in subsection 13.2.5 and the Dynamic Model, described in subsection 13.2.6 have been shown to give roughly the same results, but have subtle differences. The Dynamic Model captures the higher-frequency oscillations in lading release during the shell full condition, but it requires more inputs, specifically, the bulk modulus of the liquid lading. It also requires smaller timesteps. If the scenario you are running involves a significant amount of time in the shell full condition, and especially if failure during shell full occurs, consider using both models and comparing the results, if you have reliable data for the liquid lading's bulk modulus. Remember, too, that when running the Dynamic Shell Full Model, you will likely need smaller time steps, which are set using a button in the previous window.

4.1.3 Select TPS Window

In this window, you choose the type of thermal protection system on the tank car by selecting one of the systems that is displayed. AFFTAC has two completely separate TPS models provided through the Basic TPS Model Resource and the Advanced TPS Model Resource. Subsection 4.6.1 provides guidance on which one to use. The approach (Basic or Advanced) is selected through the large, central button on this window. Once chosen, a specific TPS model can be chosen from the displayed resource list. You can edit this list, add to it, or delete unused items from it by clicking the button below each list.

4.1.4 Setup Lading Window

In this window, you select the lading from a list of ladings stored in the Ladings Resource list. You may edit this Resource list to create new ladings by clicking the **Manage Ladings Resources** button. Also in this window, you specify the fraction of tank filled by the lading, its initial temperature, and the padding gas, if present.

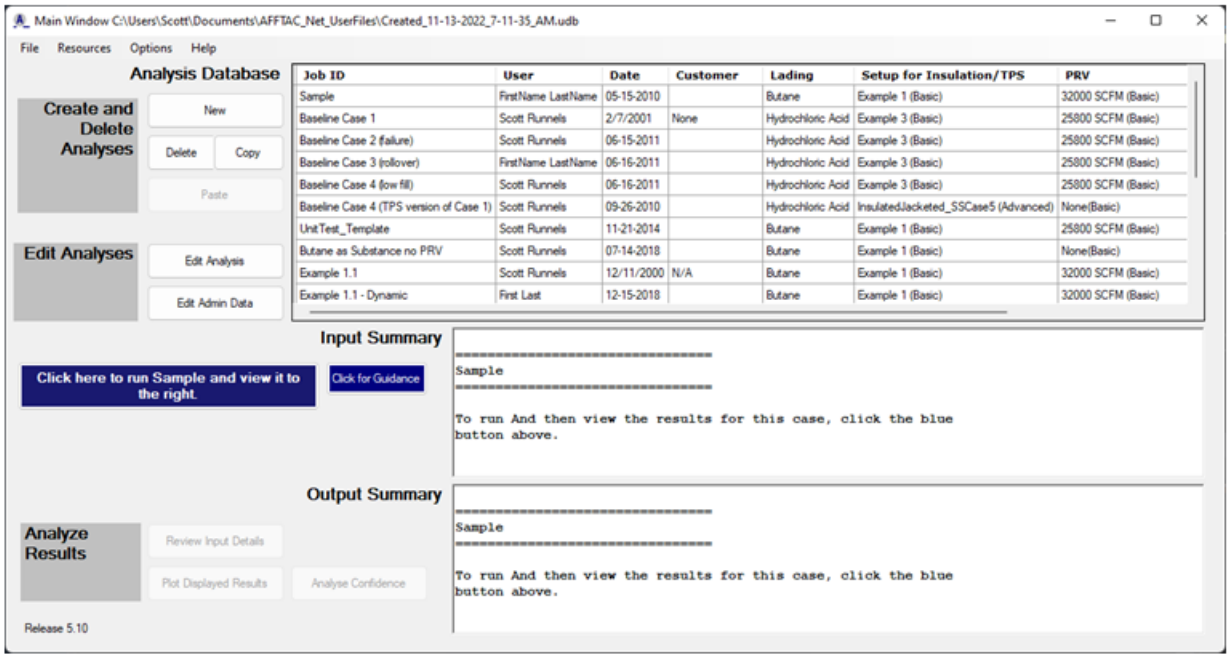

Figure 4.1: AFFTAC's **Main Window** in which the Analyses Database is displayed in the right-most pane

4.2 Running an Analysis

There are two ways to initiate the execution of an analysis. One is to highlight the analysis in the **Main Window** and then click the dark blue panel in the middle left portion of the **Main Window**. The other is to click the **Run Now** button in any of the four editing windows. In this latter option, the changes you have made during the editing sequence are automatically made part of the current highlighted analysis. However, those changes are not saved permanently in your input file until you choose the menu option **File-Save**.

The analysis is carried out by AFFTAC's Computational Module, which is a stand-alone executable invoked by the GUI. When you request the simulation to be run, the GUI writes the necessary input files for the Computational Module. It then runs the Computational Module, which executes in a DOS window that opens to display the simulation's progress. Once the simulation is completed, the GUI reads the Computational Module's output files and displays them in the two panels on the right-hand-side of the **Main Window**.

4.3 Viewing and Using Results

After a simulation is completed, the results are displayed on the right-hand-side of the **Main Window**. The middle panel of the **Main Window** displays a partial summary of your inputs for the problem. The panel below it is some of

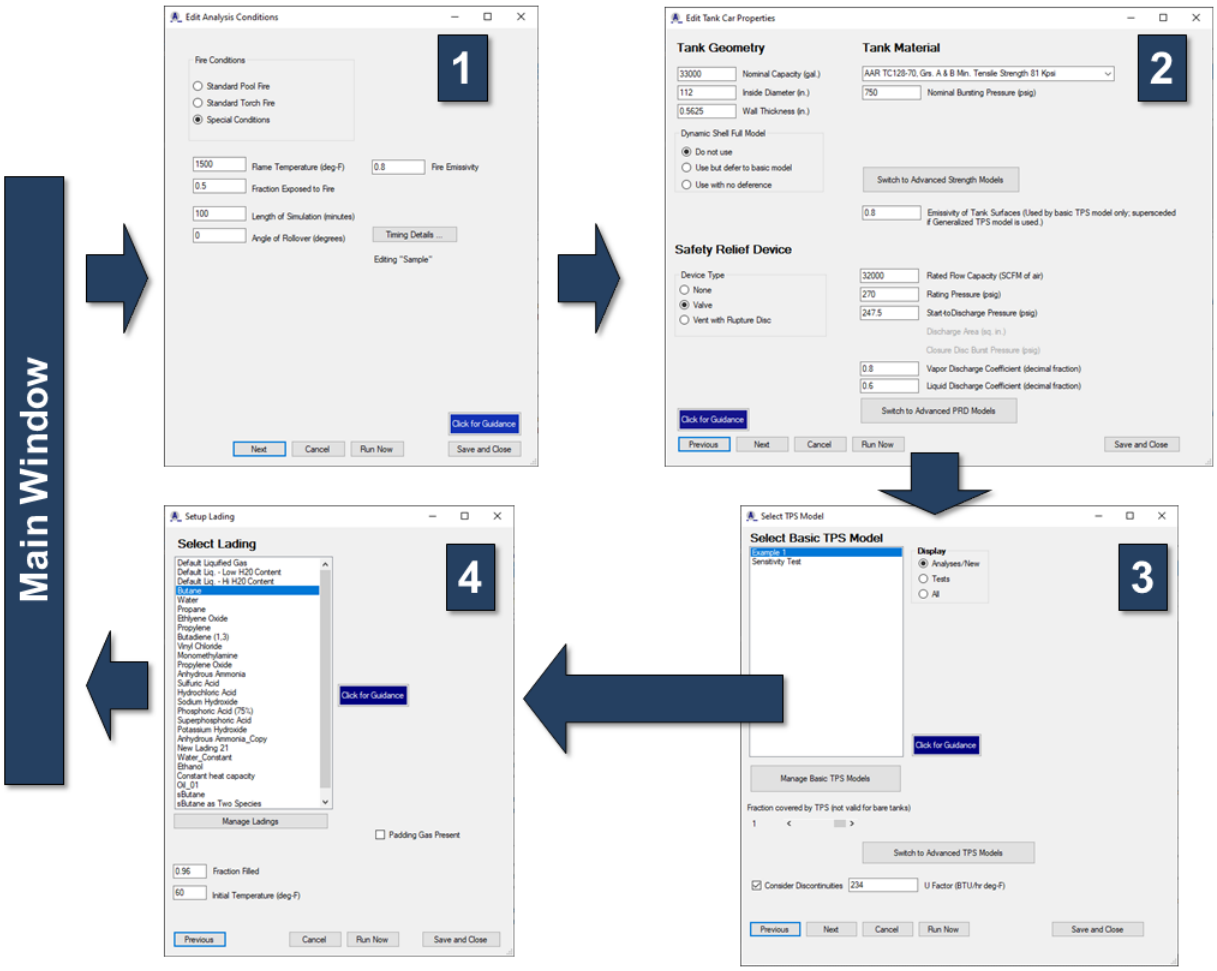

Figure 4.2: Illustration of the four-step editing process for setting up AFFTAC simulations

the key numerical output values. Typical results are shown in Figure 4.3. These results may be visualized by clicking the **Plot Displayed Results** button in the **Main Window** which displays a window like that shown in Figure 4.4. The plot window has several controls that allow some modification to the displayed plots. Clicking on a plot copies it to the Microsoft clipboard from which it can be pasted into a number of other applications.

To print the results and input summary, in the **Main Window**, select the menu option **File-Print Currently Shown Results**. Also, you may copy the contents of the displayed textual output to the Microsoft clipboard by painting the text displayed in the **Main Window** and pressing **Ctrl-C**. These contents may then be pasted into a variety of Microsoft Windows applications such as Word or PowerPoint.

A very convenient way to view and communicate results is through the PDF report, which AFFTAC can write for the displayed results (and selected Analysis setup). Click **File-PDF Report** in the **Main Window** to do that.

Of particular value is the ability to view the textual input file written by the GUI, which is read by the Computational Module. This input file contains documentation that can enhance your understanding of your inputs and also help ensure against errors. **Please take the time to look at that file** for critical runs and studies by clicking the **Review Input Details** in the lower left portion of the **Main Window**.

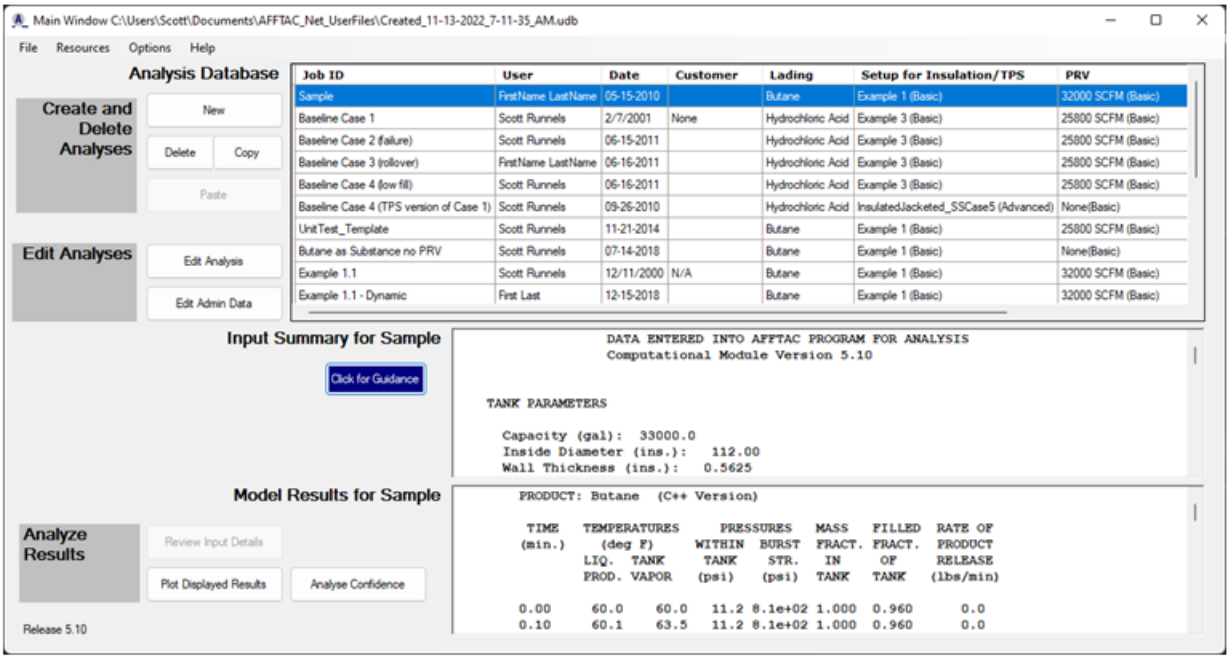

Figure 4.3: AFFTAC's **Main Window**, displaying the results of an analysis

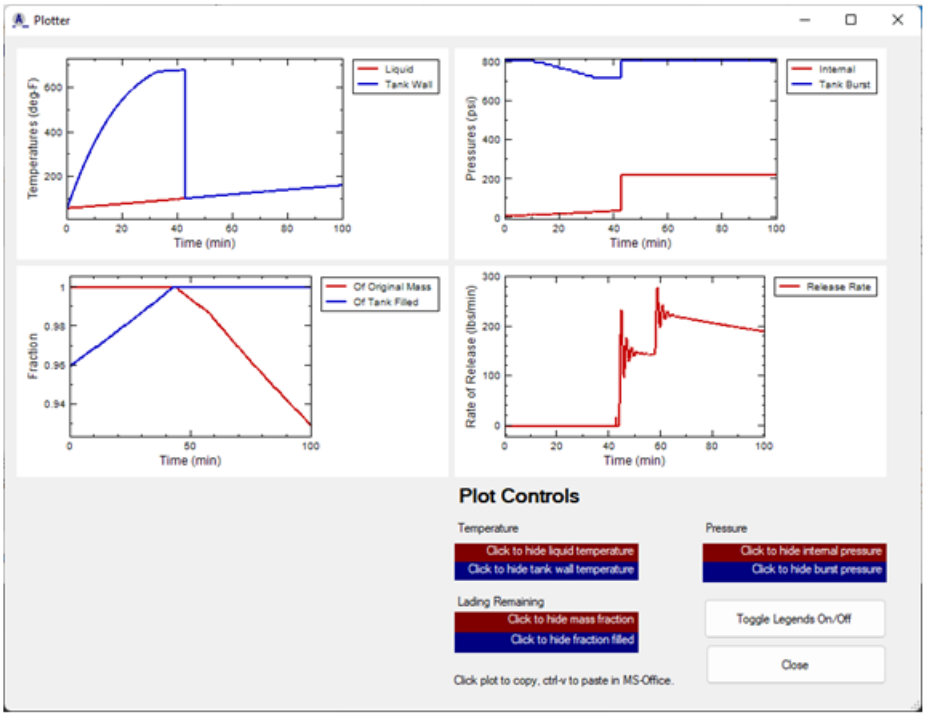

Figure 4.4: AFFTAC's plotting window, graphically displaying the results of an analysis

4.4 Administrative Information

Administrative information is required in order to print the results of an analysis or to save it. To add the administrative information, highlight the analysis and click the **Edit Admin Data** button in the **Main Window**. The window used for entering that administrative information is shown in Figure 4.5. Your name and company may be more permanently set by selecting the menu option **Options-User Information** in the **Main Window**. The rest of the user-specific information you add in the window is shown in Figure 4.5.

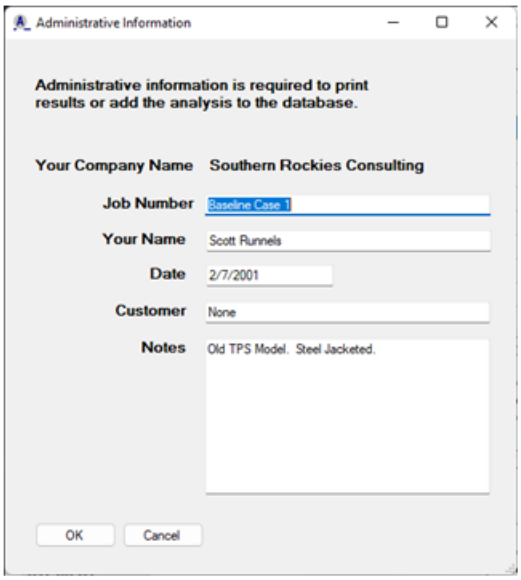

Figure 4.5: Administrative information window that must be completed for a simulation to be printed or added to the Analyses

4.5 Table of Capability Setup Options

AFFTAC is nearly forty years old and has been enhanced many times during its history. As with any code of that age and type, efforts are made to maintain older capabilities while adding enhancements. As a result of that, AFFTAC has a variety of input options and style of input methods. In many places in this manual, you will find that you have the option of using a basic (typically, older) model or an advacned (typically, newer) model. And you will find that you have the option of inputting values in different ways. To help avoid confusion, Table 4.1 is provided to clarify these aspects.

As the table indicates, some aspects of the simulation may only be entered directly into the analysis by specifying values. Others have multiple options. For example, if the Basic PRD Model setup method is used, the values are entered directly in the analysis. If you choose to use the Advanced PRD Model, you will instead access the PRD Resources and enter the values there.

Table of Capability Setup Options	
Input Value	How it is input
Length of Simulation	Value entered as part of the Analysis
Tank Geometry	Value entered as part of the Analysis
Tank Failure	Basic Strength Model: Material selection stored as part of the analysis Advanced Strength Model: Name selected from the Advanced Strength Model Resource list
Tank Wall Emissivity	When using Basic TPS Model, valued entered as part of the Analysis When using the Advanced TPS Model, entered as part of the TPS setup
Pressure Relief Device	Basic PRD Model: Values entered as part of the analysis Advanced PRD Model: Name selected from the Advanced PRD Model Resource list
Thermal Protection System	Always a selection from either the Advanced TPS Resource list or the Basic TPS Resource list
Other Heat Transfer Mechanisms	Value entered as part of the Analysis
Lading Properties Lading Initial Conditions	Always a selection from the Ladings Resource list Value entered as part of the Analysis
Padding Gas	Value specified as part of the Analysis

Table 4.1: This table provides an overview of what methods may be used for inputting values for different models in AFFTAC. Because there is a mix of Basic and Advanced modeling capabilities, input options vary.

4.6 Guidance for High-Level Choices

As Table 4.1 and the discussion leading up to it implies, there are some key high-level choices you must make when selecting which models to use in AFFTAC. In this section, some guidance is provided for those high-level choices.

4.6.1 Basic or Advanced TPS Model?

You should choose AFFTAC's Advanced TPS Model if any of these conditions are associated with your simulation:

- You need flexibility in the number of layers you want to include.
- You have a TPS defect, i.e., missing insulation, where the defect is not uniform around the tank. With the Advanced TPS Model, you can specify the insulation coverage as a function of angle around the tank.
- Your insulation deteriorates at higher temperatures.

The Basic TPS Model's configurations are more limited than those of the Advanced TPS Model, where you can specify any number of layers. However, the Basic TPS Model has one feature that the advanced version does not have, that being the detioration of the insulation with *time*, as opposed to temperature, as is done in the advanced version.

4.6.2 Basic or Advanced PRD Model?

You should use AFFTAC's Advanced Pressure Relief Device (PRD) Model if your simulation involves a pressure relief valve whose open-close behavior cannot be represented with the plot shown in Figure 11.2. AFFTAC's Advanced PRD Model allows you to modify the shape of the paths in that figure and, if necessary, create an entirely new system of paths that the PRV can follow when opening and closing due to pressure changes. If you use the Basic PRD Model, you need only input a few values as part of the standard Analysis setup. If you use the Advanced PRD Model, you will choose a model from the list of Advanced PRD Resources, which you can edit.

One advantage of using the Advanced PRD Model is that AFFTAC is shipped with a pre-calibrated set of PRD setups, already contained in the PRD Resource list. Ten entries in the PRD Resource list contain an identification number connected to particular PRDs that have been calibrated. The calibration exercise is described in the *AFFTAC Verification and Validation Testing* document; see Section 2.1 for more information.

4.6.3 Basic or Advanced Strength Model?

You should use AFFTAC's Advanced Strength Model if you have ultimate tensile strength data or Larson-Miller creep and failure data for your tank wall material. Some of that data comes shipped with AFFTAC, and so you might want to inspect the Advanced Strength Resources to help you decide. Also, if you want to see the impact of creep on the tank volume, you should choose the Advanced Strength Model. If you do choose the Advanced Strength Model, you will choose that model from the list of Advanced Strength Model Resources. Using AFFTAC's Basic Strength Model means that you will be using hard-coded polynomial-based ultimate tensile strength models for the tank wall, specifically, those in Tables 9.1, 9.2, and 9.3.

Chapter 5

Details of the Overall Thermal Model

5.1 Essential Constructs

Below are the essential constructs of AFFTAC's thermal transport model. You should be cognizant of these when seeking to understand the theory behind the Computational Module.

1. The liquid and vapor phases of the lading are assumed to be at the same temperature, T_{lading}, which changes with time but is constant in space. The part of the tank wall adjacent to the liquid phase is also assumed to be at that same temperature.

2. The innermost surface of the tank wall adjacent to the vapor is at a temperature that may be different from the lading temperature. Its temperature is denoted as $T_{wall-vapor}$.

3. As shown in Figure 5.1, heat is transferred to the lading by three mechanisms:

   (a) Conduction to the liquid through the TPS and tank wall,

   (b) Convection to the vapor by contact with the inner tank wall, and

   (c) Radiation to the liquid surface from the inner tank wall that is adjacent to the vapor.

4. The tank is heated through radiative exchange with the flame. Convection with the surrounding air is not included in the model.

Computing 4 and 3 (a) is the responsibility of the TPS model, of which there are two kinds in AFFTAC. They are each discussed in their own, subsequent, chapters. Those models take as a given the innermost surface temperature and the flame temperature. Using those two boundary conditions, they compute the heat flux transported through to the innermost surface. The process of taking the interior temperature as a known value in the TPS computations is a technique known as "nonlinear lagging" and is discussed in Chapter 3. The details of the computations in 3 (a) are discussed in the separate chapters on the two TPS models.

The details of computing the fluxes in 3 (b) and 3 (c) are discussed in this chapter. Computing these fluxes also requires knowledge of the temperature of the innermost surface of the tank wall adjacent to the vapor. That key variable, $T_{wall-vapor}$, is determined using an equation that balances the net flux into the wall from the outside with the net flux leaving the wall on the inside through convection and radiation to the lading. That heat balance is shown graphically in Figure 5.2. As with 3 (a), this method of computation uses "nonlinear lagging", as discussed in Chapter 3.

As mentioned in Section 2.1, several subtleties to the heat transfer models exist in AFFTAC; the *Programmer's Guide to the Computational Module's Unit Tests* describes some of them.

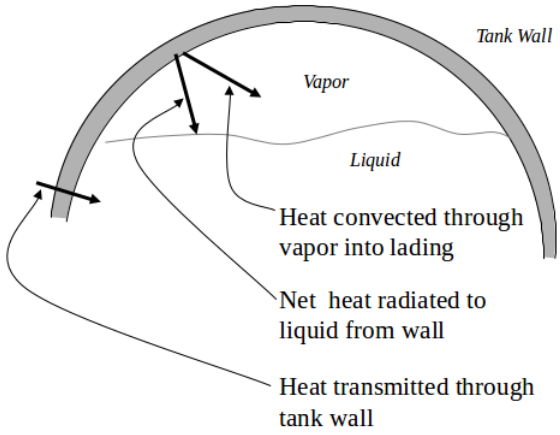

Figure 5.1: Heat flowing into the vapor and liquid phases of the lading

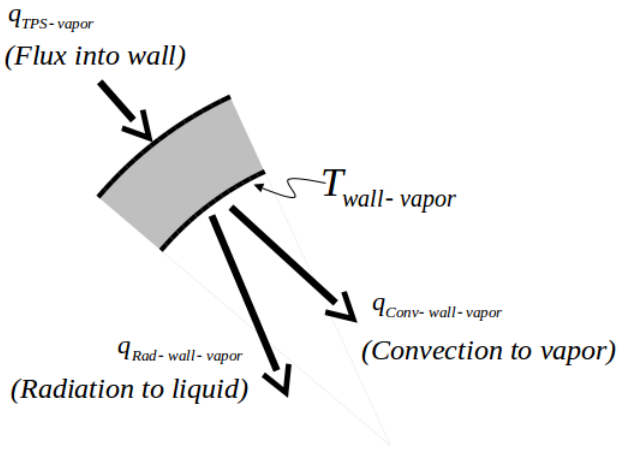

Figure 5.2: Heat balance on the tank wall adjacent to the vapor

5.2 Constructs of Radiative Heat Exchange

As discussed in the previous section, radiative heat exchange occurs between the tank car's outermost surface and the flame as well as the tank's innermost surface and the lading's liquid surface. AFFTAC models all radiative exchange using a classical law [10], and represents every surface as being gray with a constant value of emissivity.

For radiative exchange between two surfaces, the emissive powers of the two surfaces are

$$\begin{aligned} E_1 &= \epsilon_1 \sigma T_1^4 \\ E_2 &= \epsilon_2 \sigma T_2^4 \end{aligned} \tag{5.1}$$

where σ is the Stefan-Boltzmann constant. As shown in [10] a heat flux balance between two gray surfaces connected in the logical configuration indicated in Figure 5.3 results in the following relationship:

$$Q_{(1-2)} = \frac{\sigma(T_1^4 - T_2^4)}{\frac{1-\epsilon_1}{A_1\epsilon_1} + \frac{1}{A_1 F_{1-2}} + \frac{1-\epsilon_2}{A_2\epsilon_2}} \tag{5.2}$$

where

Q_{1-2} is the net heat flux from surface 1 to surface 2
F_{1-2} is the geometric view factor, which represents the line-of-sight exposure between surfaces 1 and 2 as defined in [10], and
A_i is the area of the surfaces i $(i = 1, 2)$. (5.3)

Rearranging, the above equation becomes

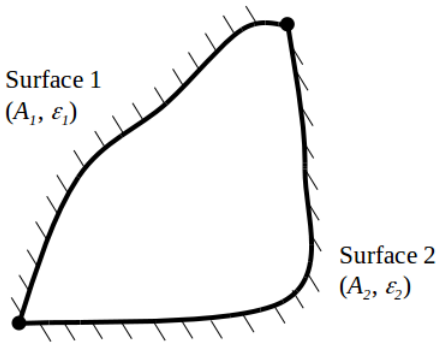

Figure 5.3: Gray body configuration used in AFFTAC

$$\frac{Q_{(1-2)}}{A_1} \equiv q_{(1-2)} = \frac{\sigma(T_1^4 - T_2^4)}{\frac{1}{F_{1-2}} + \left(\frac{1}{\epsilon_1} - 1\right) + \frac{A_1}{A_2}\left(\frac{1}{\epsilon_2} - 1\right)} \tag{5.4}$$

Through this equation the "surface configuration factor," f_{1-2}, is defined and used in AFFTAC to scale the radiative flux exchange. That factor,

$$f_{1-2} \equiv \frac{1}{\frac{1}{F_{1-2}} + \left(\frac{1}{\epsilon_1} - 1\right) + \frac{A_1}{A_2}\left(\frac{1}{\epsilon_2} - 1\right)} \tag{5.5}$$

is used in combination with the surface areas, Stefan-Boltzmann constant, and temperatures of the exchanging surfaces to predict the radiant heat flux on a per-area basis, i.e.,

$$q_{(1-2)} = f_{1-2}\sigma(T_1^4 - T_2^4) \tag{5.6}$$

In computing the radiative exchange between the inside tank wall and the liquid surface, 1 becomes "liquid" and 2 becomes "wall" to represent the tank wall. The emissivity of the tank wall is assumed to be 0.8 when using the Basic TPS Model but you may change that in the **Edit Tank Car Properties** window. When using the Advanced TPS Model, you are allowed to specify that value when editing the TPS setup. The emissivity of the liquid surface is set in the **Edit Lading Properties** window, accessible through the Ladings Resource manager. A reciprocal relationship is used to compute $f_{wall-liquid}$.

To compute the view factor, $F_{liquid-wall}$ used in the above equation, the geometry of the liquid surface relative to the tank wall must be computed. Figure 5.4 shows a cross-section of the tank. The area of the bottom quadrant is $\pi r^2/4$. The area of the gold region above that is $\theta r^2/2$. The area of the blue area is $r^2 \sin(\theta)\cos(\theta)/2$. Twice the sum of these three areas represents the entire area under the liquid surface. Therefore,

$$A_{liquid} = 2 \cdot \left[\frac{1}{4}\pi r^2 + \frac{1}{2} \cdot \theta r^2 + \frac{1}{2} r^2 \sin(\theta) cos(\theta)\right] = \frac{1}{2}\pi r^2 + \theta r^2 + r^2 \sin(\theta)\cos(\theta) \tag{5.7}$$

The ratio of this quantity to the total cross-sectional area (πr^2) is the same as the fraction of the tank volume occupied by the liquid, i.e.,

$$\frac{V_{liquid}}{V_{total}} = \frac{1}{\pi}\left[\frac{\pi}{2} + \theta + \sin(\theta)\cos(\theta)\right] \tag{5.8}$$

This equation is solved through trial and error during the simulation to determine θ at each point in time. From this value, the surface area of the liquid and the tank wall over it is computed. In addition, this value is used to determine whether or not liquid or vapor is adjacent to the pressure relief device.

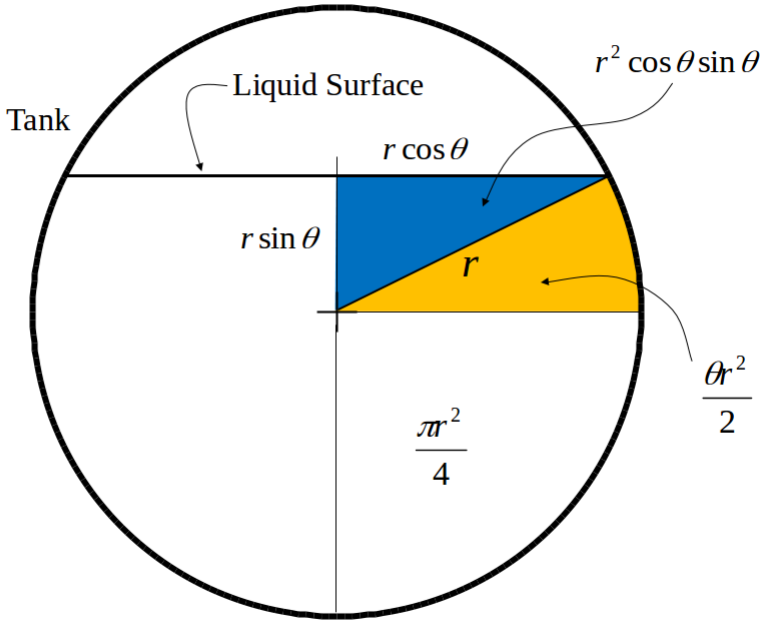

Figure 5.4: Geometry used to derive the equation relating the angle to the liquid surface endpoint to the fraction of tank filled with liquid

5.3 Temperatures of the Lading and the Tank Wall

5.3.1 Radiative Heat Exchange with the Tank Wall

As discussed above, a classical gray-body radiative exchange model is used between the innermost tank wall surface adjacent to the vapor and the surface of the liquid. That net flux, on a per-area basis, is

$$q_{(Rad-wall-liquid)} = f_{(wall-liquid)}\sigma\left(T^4_{wall-vapor} - T^4_{lading}\right) \tag{5.9}$$

The value of $f_{(wall-liquid)}$ is the surface configuration factor for the liquid lading surface and the tank wall above it as captured in Equation 5.5.

5.3.2 Convective Heat Exchange with Tank Wall

A standard engineering model is used for the convective heat exchange between the vapor and the innermost tank wall surface adjacent to it. For heat flux on a per-area basis, that model is

$$q_{(Conv-wall-vapor)} = h(T_{(wall-vapor)} - T_{lading}) \tag{5.10}$$

where h is the film coefficient.

> Aside
> The h film coefficient is difficult to estimate since it represents fluid flow that can take on a variety of forms. Film coefficients spanning an order of magnitude are reported in the literature depending on the properties of the liquid, whether or not boiling is present at the interface, and the geometry of the interface (e.g., see [17]). An indication of a representative value to use for this parameter can be inferred from the results of the full-scale fire test on a tank car filled with propane [20]. The results of this test indicated that the average conductance over the surface of the car was $300\left[\frac{\text{BTU}}{\text{hr}\cdot\text{ft}^2\cdot\text{R}}\right]$. The conductance of the 5/8 in. thick steel wall can be estimated at approximately $500\left[\frac{\text{BTU}}{\text{hr}\cdot\text{ft}^2\cdot\text{R}}\right]$, which implies that the conductance for the film would be about $750\left[\frac{\text{BTU}}{\text{hr}\cdot\text{ft}^2\cdot\text{R}}\right]$. A value of $1000\left[\frac{\text{BTU}}{\text{hr}\cdot\text{ft}^2\cdot\text{R}}\right]$ is recommended as a conservative representative value. When only vapor is present, the convection coefficient is set to approximately $1.0\left[\frac{\text{BTU}}{\text{hr}\cdot\text{ft}^2\cdot\text{R}}\right]$ but varies with fill and venting status. The proprietary document *Programmer's Guide to the Computational Module's Unit Tests* contains more information on this topic (see the note in Section 2.1 of this manual).

In both the legacy and new, generalized TPS model, the convective heat transfer is modeled as an additional "virtual layer" of resistance, because it has exactly the same mathematical form as a heat conductance model (linear in the temperature difference).

5.3.3 Temperature Change in the Tank Wall Adjacent to the Vapor

In both of the heat flux terms in the preceding two subsections, the value for $T_{wall-vapor}$ is considered known. But, as discussed at the beginning of this chapter and shown in Figure 5.2, it is determined by considering the heat balance on that part of the tank wall. The net heat flux is the heat entering the wall from the outside minus the heat leaving the wall and going into the lading. The difference in those fluxes is used to evolve $T_{wall-vapor}$ over time as follows:

$$m_{wall-vapor}\frac{dT_{wall-vapor}}{dt} = q_{TPS-vapor} - q_{Rad-wall-liquid} - q_{Conv-wall-vapor} \tag{5.11}$$

where each term is on a per-area basis, including $m_{wall-vapor}$, which is the thermal mass of the tank wall over the vapor space, on a per-area basis. It is the product of its density and specific heat.

Clearly, the last two heat flux terms are the very ones in the preceding subsections that depend on $T_{wall-vapor}$. This is not surprising because all of these variables are, in fact, linked simultaneously in time. But as has been mentioned multiple times at this point in the manual, these linked governing equations are split and solved in pieces. Thus, using $T_{wall-vapor}$ and other values from the previous time step, $q_{Rad-wall-liquid}$ and $q_{Conv-wall-vapor}$ are computed. Those values are then used to update $T_{wall-vapor}$ and other variables as well, such as T_{lading}.

In Figure 5.2 and the above equation, $q_{TPS-vapor}$ is the heat conducted from the outer part of the TPS into the tank wall. Along with its counterpart in the liquid region, $q_{TPS-liquid}$, it is a principle output of the TPS models and its computation is described in detail later.

5.3.4 Temperature Change of the Lading and Tank Wall Adjacent to the Liquid

As already mentioned, AFFTAC assumes the vapor and liquid temperatures are equal and the tank wall adjacent to the liquid is at the same temperature as the liquid. The liquid phase of the lading and the part of the tank wall adjacent to it are lumped into one thermal mass denoted here as $M_{liquid+wall(adjacent)}$. The mass of the vapor is negligible by comparison and although it could be included in principle, it is neglected here. The net flux into the lading is

$$\begin{aligned} Q_{net} &= A_{wall-liquid} \cdot q_{TPS-liquid} \cdot \text{Fraction Engulfed} \\ &+ A_{wall-vapor} \cdot q_{Rad-wall-liquid} + A_{wall-vapor} \cdot q_{Conv-wall-vapor} \end{aligned} \tag{5.12}$$

The first term on the right-hand side is the conductive exchange between the tank wall and the liquid, which is scaled by the area of contact between the liquid and tank wall, $A_{wall-liquid}$. It is one of the primary outputs of the TPS model. If you refer to the theory sections for both the Basic and Advanced TPS models, you will see sections where the computation of that quantity is described. Keeping in mind that the thermal model is one-dimensional, the "Fraction Engulfed" term is used to represent the fact that some of the tank may not be engulfed in the flame. It changes depending upon whether a pool fire or a torch fire is being considered.

During times when the pressure relief device is open and lading is being expelled, the amount of work, W_{flow}, performed by pushing part of itself through the device is subtracted from Q_{net}. Also, the latent heat of vaporization for the expelled lading is subtracted. Thus the temperature change is given by

$$M_{liquid+wall(adjacent)} \frac{dT_{lading}}{dt} = Q_{net} + W_{flow} - \dot{m} H_f \tag{5.13}$$

Here, $M_{liquid+wall(adjacent)}$ is the thermal mass and H_f is the latent heat of vaporization.

> Aside
> Modeling the tank wall over the vapor space and liquid each as having a uniform temperature is based on the assumption that the conditions are uniform on the respective inside surfaces of the tank. This assumption is not strictly without consequence because the temperature of the inner wall surface could be colder for regions close to the liquid's surface. The temperature would depend on the length of time the wall has been exposed to the vapor and also the amount of radiant energy that has been received from the hotter part of the wall. Uniform conditions will be closely approached when the liquid level is near the top of the tank, because a slight drop in the liquid level will expose a large area of the inner surface of the tank. Uniform conditions will also be approached when the level of the liquid is low. Although the transient difference in temperature may be larger when the liquid level is near the center of the tank, calculations show that the difference would only have a small effect on the total heat transfer.

5.3.5 Additional Heating Mechanisms

Although AFFTAC models the tank car as a perfect cylinder, in reality, there are other connections to the tank that can enhance heat transfer to it; these were originally referred to as "discontinuities" in the thermal protection system. While those are not modeled explicitly, AFFTAC does allow you to enter a factor that helps accommodate their effects. The selection is made in the **Edit TPS** window and is labeled **Consider Discontinuities**. If you select that option, you can then enter a value for a constant, which is referred to as the "USum" value. That constant is multiplied by the difference between the tank wall's outer and inner temperatures to compute an additional heat conduction mechanism into the lading. Typical "U" values for different "discontinuities" in the TPS are shown in Table 5.1.

Note that the use of special insulation on the components in Table 5.1 could reduce their "U" value. AFFTAC accepts a single value that represents the sum of the above applicable values. A value of 234 BTU/hr deg-F is the default in AFFTAC, which is more conservative since a higher value results in more heat transferred to the tank.

Component Considered	"U" Value (BTU/hr-deg-F)
Manway Nozzle and Manway Cover	14.6
Siphon and Air Vent Nozzle	6.1
Safety Relief Valve Nozzle	3.2
Jacket Spacers	15.5
Bottom Outlet Saddle	13.1
Draft Sills (2, one each end of car)	72.9
Body Bolsters (2, one each end of car)	65.0
Brake Cylinder Support	4.6
Brake Rod Lever Support	3.2

Table 5.1: This table of USum values, an input into AFFTAC.

Chapter 6

Modeling Ladings with the Ladings Resource

Ladings are modeled using multiple thermodynamic properties, including specific heat, specific volume, vapor pressure, heat of vaporization, and more. Furthermore, each of those properties are often functions of temperatures and are therefore represented as tabular data. Thus, there are several numerical values associated with any lading. In AFFTAC, all of those values are collected together and referred to using a single name, such as “Butane” or “Propane”, when setting up a simulation. When the simulation is run, AFFTAC extracts the appropriate thermodynamic data for that lading and writes it to a file for the Computational Module to read.

Each lading, as described above, is part of a bigger collection of data for multiple ladings, in what is together referred to as the “Lading Resources”. Part of setting up an AFFTAC simulation is ensuring that the properties for the lading you are modeling are present in the Ladings Resource list, that the values for that lading are approproriate, and making the necessary changes and additions. This chapter addresses that process.

The Ladings Resources may be edited by choosing the **Resources-Ladings** menu option in the **Main Window**, or by clicking the **Manage Ladings** button in the **Setup Lading** window, which is displayed during the editing of an analysis.

When you choose to manage the Ladings Resources, a window like that shown in Figure 6.1 is displayed. In this window, ladings can be edited by highlighting them and clicking the **Edit** button. New ladings can be created by either highlighting an existing one and clicking **Copy** then **Paste**, which creates a copy of the highlighted lading, or by clicking **New**, which creates a new lading from scratch.

6.1 Using Default Ladings

The first three entries in the Ladings Resource list are referred to as “default ladings”. These cannot be used for an analysis but instead serve as a template from which new ladings can be created when not all of the thermodynamic properties are known. The process for creating a new lading from a default lading is similar to creating one from any other existing lading. Simply highlight the default lading of interest, click **Copy** and then click **Paste**. However, when pasting from a default lading, the dialog box shown in Figure 6.2 appears. This window asks for the name of the new lading, the molecular weight, and the density at ambient. The creation of the new lading cannot proceed without these values. The use of default ladings is not recommended. If they are used, you should understand how their thermodynamic properties were chosen, as described in Appendix B.

6.2 Editing Pure Substances or Simple Binary Mixtures

When you double-click a lading or highlight it and then click the **Edit** button, the **Edit Lading** window like those shown in Figure 6.3 appears. This multi-faceted window allows for the input of the thermodynamic properties of the

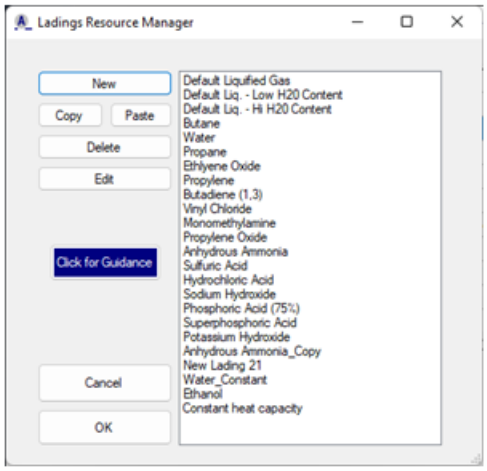

Figure 6.1: The window used for managing the Ladings Resource

lading.

The **Edit Lading Properties** window changes its appearance depending upon the options chosen. The most significant change is when you select the **Substance** or **Solution** option. Here "substance" means a pure substance, comprised of only one constituent. A "solution" here means a binary solution only, i.e., that which is comprised of two different constituents.

Returning now to the pure substance or simple binary solution model, in the upper window of Figure 6.3, we see that the Substance option is chosen. In this mode, you need only enter thermodynamic properties for the substance. In the lower part of Figure 6.3, is the same window with the Solution option chosen, where you are required to enter some of the thermodynamic properties for the solvent and solute at high and low concentrations. To the extent possible, those concentrations should bracket the solution concentration used in the analysis. Inaccuracies can result from the bracketing being too wide. Also see Appendix A.

You may enter any of the lading's thermodynamic properties as a constant or as a function of temperature. If they are a constant, the values are simply typed into the associated entry box. AFFTAC converts that constant value into a table of two rows, each with the same value you entered. To enter properties that vary as a function of temperature, you must enter the data by first clicking the appropriate **Edit Table** button that appears next to the property name.

The bulk modulus entry represents the amount of pressure the liquid lading generates upon volumetric compression. It is only used if the "Dynamic Shell Full" model is selected in the **Edit Tank Car Properties** window; see subsection 4.1.2 for information and guidance on that model. The model is described fully in subsection 13.2.6.

Shown in Figure 6.4 is the **Property Entry** window for one of the lading's specific heat, as an example. The table may be edited by entering the values as a function of temperature. Note that you can cut and paste from Excel into this window, which can sometimes accelerate the process. By clicking on the plot itself, the plot is copied to the Microsoft clipboard and can then be pasted into a variety of Microsoft Windows applications such as PowerPoint and Word. All of the thermodynamic properties for the lading used in a simulation are written to the PDF report, when that report is requested (in the **File-Write to PDF** menu option in the **Main Window**).

Check the **Has Critical Temperature** box if there is an upper temperature limit for any of the lading's thermo-

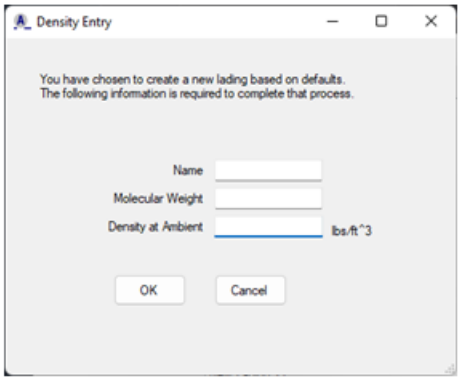

Figure 6.2: Dialogue box asking for additional information when creating a new lading from a default lading

dynamic properties' validity. The thermodynamic properties you enter for a lading are extremely important in AFFTAC calculations. If you are not confident of those values' validity past a certain temperature, check the box and enter that temperature. AFFTAC will stop the simulation if the lading's temperature reaches that temperature, which represent the onset of invalidity.

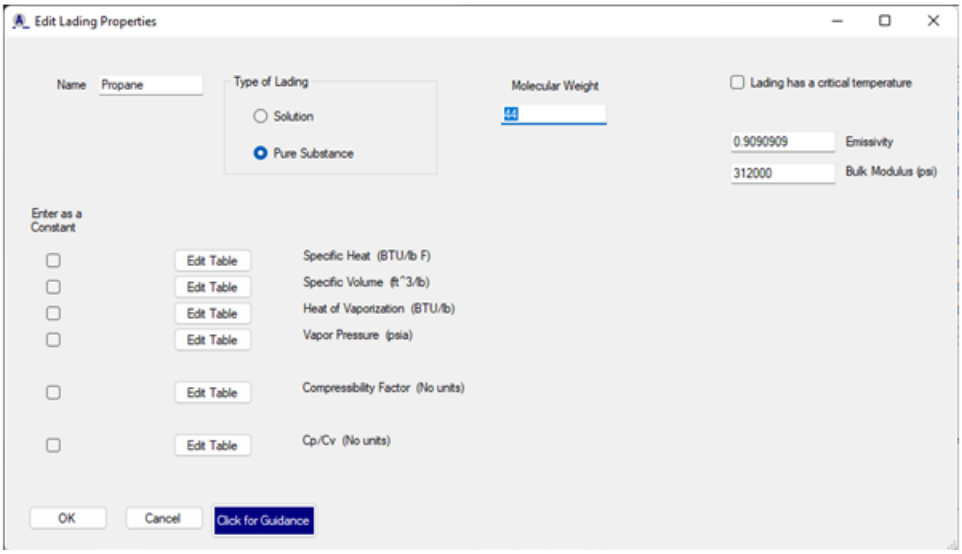

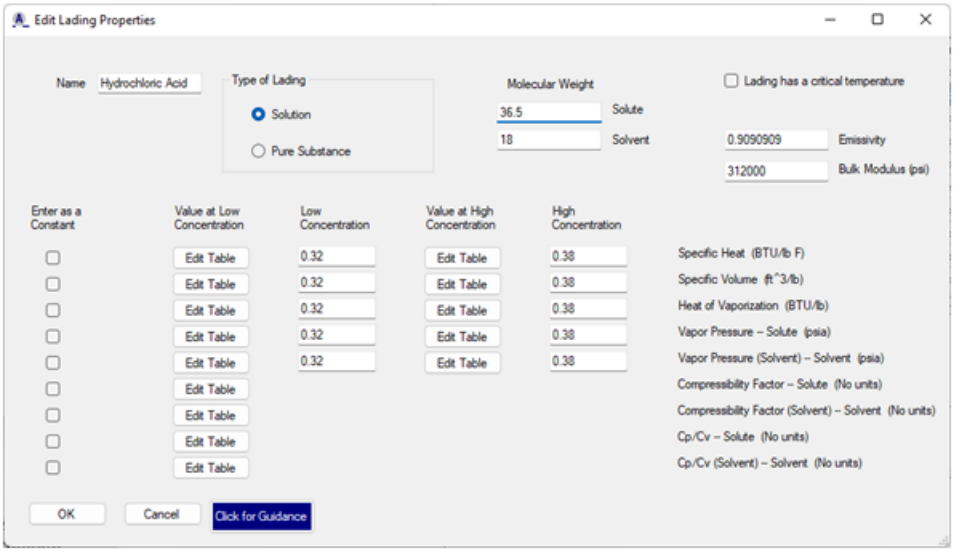

Figure 6.3: Example **Edit Lading Properties** window where the thermodynamics properties of the lading are entered for a pure substance (top) or simple binary solution (bottom)

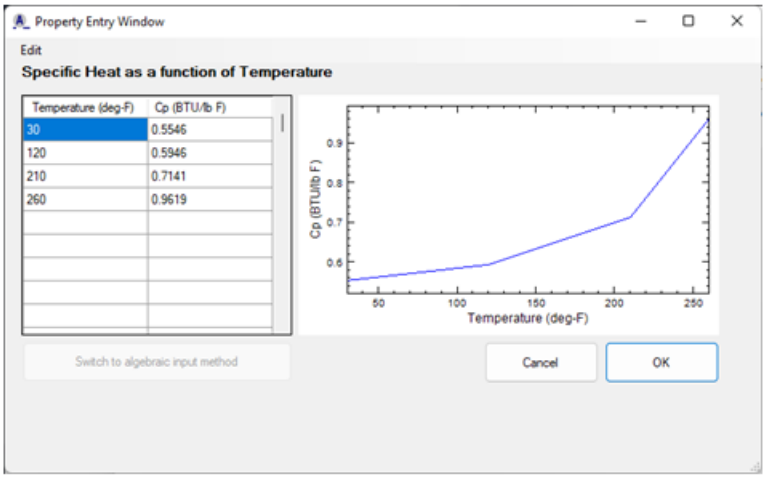

Figure 6.4: Example window for editing tabular input of thermodynamic properties

Chapter 7

AFFTAC's Basic TPS Model

There are two separate ways to model thermal protection systems (TPSs) in AFFTAC. You are required to choose one of them when setting up an analysis even if the tank is bare. The TPS model described in this chapter is the Basic TPS Model, which is the older of the two models. It provides important capabilities and also provides an important reference point for calculations that use the Advacned TPS Model, discussed in the next chapter. How to choose which to use is discussed in subsection **??**. Here we discuss the Basic TPS Model.

The inputs that specify the Basic TPS Model are grouped together and stored by name in the Basic TPS Model Resource list. Thus, each named entry in the Basic TPS Resource list represents multiple pieces of data. When setting up an analysis, the third editing window requires you to select which TPS model you want to use, the Basic TPS Model or the newer, Advanced TPS Model. If you select the Basic TPS Model, you will see the list of named entries in the Basic TPS Model Resource list. In that same window, you may launch a window from which you may edit the Basic TPS Model Resource list. You may also edit the Basic TPS Model Resource List from the **Main Window** by choosing the option **Resources-Basic TPS Model**.

7.1 Managing the Basic TPS Model Resource List

When you choose to manage the Basic TPS Resource, a window like that shown in Figure 7.1 is displayed. In this window, TPS setups can be edited by double clicking them or by highlighting them and clicking the **Edit** button. New Basic TPS Model setups can be created by either highlighting an existing one and clicking **Copy** then **Paste**, which creates a copy of the highlighted TPS, or by clicking **New**, which creates a new insulation using default values.

When you double-click a TPS or highlight it and then click the **Edit** button, the **Basic TPS Model Setup** window appears. This multi-faceted window provides opportunities to create and customize six different TPS types. Its appearance changes depending upon which type of TPS type is chosen. The next section describes those TPS types.

7.2 Setting up a TPS in the Basic TPS Model

The **Basic TPS Editing** window provides six different type TPS configujrations: Bare Tank, FRA Standard, Steel-Jacketed, Temperature-Independent, Temperature-Dependent, and Steel Jacketed (2-component). Those TPS types are summarized in Figure 7.2 and are discussed in more detail, below. There are also informative tests described in the *Programmer's Guide to the Computational Module's Unit Tests* document (see Section 2.1 of this manual for more information).

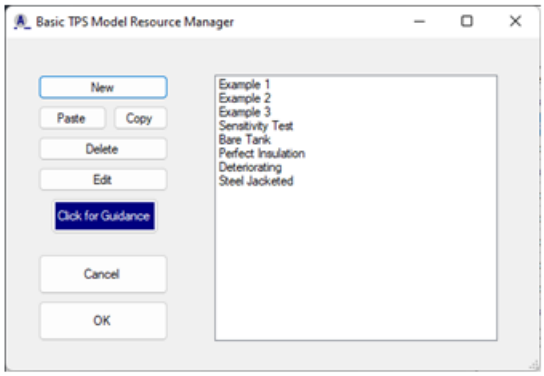

Figure 7.1: The Basic TPS Model Resource Manager

7.2.1 Bare

The “Bare” option simply means that the thermal protection system (TPS) consists entirely of the tank wall, plus the optional liner that can be added. The conductance of the tank wall is computed automatically from the material you select for the tank wall in the Basic Strength Model along with the thickness of the tank wall you specify in the analysis.

7.2.2 FRA Standard

This TPS sets an overall thermal conductance of 4.0 $\left[\frac{\text{BTU}}{\text{hr}\cdot\text{ft}^2\cdot\text{R}}\right]$ for the TPS, which is the maximum conductance that will pass the FRA performance test specified in Appendix B to CFR 179. Insulation systems that pass the test would likely have conductances that are less than this value.

7.2.3 Steel Jacketed

This option allows for an insulating layer with a time-varying conductance on the outside of the tank wall, where the tank wall conductance is computed as in the “Bare” option above. A jacket is placed outside the insulation such that there is an air gap between them. The coverage of the insulation is specified in the analysis, in the third window of the four-step editing process. Note that the coverage is averaged over the entire tank. If you want to specify an insulation defect as a function of position on the tank’s cross section, use the Advanced TPS Model, not the Basic TPS Model.

7.2.4 Temperature-Independent Insulation

This type of TPS uses an insulation that is constant with temperature but is allowed to change with time. The conductance of the insulation is combined in series with that of the tank wall, as in the “Bare” option, above. Two alternatives are offered, one where the conductance of the system is constant and the other where the conductance changes linearly over a given time period from an initial value to a steady-state value. The coverage of the insulating layer is set in the same way as in the Steel Jacketed TPS type, and has the same limitations.

7.2.5 Temperature-Dependent Insulation

The configuration of this TPS type is the same as the Temperature-Independent Insulation. The difference is that instead of specifying a time-dependent conductance, you specify a thermal conductivity that is a function of temepra-

ture, in particular:

$$k = k_1 + k_2 T + k_3 T^2 \tag{7.1}$$

Note that conductivity divided by thickness of the layer yields the conductance, which is the factor that determines the heat flux through the layer. Thus, since *conductivity* is specified here, you must also specify the layer's thickness.

Note also that conductivity typically has units of $\left[\frac{\text{BTU}}{\text{hr·ft·R}}\right]$. When conductivity is computed using the temperature-dependent form, temperature is in thousands of [deg-F] ([deg-R]) and length is in feet. So the units of conductivity are, in the Computational Module, $\left[\frac{\text{BTU}}{\text{hr·ft·thousands of·R}}\right]$. The k_1 parameter has those units while the other two parameters have units that accommodate the temperature function that multiplies them. In summary, see Table 7.1. The resulting conductance of the insulation is combined with that of the tank wall as is computed in the "Bare" option. The coverage of the insulating layer is set in the same way as in the Steel Jacketed TPS type, and has the same limitations.

Parameter	Units
k1	BTU/(hr-ft-(thousands of deg-F))
k2	BTU/(hr-ft-(thousands of deg-F)^2)
k3	BTU/(hr-ft-(thousands of deg-F)^3)

Table 7.1: This table shows the units of the coefficients used in the temperature-dependent insulation of the Basic TPS Model.

7.2.6 Steel Jacketed (2 component) Insulation

This option combines the Steel Jacketed option and the Temperature Dependent option, making the time-varying conductance layer the outer layer while the temperature-dependent layer is the inner layer. The conductances of these layers are combined with that of the tank wall, as discussed in subsection 7.2.1. The coverage of the insulating layers is set in the same way as in the Steel Jacketed TPS type, and has the same limitations.

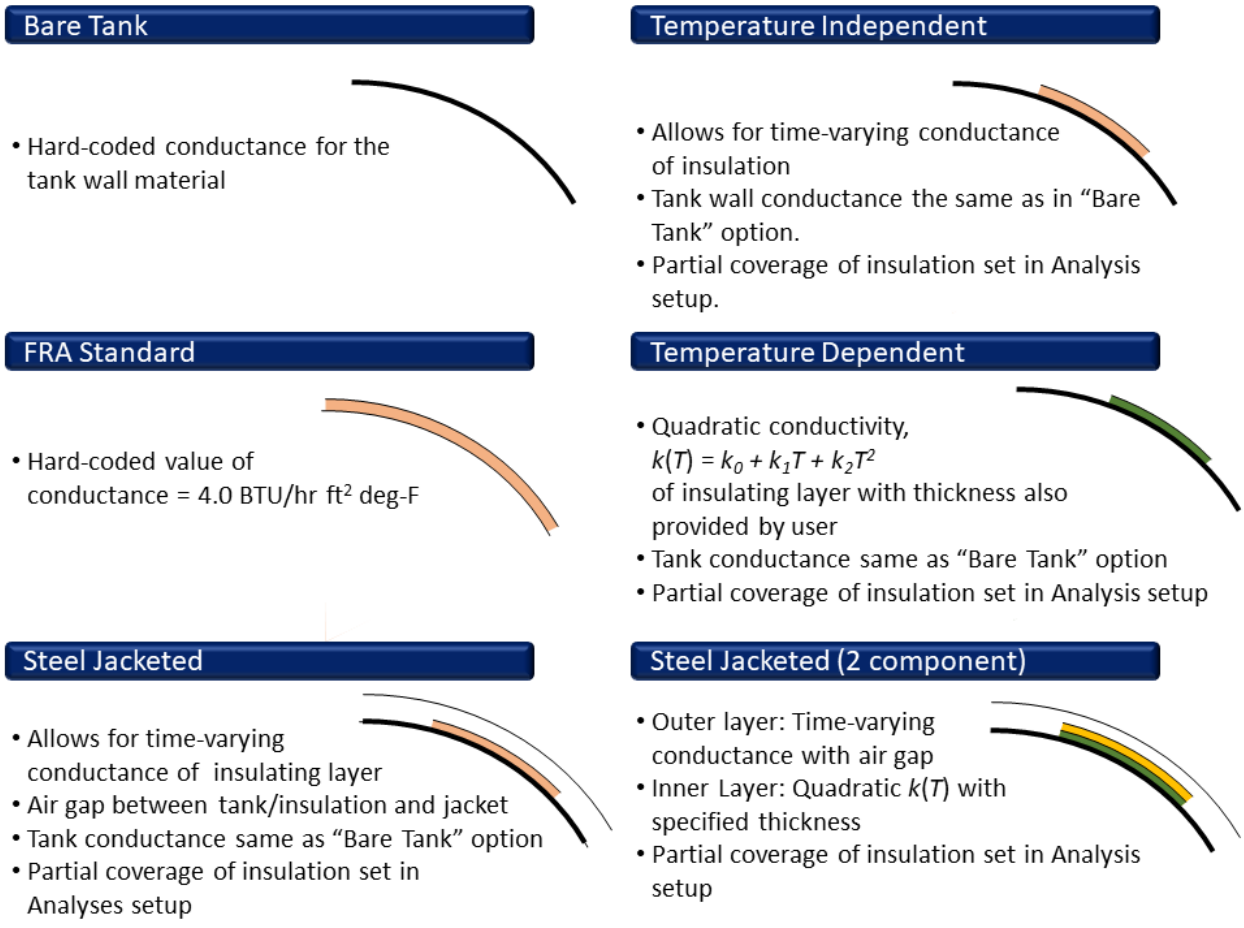

Figure 7.2: Summary of options provided by the Basic TPS Model.

7.3 Basic TPS Model Theory

Before attempting to understand the theory for the Basic TPS Model, it is highly recommended that you read chapter 5. The material there will help you understand how the calculations in the TPS model fit into the overall solution process and also some of the parameters used in the model description.

As discussed in that chapter, the primary role of the TPS model is to compute the heat flux through the TPS. The Basic TPS Model operates in two modes, one in which the tank is bare or perhaps partially covered by an insulating layer and another mode in which an air gap exists between the insulated tank and a steel jacket. Although all of the underlying assumptions and approaches are the same for the two modes, it is convenient to describe them separately.

The overall thermal model discussed in Chapter 5 has certain constructs, such as the fact that the lading is a uniform temperature and that same temperature is shared by the part of the tank wall adjacent to the liquid. Likewise, the Basic TPS Model has certain constructs. The most important one is that it assumes the tank's outermost surface can have up to four distinct temperatures. Since partial insulation coverage is modeled, different outermost temperatures exist for the regions with insulation compared to those regions without insulation. Also, both of those regions may exist in the part of the tank adjacent to the vapor or the liquid. Thus four combinations result, as listed in Table 7.2. And to solidify these definitions, the temperatures are shown in Figure 7.3 for the two different cases (jacketed and non-jacketed). Notice in both cases that there is one temperature for the lading, both vapor and liquid, and that same temperature is the temperature of the interior tank wall adjacent to the liquid.

Adjacent to	Insulation Present?	Outermost Temperature in that Region
Liquid	Yes	$T_{outer-Ins-liquid}$
	No	$T_{outer-noIns-liquid}$
Vapor	Yes	$T_{outer-Ins-vapor}$
	No	$T_{outer-noIns-vapor}$

Table 7.2: The four outermost temperatures in the Basic TPS Model when a steel jacket is not present.

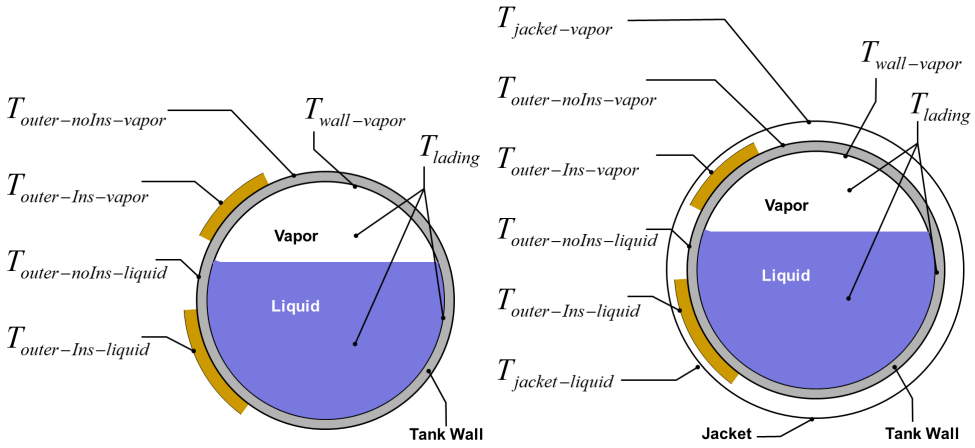

Figure 7.3: Temperature definitions for the case of an unjacketed (Left) and jacketed (Right) TPS

7.3.1 Bare Tank or Non-Jacketed Tank with Partial Insulation Coverage

Although a bare tank may perform and appear very different than a tank with insulation, from the Basic TPS Model's standpoint, the two cases are identical in structure. Specifically, the heat transfer from the inside of the tank wall to the outermost surface is equal to the temperature difference on those two surfaces times a thermal conductivity, divided by a thickness. Granted, the conductivity in the bare tank case will be much higher than in the insulated case, but that does not change the fact that the equations are the same form.

And so, in AFFTAC, the bare tank and insulated tank are treated exactly the same way, with different values for conductivity. The treatment is a heat balance on the outermost surface that accommodates areas with and without insulation. The equations are of the same form for all the regions:

$$\sigma\epsilon_f f T_f^4 - \sigma\epsilon T_{outer}^4 + c(T_{outer} - T_{inner}) = 0 \tag{7.2}$$

where T_f is the flame temperature, c is thermal conductance, and ϵ_f is the emissivity of the fire. The value for c and the other variables take on the following meanings in the different regions to which the equation is applied, as shown in Table 7.3.

Adjacent to	Insulation Present?	T_{outer}	T_{inner}	c
Liquid	Yes	$T_{outer-Ins-liquid}$	T_{lading}	$c_{Tank+Ins}$
	No	$T_{outer-noIns-liquid}$	T_{lading}	c_{Tank}
Vapor	Yes	$T_{outer-Ins-vapor}$	$T_{wall-vapor}$	$c_{Tank+Ins}$
	No	$T_{outer-noIns-vapor}$	$T_{wall-vapor}$	c_{Tank}

Table 7.3: The values that the variables in Equation 7.2 take on for the four regions of the tank wall present in the Basic TPS Model when a steel jacket is not present.

The nonlinear equation is solved four times, twice for the tank wall adjacent to the liquid and twice for the tank wall adjacent to the vapor. The reason AFFTAC makes the distinction between the liquid and vapor regions was explained in Chatper 3, but is worth reviewing here. When the liquid lading is touching the tank wall, it provides a great deal of thermal mass in intimate contact with the tank wall. Therefore, the tank wall touching the liquid is assumed to be at the same temperature as the liquid. However, the tank wall adjacent to the vapor has no intimate contact with a large thermal mass. Thus it can be at a different temperature from the lading.

Once the outermost surface temperature is determined for the four regions in Tables 7.2 and 7.3, it is used in combination with the appropriate innermost surface temperature to compute the heat flux into the innermost layer via conduction

$$q_{region} = c(T_{outer} - T_{inner}) \tag{7.3}$$

which is simply the third term in Equation 7.2. Thus, for the four combinations considered, heat fluxes computed are as shown in Table 7.4.

To compute the total average flux through the tank wall for the liquid and vapor regions, the fluxes for those regions in the parts that do and do not have insulation are combined using a weighted average:

$$\begin{aligned} q_{TPS-liquid} &= q_{Ins-liquid}F_{Ins} + q_{noIns-liquid}(1 - F_{Ins}) \\ q_{TPS-vapor} &= q_{Ins-vapor}F_{Ins} + q_{noIns-vapor}(1 - F_{Ins}) \end{aligned} \tag{7.4}$$

where F_{Ins} is the fraction of insulation coverage.

Adjacent to	Insulation Present?	q_{region}
Liquid	Yes	$q_{Ins-liquid}$
	No	$q_{noIns-liquid}$
Vapor	Yes	$q_{Ins-vapor}$
	No	$q_{noIns-vapor}$

Table 7.4: The heat fluxes computed by Equation 7.3 for the four regions in the Basic TPS Model when a jacket is not present.

7.3.2 Partial Insulation Coverage Inside the Jacket

In this case, the model accommodates a variable amount of coverage from the insulation that is between the steel jacket and the tank wall.

The model assumes that the steel jacket is so thin that it does not support a temperature gradient, i.e., it is a uniform temperature T_j. The heat transfer equation is solved twice, once for the part of the tank wall touching the liquid, and once for where it is touching the vapor.

Analogous to the previous subsection, the governing equation can be written once and applied to multiple regions by appropriately defining the variables. When solving for the part of the tank wall adjacent to the liquid, the inner temperature of the tank wall T_i is set to T_{lading}. When solving for the part of the tank wall adjacent to the vapor, the inner temperature of the tank wall is set to $T_{wall-vapor}$. When solving for the liquid region, the solution obtained for $T_{outer-Ins}$ is used for $T_{outer-Ins-liquid}$ and the solution obtained for $T_{outer-noIns}$ is used for $T_{outer-noIns-liquid}$. The exact analogy is used for the vapor region.

The following equation represents the heat balance on the jacket:

$$\sigma\epsilon f T_f^4 - \sigma\epsilon T_j^4 - \sigma\left(\frac{\epsilon}{2-\epsilon}\right)T_j^4 + \sigma\left(\frac{\epsilon}{2-\epsilon}\right)T_{outer-noIns}^4(1-F_{SP}) + \sigma\left(\frac{\epsilon}{2-\epsilon}\right)T_{outer-Ins}^4 F_{SP} = 0 \quad (7.5)$$

This is the heat balance on the bare tank surface:

$$\sigma\left(\frac{\epsilon}{2-\epsilon}\right)T_j^4 - \sigma\left(\frac{\epsilon}{2-\epsilon}\right)T_{outer-noIns}^4 - C_w(T_{outer-noIns} - T_i) = 0 \quad (7.6)$$

And this is the heat balance on the insulation surface:

$$\sigma\left(\frac{\epsilon}{2-\epsilon}\right)T_j^4 - \sigma\left(\frac{\epsilon}{2-\epsilon}\right)T_{outer-Ins}^4 - \overline{C}(T_{outer-Ins} - T_i) = 0 \quad (7.7)$$

In the above equations, σ is the Stefan-Boltzmann constant, and the f parameters are the surface configuration factors. The surface configuration factors rely upon the emissivities, geometric view factors, and areas of the surfaces involved (see Equations 5.2-5.6). The C_w and $\overline{C}$ are thermal conductances of the wall and wall+insulation, respectively.

The unknowns in the above equations are T_j, $T_{outer-Ins}$, and $T_{outer-noIns}$. To solve the equations using the Newton-Raphson method, first the left-hand-side of the equations are given names, f_1, f_2, and f_3:

$$f_1 \equiv \sigma\epsilon f T_f^4 - \sigma\epsilon T_j^4 - \sigma\left(\frac{\epsilon}{2-\epsilon}\right)T_j^4 + \sigma\left(\frac{\epsilon}{2-\epsilon}\right)T_{outer-noIns}^4(1-F_{SP}) + \sigma\left(\frac{\epsilon}{2-\epsilon}\right)T_{outer-Ins}^4 F_{SP} \quad (7.8)$$

$$f_2 \equiv \sigma\left(\frac{\epsilon}{2-\epsilon}\right)T_j^4 - \sigma\left(\frac{\epsilon}{2-\epsilon}\right)T_{outer-noIns}^4 - C_w(T_{outer-noIns} - T_i) \quad (7.9)$$

$$f_3 \equiv \sigma\left(\frac{\epsilon}{2-\epsilon}\right)T_j^4 - \sigma\left(\frac{\epsilon}{2-\epsilon}\right)T_{outer-Ins}^4 - \overline{C}(T_{outer-Ins} - T_i) \quad (7.10)$$

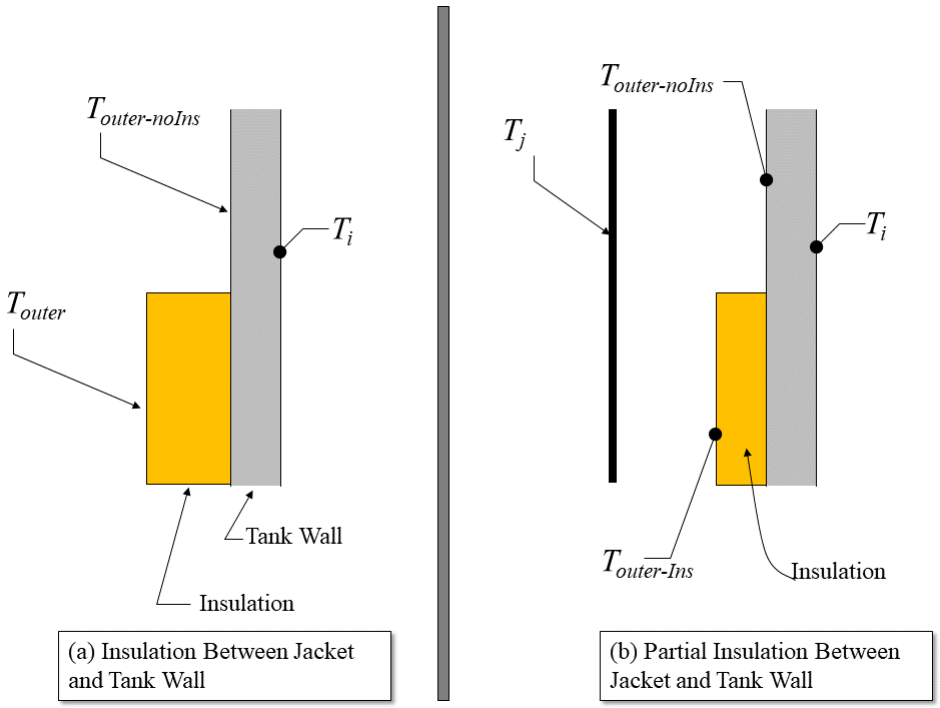

Figure 7.4: Heat exchange diagram for jacketed systems showing relevant nomenclature

Second, an array containing the three unknown temperatures and an array containing the three functions are defined:

$$\mathbf{T} \equiv \begin{bmatrix} T_j \\ T_{outer-noIns} \\ T_{outer-Ins} \end{bmatrix} \text{ and } \mathbf{f}(\mathbf{T}) \equiv \begin{bmatrix} f_1(T) \\ f_2(T) \\ f_3(T) \end{bmatrix} \tag{7.11}$$

The nonlinear system of three equations may now be expressed as follows:

$$\mathbf{f}(\mathbf{T}) = \mathbf{0} \tag{7.12}$$

The Newton-Raphson method of solving a nonlinear system such as that in Equation 7.11 is to start with an initial guess, $\mathbf{T}^0$ and then update that guess as follows:

$$\mathbf{T}^{i+1} = \mathbf{T}^i + \boldsymbol{\delta}^i \tag{7.13}$$

where $\boldsymbol{\delta}^i$ is the solution to the following linear system of equations:

$$\begin{bmatrix} \frac{\partial f_1}{\partial T_j} & \frac{\partial f_1}{\partial T_{outer-noIns}} & \frac{\partial f_1}{\partial T_{outer-Ins}} \\ \frac{\partial f_2}{\partial T_j} & \frac{\partial f_2}{\partial T_{outer-noIns}} & \frac{\partial f_2}{\partial T_{outer-Ins}} \\ \frac{\partial f_3}{\partial T_j} & \frac{\partial f_3}{\partial T_{outer-noIns}} & \frac{\partial f_3}{\partial T_{outer-Ins}} \end{bmatrix} \boldsymbol{\delta}^i = -\boldsymbol{f}(\boldsymbol{T}^i) \tag{7.14}$$

The right hand side is an array of three entries, which are the $\boldsymbol{f}$ functions evaluated at the previous guess. The matrix is comprised of partial derivatives of the three functions with respect to the different temperatures, also evaluated at the previous guess.

Working from Equations 7.8-7.10, the partial derivatives are as follows:

$$\begin{aligned}
\frac{\partial f_1}{\partial T_j} &= -4\sigma\epsilon T_j^3 - 4\sigma\left(\frac{\epsilon}{2-\epsilon}\right)T_j^3 \\
\frac{\partial f_1}{\partial T_{outer-noIns}} &= 4\sigma\left(\frac{\epsilon}{2-\epsilon}\right)T_{outer-noIns}^3(1-F_{SP}) \\
\frac{\partial f_1}{\partial T_{outer-Ins}} &= 4\sigma\left(\frac{\epsilon}{2-\epsilon}\right)T_{outer-Ins}^3 F_{SP} \qquad (7.15) \\
\frac{\partial f_2}{\partial T_j} &= 4\sigma\left(\frac{\epsilon}{2-\epsilon}\right)T_j^3 \\
\frac{\partial f_2}{\partial T_{outer-noIns}} &= -4\sigma\left(\frac{\epsilon}{2-\epsilon}\right)T_{outer-noIns}^3 - C_w \\
\frac{\partial f_2}{\partial T_{outer-Ins}} &= 0 \\
\frac{\partial f_3}{\partial T_j} &= 4\sigma\left(\frac{\epsilon}{2-\epsilon}\right)T_j^3 \\
\frac{\partial f_3}{\partial T_{outer-noIns}} &= 0 \\
\frac{\partial f_3}{\partial T_{outer-Ins}} &= -4\sigma\left(\frac{\epsilon}{2-\epsilon}\right)T_{outer-Ins}^3 - \overline{C} \qquad (7.16)
\end{aligned}$$

An initial guess is required to start the Newton-Raphson iterations. For all but the first time step, the solution from the previous time step is sufficient. But for the first time step, the initial guess is provided using an approximation. The geometric view factor for the flame-tank exchange is assumed to be unity except in the case of a torch fire where it is assumed to be 0.536. The geometric view factor for the jacket-wall exchange is unity.

7.4 Heat Flux Into Lading and the Tank Wall over the Vapor Space

Once the nonlinear system is solved to determine the temperatures on the outer surfaces, those values can be used to compute the flux as follows:

$$q_{TPS-liquid} = F_{SP}(T_{outer-Ins-liquid} - T_{lading})\overline{C} + (1-F_{SP})(T_{outer-noIns-liquid} - T_{lading})C_w \qquad (7.17)$$

$$q_{TPS-vapor} = F_{SP}(T_{outer-Ins-vapor} - T_{wall-vapor})\overline{C} + (1-F_{SP})(T_{outer-noIns_vapor} - T_{wall-vapor})C_w \qquad (7.18)$$

Here, $\overline{C}$ and C_w represent the conductivities for the regions with and without insulation.

7.5 Conductances for Multi-Layer TPSs

The thermal transport models described in the previous section rely heavily on composite conductances. Considering one-dimensional heat conduction through several layers, it is well known that the effective conductance, C, of the composite layer is related to the conductance, C_i, of each layer as follows:

$$\frac{1}{C} = \sum_{i=1}^{n} \frac{1}{C_i} \qquad (7.19)$$

where n is the number of layers. Here, each C_i represents a layer in the composite system. Those layers include the tank wall itself, but also insulation and tank linings. Although not shown explicitly in Figure 7.4, other layers may exist (such as a lining). Their conductance is used to modify the C_w using the equation above.

AFFTAC's Basic TPS Model accommodates different behaviors for the insulation layers and linings. For example, you can specify an amount of time during which some layers deteriorate. Also, you can specify a temperature-dependent conductivity. Note that conductivity is a material property and conductance is conductivity divided by thickness. In that case, a nonlinear system must be solved to determine the effective conductivity of the entire layer. As discussed earlier in this chapter, the conductivity may be expressed by the user as follows:

$$k(T) = k_1 + k_2 T + k_3 T^2 \tag{7.20}$$

To solve the heat conduction equation when the conductivity is of this form, the algorithm divides the insulation layer into 50 elements. It then starts at the inside of the layer and, using the previous value for the effective conductance and the heat flux that it allows, marches through the 50 elements computing the temperature distribution as it proceeds. When it arrives at the outside of the insulation, it checks to see if the temperature matches that predicted by using the previous effective conductivity. If it does not, the effective conductivity is adjusted and the process is repeated until convergence is achieved.

The other insulation behaviors in AFFTAC's Basic TPS Model accommodate different insulations used in tank cars. For example, rubber liners are used on some acid cars. They would initially offer a high value of insulation. A typical value for the conductivity of rubber is 0.1 $\left[\frac{\text{BTU}}{\text{hr·ft·R}}\right]$. This value would imply a conductance of 6.4 $\left[\frac{\text{BTU}}{\text{hr·ft}^2\text{·R}}\right]$ for a 3/16 in. thick rubber liner, which would provide a high degree of resistance to heat flow into the tank. It is likely, however, that the effectiveness of the rubber as a thermal insulator would soon be destroyed on cars that do not have any exterior insulation because the adjacent steel tank wall would soon be heated to over 1000 deg-F, which would melt the surface of the rubber in contact with it. Therefore, in an analysis of this condition, it is recommended that the rubber liner be considered to have an initial conductance of 6.4 $\left[\frac{\text{BTU}}{\text{hr·ft}^2\text{·R}}\right]$, but that this would be degraded linearly over a 15 minute period. The rubber liner on an insulated car is likely to remain effective for a much longer time because the exterior insulation would keep the tank wall at a moderate temperature.

Some cars have an organic coating on the inside of the tank. It would offer less resistance to heat flow than a rubber liner because of its small thickness. An estimate of its conductivity is 0.25 $\left[\frac{\text{BTU}}{\text{hr·ft·R}}\right]$, which implies a thermal conductance of 500 $\left[\frac{\text{BTU}}{\text{hr·ft}^2\text{·R}}\right]$ for a 6 mil thickness. Its effectiveness would be expected to be retained for a fairly long period of time because its conductance is high, which means the temperature of the inside of the tank wall would be close to the temperature of the lading. Thus, it is less likely to be damaged by high temperature.

Again, for all such liners, the C_w value is modified according to Equation 7.19. Values for the three liner options are given in the *Programmer's Guide to the Computational Module's Unit Tests document*. See Section 2.1 of this manual for more information.

Chapter 8

AFFTAC's Advanced TPS Model

This chapter discusses the scope and use of AFFTAC's Advanced TPS Model, which is a separate modeling option that can be chosen instead of the Basic TPS Model described in the previous chapter. The Basic TPS Model, although simpler and in many ways less flexible than the Advanced TPS Model discussed here, is important because it has been part of AFFTAC longer and, through its many uses, has undergone significant debugging and hardening. Which model to ultimately choose is discussed in subsection **??**.

The Advanced TPS Model offers several sophisticated advances over the Basic Model. Because of its complexity, it has also undergone significant testing as described in the accompanying *AFFTAC Verification and Validation Test* document and the *Programmer's Guide to the Computational Module's Unit Tests*. The capabilities of the Advanced TPS Model include:

1. The ability to accommodate an arbitrary number of material layers in the TPS,

2. Each layer of the TPS can have an arbitrary coverage (defects) that varies as a function of position around the tank,

3. Each layer of the TPS may have its thermal conductivity specified using tabular data or quadratic algebraic form,

4. Each layer of the TPS may undergo a change of phase at a certain temperature wherein the thermal conductivity is described by a different table.

These capabilities are partially represented in Figure 8.1, which highlights the fact that each layer can have multiple thermal conductivity curves, and Figure 8.2, which highlights how the amount of material present (its "coverage") can vary as a function of angle around the tank car.

8.1 How to Access the Advanced TPS Model

While editing an analysis, the third window of the four-window editing sequence requires you to choose either the Basic TPS model or the Advanced TPS Model. If you choose the Advanced TPS Model, you will see the list of previously established TPS setups for that model. You may select one of the setups in the list for your analysis. Also, you may edit that list of setups by clicking the **Manage Advanced TPS Models** button. You may also manage the Advanced TPS Resources by choosing the **Main Window** menu option **Resources-Advanced TPS Models**.

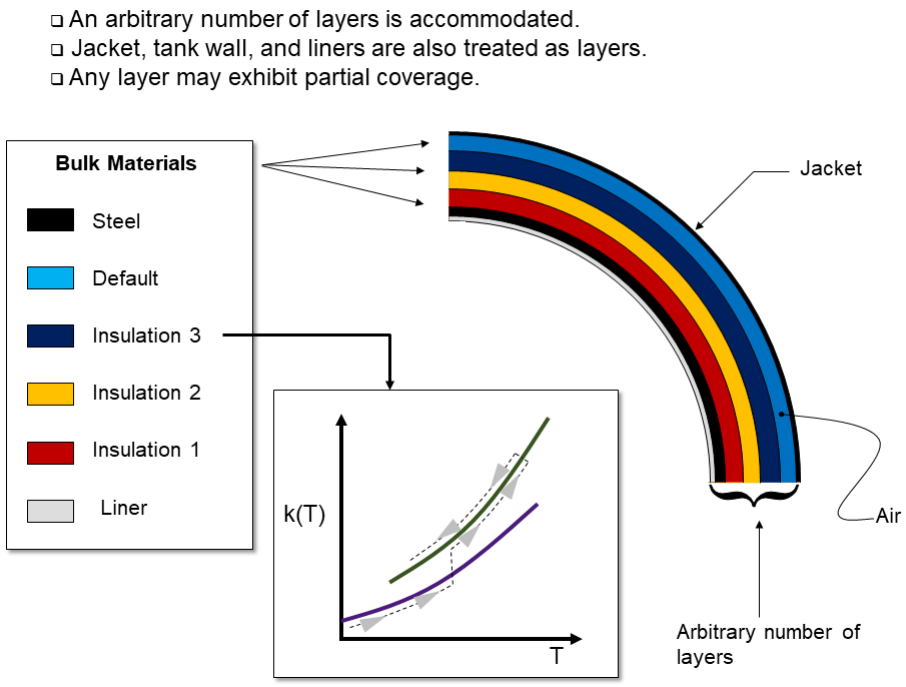

Figure 8.1: The Advanced TPS Model allows for an arbitrary number of layers. Each layer is characterized by thermal conductivity as a function of temperature, $k(T)$. Phase change, e.g., charring, is represented by switching from one $k(T)$ curve to another, permanently, as shown for one of the insulation layers.

8.2 How to Use the Advanced TPS Model

8.2.1 Basic Ideas

There are two key steps involved in setting up an Advanced TPS Model:

1. Add layers, or delete them if necessary, and
2. Provide the details regarding the makeup of each layer.

To accomplish the first step, hover over one of the existing layers in the graphics box, which is in the far right of the **Advanced TPS Setup Window** and right click. When you do, you will be given the option to add a layer on the inside or the outside of that layer. Once the layer is added, right click on it to provide its specifications, selecting **Edit this layer**. You must provide the following for the layer:

1. Its thickness,
2. The emissivity of its inner and outer surfaces, and
3. Its “coverage”, a quantity that is explained next.

In the Advanced TPS Model, you can specify TPS defects (gaps in the insulation) as a function of angle around the tank. You do that by modifying the “coverage” specification for the insulating layer(s). Coverage is a quantity that describes how much of the layer is present at a particular angular location. When coverage is 100%, the layer has no gaps and the only method of heat flow through it is conduction. When coverage is less than 100%, conduction occurs through the part of the layer present, while natural convection and radiation occurs where the layer is missing.

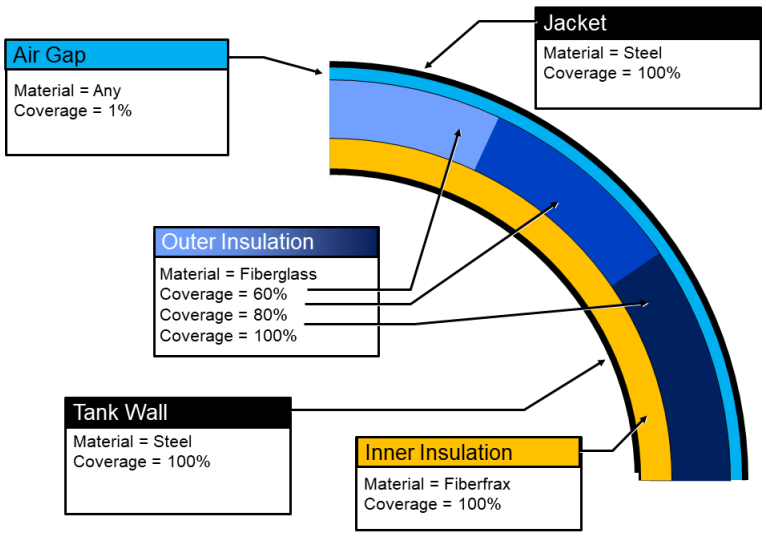

Figure 8.2: The Advanced TPS Model allows for the "percent coverage" of a layer to be specified by region. In this example, one of the insulating layers varies in its coverage. When a layer has defects, e.g., its coverage is less than 100%, radiation and convection can occur between the layers surrounding that defective layer.

AFFTAC allows for any value to be input for coverage. Clearly, insulation that is completely missing in one area of the tank is technically 0% coverage. For numerical reasons, it is necessary to instead enter a very small value for coverage, e.g., 1%, to represent missing insulation. But you can enter a value for 20%, 90%, etc., for insulation with defects. In those cases, AFFTAC assumes that the missing portions are evenly distributed in the region where that coverage is specified. For example, suppose you specify 90% coverage in the region between the top of the tank and half way down to the ground. In that case, conduction occurs across 90% of that area, while convection and radiation occurs in 10% of the area. AFFTAC inherently assumes that the voids, which are 10% of the area, are *not* gathered together in one place. Rather, AFFTAC assumes those voids are evenly distributed through the region (from the tank top to half way down, in this case). Figure 8.3 shows a conceptual five-layer TPS, each with its own coverage. Layers 2-4 have coverage less than 100%. As the illustration represents, AFFTAC not only assumes the voids are randomly distributed but, also as a consquence, that they are not necessarily aligned.

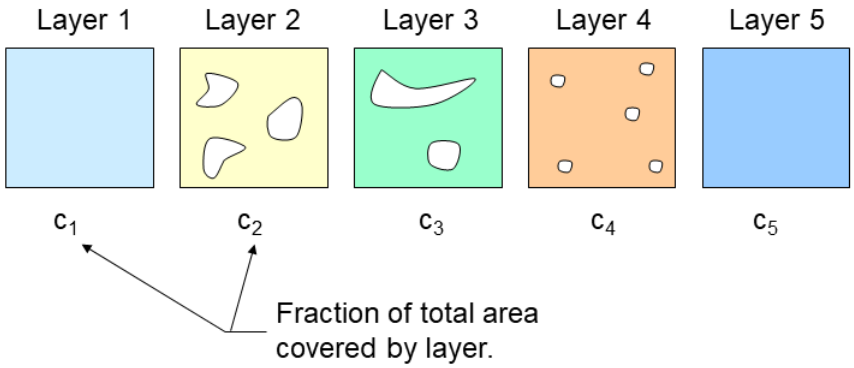

Figure 8.3: Illustration of a disassembled conceptual TPS, which each layer laid out separately thereby exposing the voids in each layer

How to Specify an Air Gap

If need to specify an air gap in your TPS, you must declare a layer and decrease its coverage to near 0%. Again, due to numerical reasons, 0% is not allowed, but 1% should suffice. Note that it is not possible to represent an air gap by adding a layer, calling it air, and entering the thermal conductivity of air for that layer. That is because the Advanced TPS Model does not allow convection or radiation through any layer, except where that layer has less than 100% coverage.

8.2.2 Using the Advanced TPS Setup Window

Shown in the top part of Figure 8.4 is the window for setting up Advanced TPS Models, and managing the list of models you already have as Resources. Toward the far left of that window, bulk materials are defined and, for each one, at least one table describing their thermal conductivity is specified. You can add to, delete from, or modify this list through the **Edit List of Materials** button. You also can add to, delete from, copy/paste, or modify any of the existing Advanced TPS Models in the list under the red "Thermal Protection Systems" banner in the middle of the window. And, as already mentioned, you can add, delete, and edit layers using a right click in the far-right graphics box.

8.2.3 Using the Edit TPS Layer Window

Whenever you choose to edit a layer through a right click in the TPS graphics window, a layer editing window like that shown in the bottom part of Figure 8.4 appears. In that window, you can change the name of the layer, specify the bulk material of which it is comprised, specify its thickness, and provide emissivity values for its inner and outer surfaces. The coverage of the layer is specified graphically by left-clicking and dragging your mouse. You can sweep out new coverage regions or adjust existing coverage regions by dragging the any of the blue balls (except those at the top and bottom which are fixed).

It is recommended that, when computing the percent coverage for an angular segment of the tank wall cross section, you use the minimum value along the axis of the tank. For example, suppose there is a region of insulation, 10 foot long (axially), that is missing toward the top of the tank. Instead of averaging the effect of the 10 foot long region, it is recommended that you imagine the 10 foot long region to extend the entire length of the tank, i.e., "sample" the cross section of the tank in the middle of the defect, and use those values for the coverage around the semicircule.

8.2.4 Using the Bulk Materials Editing Window

Whenever you choose to edit a specific bulk material, a window such as that in Figure 8.5 will appear. The purpose of this window is to allow you to enter values for the bulk material's thermal conductivity as a function of temperature, i.e., $k(T)$. Those values may be entered in tabular form or in quadatric form, and each bulk material is allowed to have multiple tables or quadratic represention because as the material is heated, it might change phase or deteriorate such that its fundamental conduction properties are permanently altered. For that reason, there is a *list* of conductivity tables/functions, where each one is activated at a specified temperature. Add to, subtract from, or modify that list of tables in this window. Double-clicking on any entry in that list allows you to enter the specific $k(T)$ values as a table or quadratic function.

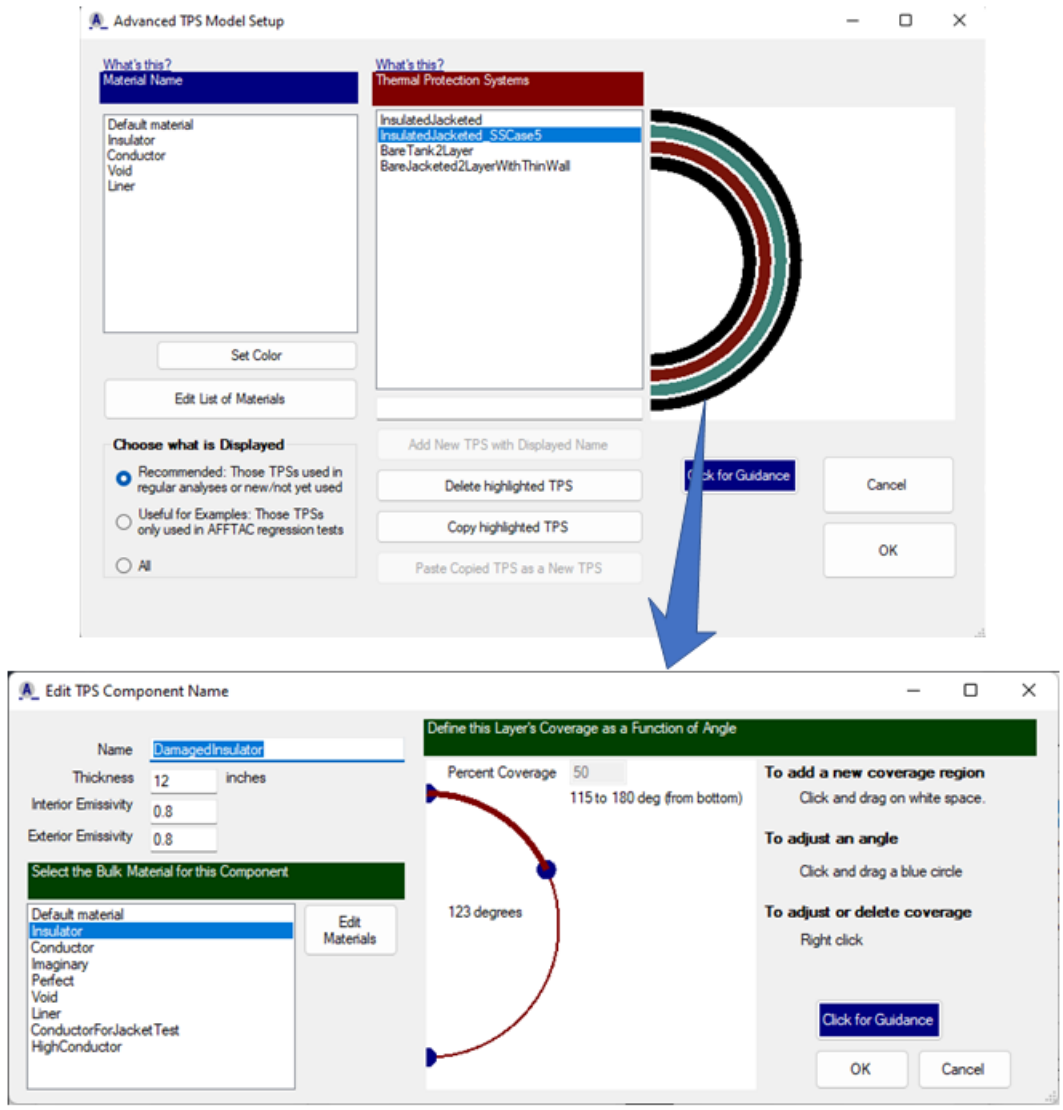

Figure 8.4: **Upper:** Main management and editing window for the Advanced TPS Model Database, **Lower:** Editing an individual layer.

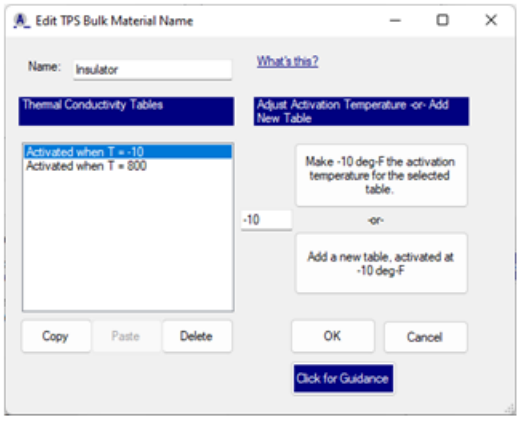

Figure 8.5: Editing a bulk material in the Advanced TPS Model allows you to establish multiple thermal conductivity curves that become activated at different temperatures. In this way, you can represent permanent, irreversible change of state in a material, e.g., charring of insulation.

8.3 Highlights of the Advanced TPS Model's Theory

Consider Figure 8.3, which shows each layer of a five-layer system as if the system had been disassembled, and each layer laid out side by side. As the figure shows, each of the inner layers may have a coverage value, c_i, less than unity. The voids in these layers affect how heat is transferred through the system, as illustrated in Figure 8.6, which shows that there are three temperatures at each material interface. One temperature is that of the area where the two adjacent layers are in contact. Specifically, T_2 is the temperature where Layer 2 and Layer 3 are in contact. T_{R2} is the temperature of Layer 2's right side that is exposed to convection and radiation with layers to its right. T_{L3} is the temperature of Layer 3's left side that is exposed to convection and radiation with layers to its left. A governing equation is required for each one of these areas.

The Advanced TPS Model makes the following assumptions:

1. The voids have a random size distribution, meaning that on average there is no pattern that would require voids to line up, thereby unduly exposing one layer to another layer several layers away. Instead, the exposure of each layer to other layers is gradually reduced by the coverage of the intermediate layers.

2. The voids are large enough such that lateral conduction (i.e., in the plane of Figure 8.3) need not be considered.

Because the Advanced TPS Model is designed to handle an arbitrary number of layers, each with an arbitrary amount of coverage, there is a non-trivial amount of nomenclature that must be established before the actual governing equations can be written. Appendix G describes that nomenclature and proceeds to give an exhaustive account of the governing equations and solution algorithm. Here, the equations are summarized so you can get a reasonably good understanding of the model's basic theory.

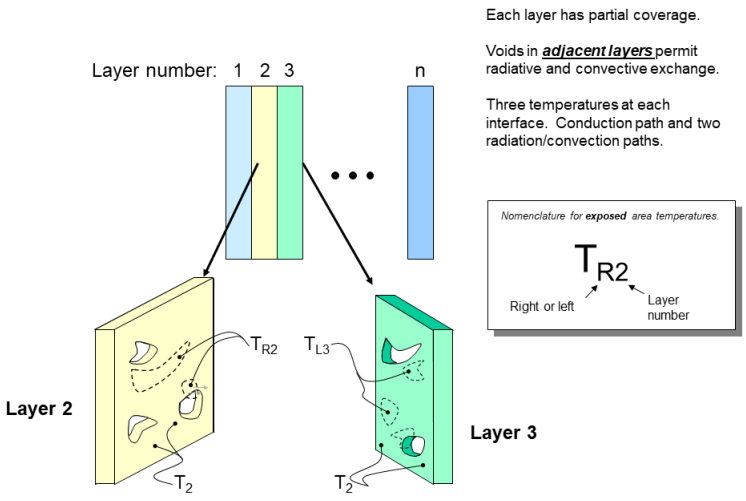

Figure 8.6: Illustration of a conceptual TPS with layer numbers, showing how the voids and non-void areas interact between layers, and establising the temperature nomenclature

8.3.1 Area in Contact

Interface i is the interface between Layer i and Layer $i + 1$. Since this area is in contact with two layers, conduction is the only mechanism for heat transfer. A heat balance on the interface states that the heat flowing into it must equal

the heat flowing out of it. That requirement is embodied in the following equation:

$$\frac{k_i}{w_i}A_i(T_i - T_{i-1}) + \frac{k_i}{w_i}A_{i,L}(T_i - T_{L_i}) + \frac{k_{i+1}}{w_{i+1}}A_{i+1}(T_i - T_{i+1}) + \frac{k_{i+1}}{w_{i+1}}A_{i,R}(T_i - T_{R_{i+1}}) = 0 \tag{8.1}$$

where k_i and w_i are the thermal conductivity and thickness, respectively, of layer i. Also, regarding A_i in the above equation, you can see some of the complexities of the nomenclature. In particular, there are area terms, "A" variables, that describe how much area is available for conduction. That value depends on the amount of coverage specified for the layers.

8.3.2 Right Side's Exposed Area

Consider again interface i, but this time, the part of that interface that is exposed due to a lack of coverage in Layer $i+1$. Heat conduction still occurs to the left, but radiative and convective heat transfer occurs to the right. Again, a heat balance on the interface states that the heat flowing into it must equal the heat flowing out of it. That requirement is embodied in the following equation, where heat conduction to the left is represented in the first terms and radiative plus convective heat flow is represented in the last terms:

$$\begin{aligned}\frac{k_i}{w_i}A_{i-1,R}(T_{R_i} - T_{i-1}) + \frac{k_i}{w_i}A_{L,R}(T_{R_i} - T_{L_i}) \\ + \sum_{k=i+1}^{n} A_{R_iL_k}h_{i,k}(T_{R_i} - T_{L_k}) \\ + \sum_{k=i+1}^{n} A_{R_iL_k}(T_{R_i}^4 - T_{L_k}^4)/(1/\epsilon_{R_i} + 1/\epsilon_{L_k} + 1) = 0\end{aligned} \tag{8.2}$$

Again, while not all of the nomenclature is defined here (it is in Appendix G), the above equation can still give you a feel for this part of the theory. Part of the heat leaving a surface that is exposed is due to conduction through its own layer; those are the first two terms. The third term represents the convective heat transfer between the exposed area and all of the other exposed areas it sees. Note that the value for the convective heat transfer coefficient within layers in the Advanced TPS Model is currently set to be 1.08 BTU/hr-ft-deg R. Keep in mind that there are an arbitrary number of layers, which explains why the summation sign is needed. The last term is the radiative exchange between the exposed area and all the other exposed areas it sees.

8.3.3 Left Side's Exposed Area

The equation for the left side's exposed area is exactly analogous to that for the right:

$$\begin{aligned}\frac{k_i}{w_i}A_{i,L}(T_{L_i} - T_i) + \frac{k_i}{w_i}A_{L,R}(T_{L_i} - T_{R_i}) \\ + \sum_{k=1}^{i-1} A_{L_iR_k}h_{i,k}(T_{L_i} - T_{R_k}) \\ + \sum_{k=1}^{i-1} A_{L_iR_k}(T_{L_i}^4 - T_{R_k}^4)/(1/\epsilon_{L_i} + 1/\epsilon_{R_k} + 1) = 0\end{aligned} \tag{8.3}$$

Again, the theory is thoroughly developed in Appendix G, and you are encouraged to explore that material.

8.3.4 Flux Computation

The key output of the TPS model is the flux into and through the innermost surface of the TPS, which may be a liner or the tank wall itself. Once all of the temperatures in Figure 8.6 and Equations 8.1-8.3 are known, the flux through and into the innermost surface is computed using the conduction term, i.e.,

$$q_{TPS-liquid} = \frac{k_1}{w_1}(T_{L_1} - T_{lading})$$
$$q_{TPS-vapor} = \frac{k_1}{w_1}(T_{L_1} - T_{wall-vapor}) \quad (8.4)$$

Chapter 9

AFFTAC's Basic Strength and Failure Model

There are two separate methods for modeling strength and failure of the tank wall in AFFTAC, the Basic Strength Model and the Advanced Strength Model. The Basic Model is described here while the Advanced Model is described in the next chapter. For guidance on which to choose, see subsection 4.6.3.

The Basic Strength Model is relatively straightforward to explain and use. You make the choice regarding which strength model to use in the **Edit Tank Car Properties** window, which is the second of the four-window editing sequence for any analysis. The upper right part of that window has two modes, one of which is displayed when using the Basic Strength Model and the other when using the Advanced Strength Model. The modes are toggled by clicking the button that says either **Switch to Advanced Strength Model** or **Switch to Basic Strength Model**. Figure 9.1 shows the window with the Basic Strength Model options displayed.

The Basic Strength Model is based on an estimate of the material's room-temperature ultimate tensile strength, which is a constant, multiplied by a factor that decreases with increasing temperature. More explicitly, in AFFTAC, the tensile strength of the tank wall material is

$$S(T) = S_r f(T) \tag{9.1}$$

where S_r is the hard-coded value of the material's ultimate tensile strength at room temperature and $f(T)$ is the multiplier that decreases with increasing temperature. Values of S_r are provided inside AFFTAC for twenty-seven different materials. And for each material, there is a hard-coded model for $f(T)$. Tables 9.1 - 9.3 on the subsequent pages show these models for each of the materials. The units in the tables are

$$\begin{aligned} T &: R^o/1000 \\ S_r &: \text{Kpsi} \end{aligned} \tag{9.2}$$

Note that the adjustment factor, $f(T)$, is not a function of time, meaning that it does not accommodate the widely observed phenomenon of creep.

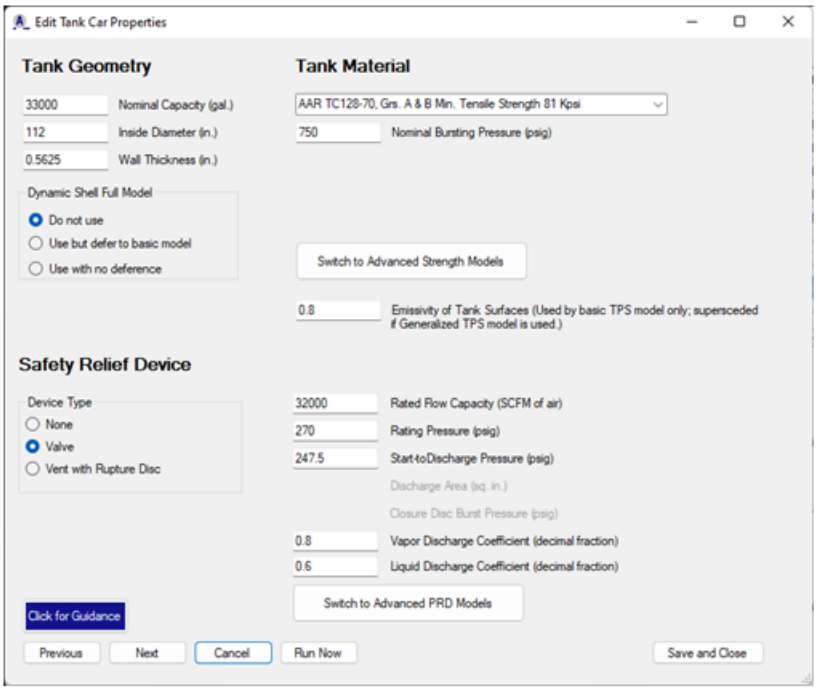

Figure 9.1: **Edit Tank Car Properties** window in which the Basic Strength Model is selected.

Carbon Steels			
ID	Description	S_r	Adjustment Factor
1	ASTM A 515-70, Gr. 55 Min.	55,000	$f = \begin{cases} 1 - 0.54(T - 0.460)^4 & T < 1.260 \\ 1.74 - 1.17(T - 0.460) & T > 1.260 \\ 0. & T > 1.947 \end{cases}$
2	ASTM A 515-70, Gr. 60 Min.	60,000	
3	ASTM A 515-70, Gr. 65 Min.	65,000	
4	ASTM A 515-70, Gr. 70 Min.	70,000	
5	ASTM A 285-70a, Gr. A Min.	45,000	
6	ASTM A 285-70a, Gr. B Min.	50,000	
7	ASTM A 286-70a, Gr. C Min.	55,000	
8	ASTM A 516-70a, Gr. 55 Min.	55,000	
9	ASTM A 516-70a, Gr. 60 Min.	60,000	
10	ASTM A 516-70a, Gr. 65 Min.	65,000	
11	ASTM A 516-70a, Gr. 70 Min.	70,000	
12	AAR TC128-70, Grs. A & B Min.	81,000	
13	ASTM A 537-80, Class 1 Min.	70,000	
14	ASTM A 302-69a, Gr. B Min.	60,000	
15	ASTM A 302-70a, Gr. B Min.	60,000	

Table 9.1: For carbon steels, hard-coded room temperature tensile strength (column 3) and multiplicative adjustment factor that reduces that strength due to higher temperatures (column 4). Here, temperature, T, is in thousandths of Rankines. See [4].

Stainless Steels			
ID	Description	S_r	Adjustment Factor
16 17	ASTM A 240-70, Type 304 Min. ASTM A 240-70, Type 304L Min.	75,000 70,000	$f = \begin{cases} 1 - 0.45(T - 0.86)/0.9 & 8.6 < T < 1.76 \\ 0.55 - 0.55(T - 1.76)/0.4 & 1.76 < T < 2.16 \\ 0. & T > 2.16 \end{cases}$
18 19	ASTM A 240-70, Type 316 Min. ASTM A 240-70, Type 316L Min.	75,000 70,000	$f = \begin{cases} 1 - 0.55(T - 0.86)/0.9 & 8.6 < T < 1.76 \\ 0.45 - 0.45(T - 1.76)/0.4 & 1.76 < T < 2.16 \\ 0. & T > 2.16 \end{cases}$

Table 9.2: For stainless steels, hard-coded room temperature tensile strength (column 3) and multiplicative adjustment factor that reduces that strength due to higher temperatures (column 4). Here, temperature, T, is in thousandths of Rankines. See [6] and [5].

Aluminum			
ID	Description	S_r	Adjustment Factor
20 21 22 23 24 25	ASTM B 209-70, Alloy 5052 Min. ASTM B 209-70, Alloy 5083 Min. ASTM B 209-70, Alloy 5086 Min. ASTM B 209-70, Alloy 5154 Min. ASTM B 209-70, Alloy 5254 Min. ASTM B 209-70, Alloy 5454 Min.	75,000 38,000 35,000 30,000 30,000 31,000	$f = \begin{cases} 1 - 0.55(T - 0.86)/0.9 & 0.610 < T < 1.260 \\ 0. & T > 2.6 \end{cases}$
26	ASTM B 209-70, Alloy 5652 Min.	75,000	$f = \begin{cases} 1 - 0.55(T - 0.86)/0.9 & 0.610 < T < 1.260 \\ 0. & T > 2.6 \end{cases}$
27	ASTM B 209-70, Alloy 6061 Min.	34,000	$f = \begin{cases} 1 - 0.48(T - 0.610)/0.25 & 6.1 < T < 8.6 \\ 0.52 - 0.52(T - 0.86)/0.40 & 8.6 < T < 1.26 \\ 0. & T > 1.26 \end{cases}$

Table 9.3: For different types of aluminum, hard-coded room temperature tensile strength (column 3) and multiplicative adjustment factor that reduces that strength due to higher temperatures (column 4). Here, temperature, T, is in thousandths of Rankines. There were possible corrections needed to the legacy strength model found as part of this background research. See [16].

Chapter 10

AFFTAC's Advanced Strength and Failure Model

In contrast to the Basic Strength Model discussed in the previous chapter, the other way to model strength of the tank wall is to use AFFTAC's Advanced Strength Model. Because there are multiple inputs involved in an Advanced Strength Model setup, each setup is grouped together as a single "Resource", as are inputs for ladings. They are then managed using the Advanced Strength Model Resource Manager.

You can switch to using the Advanced Strength Model in a simulation by clicking the button **Switch to Advanced Strength Model** in the **Edit Tank Car Properties** window. The Advanced Strength Model Resource is like the other Resources used in AFFTAC in that by choosing a particular name, you are potentially drawing upon several pieces of data.

The Advanced Strength Model accommodates two types of strength models which may be used individually or in combination. One is the Larson-Miller failure model; the other is ultimate tensile strength data that you can enter as a function of temperature. Also, it contains the model for specifying how much the tank wall creeps under the thermal and pressure loading during a simulation. Before moving into a discussion of these models, it is worth noting that although the legacy hard-coded algebraic models mentioned at the beginning of this chapter are less general and are not available for editing by the user, they have been part of AFFTAC longer. Therefore, they have been used more and have been part of more tests. Most importantly, however, they are simpler. Therefore, it is recommended that, critical simulations, you also try the Basic Strength Models for comparison.

As mentioned above, to use an entry in the Advanced Strength Model, when editing an analysis, click the **Switch to the Advanced Strength Model** button in the Edit Tank Car Properties window, which is the second in the four-window editing sequence. When you do that, the list of current model setups in the Advanced Strength Model Resource list appears, and you may select one for the current analysis. That editing window, displaying the Advanced Strength Model Resource Manager, is shown in Figure 10.1. Note that, currently in AFFTAC, when you choose to use the Advanced Strength Model the conductivity of the tank wall and the thermal expansion coefficient are automatically set to that of carbon steel.

To edit or expand the entries in the Advanced Strength Model Resource, click the **Manage Advanced Models** button, which appears when you click the **Switch to Advanced Strength Model**. When you click the **Manage Advanced Models** button, the **Advanced Strength Model Resource Manager** window appears, like that shown in Figure 10.2. From that window you may create new or delete existing entries. If you choose to edit an entry, the window in Figure 10.3 appears, which shows that each strength model can implement either the Larson-Miller strength model, the ultimate tensile strength data, or both. The ultimate tensile strength model is described by the ultimate tensile strength entered as a function of temperature. The Larson-Miller model is described by the "Larson-Miller parameter" entered as a function of stress; the Larson-Miller model will be described in more detail in a later section. If you choose to model the strength of the tank wall using the Larson-Miller model, AFFTAC also gives you

the option of including creep in the tank volume calculation. If you choose that option, you must enter data that specifies the amount of creep that was measured just before failure during a Larson-Miller experimental test. To be clear on this point, when tank car material is tested in the laboratory under constant stress and constant temperature conditions, it eventually fails. The strain just before failure is what we call here the "failure creep strain". It may be entered into AFFTAC as a function of temperature. If you select this option and enter the data, the creep of the tank car walls will be included along with elastic strain and thermal expansion at each time step when AFFTAC recomputes the changing volume of the tank car. These details are discussed in subsection 14.2.3.

Data is entered for these models by clicking the appropriate buttons in Figure 10.3, which opens a property data entry window. An example of that window is shown in Figure 10.4 and allows for tabular entry of data (top of Figure 10.4) or, conversely, algebraic data entry (bottom of Figure 10.4).

The Larson-Miller strength model output is in two forms, which occupy two columns in the output viewed in the **Main Window**. The primary output of the Larson-Miller model is a metric referred to here as "Life Depleted." This value, which starts at zero, represents the amount of accumulated damage in the tank material due to temperature and stress. It is a non-dimensional value; once it reaches the value of unity, the life is completely depleted from the tank wall and it fails, thereby ending the simulation. The "Life Depleted" output might change very slowly at first and then grow rapidly as failure is neared. Therefore, the log of its value is displayed.

Another useful metric output by the Larson-Miller model is the internal tank pressure that would cause the tank wall to fail in one minute, given the damage that has accumulated in the tank wall up that that point in time. That internal burst pressure output takes the place of the "burst pressure" column of data, which is displayed using the Basic Strength Model.

Shown in Figure 10.5 is a set of plots from a simulation that uses the Larson-Miller strength model. In the bottom left plot, the life depleted is shown. In the upper right plot, the "burst pressure" is plotted; again, this is the pressure at which the tank would fail in one minute given its accumulated damage.

When both options are selected in Figure 10.3, AFFTAC outputs the minimum value for burst pressure between the two models (Ultimate Tensile Strength versus Larson-Miller).

10.1 Validated Entries in the Advanced Strength Model Resource List

AFFTAC comes shipped with a handful of steels that have been successfully validated against the Larson-Miller failure model in recent small-scale experiments. The validation procedure is described in [21]. In that report, the fits to the experimental data are shown. Also, verification tests for the Larson-Miller model that are part of the AFFTAC Regression Test Database are described in the *Verification and Validation Testing* document.

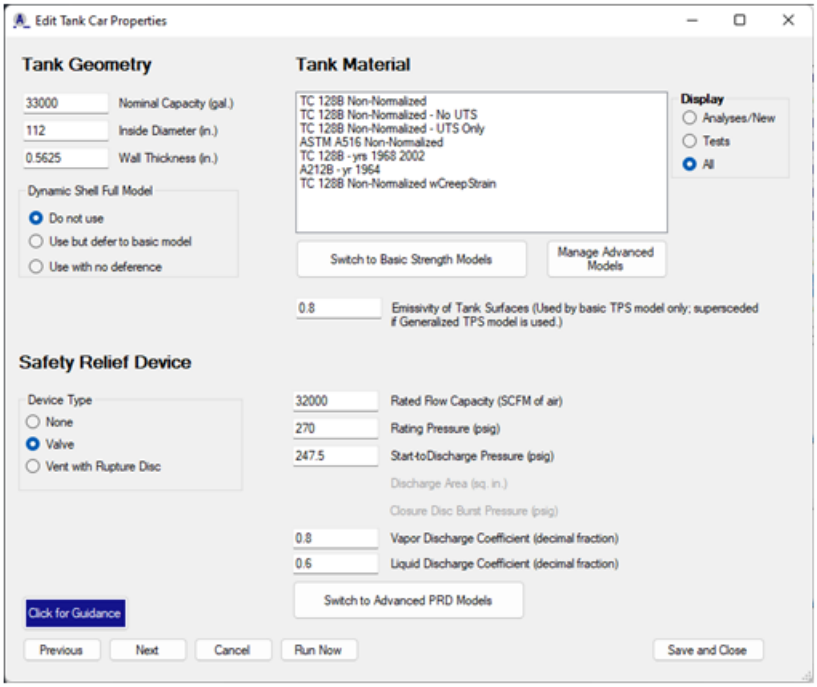

Figure 10.1: The **Edit Tank Car Properties** window in which the Advanced Strength Model has been selected.

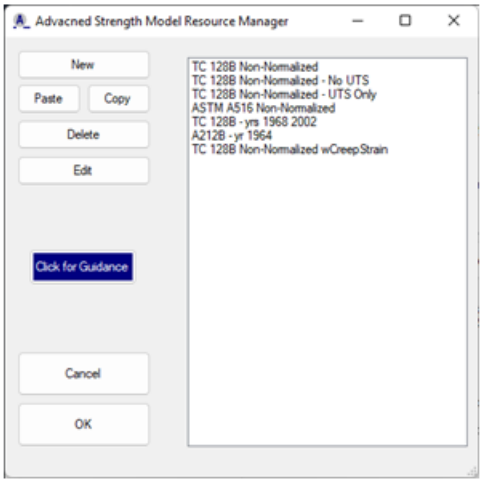

Figure 10.2: Advanced Strength Model Resource management window.

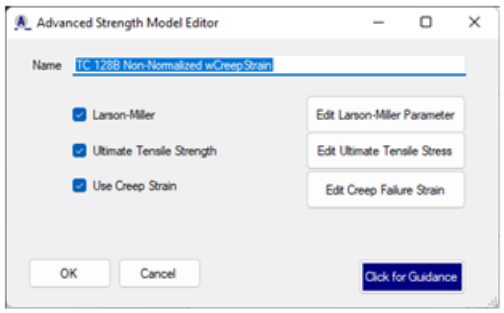

Figure 10.3: Editing window for Advanced Strength Model setup. Larson-Miller and Ultimate Tensile Strength models are two options. When Larson-Miller is selected, you may also choose to enter creep strain at failure as a function of temperature. In so doing, creep strain will be used with elastic and thermal strain to compute the changing tank volume during a simulation.

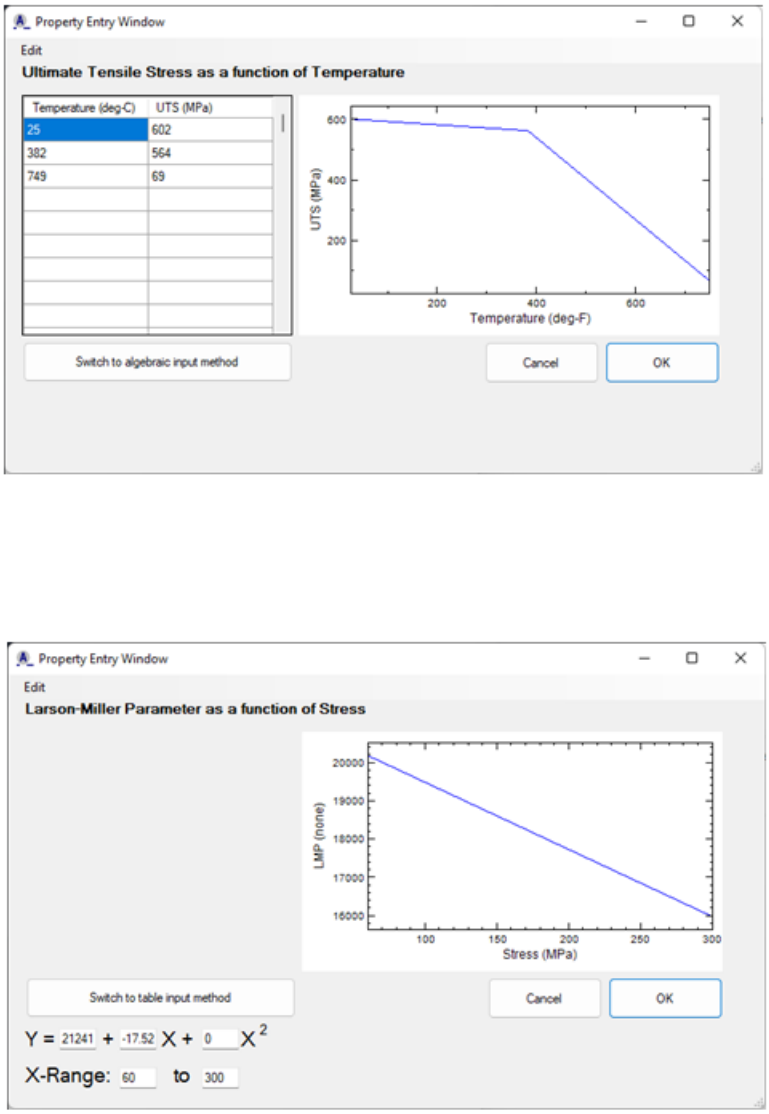

Figure 10.4: Property entry window. The tabular of data entry is still available (top). But this window also accommodates polynomial data entry (bottom). The two modes are activated using the large button between the table and polynomial entry regions of the window.

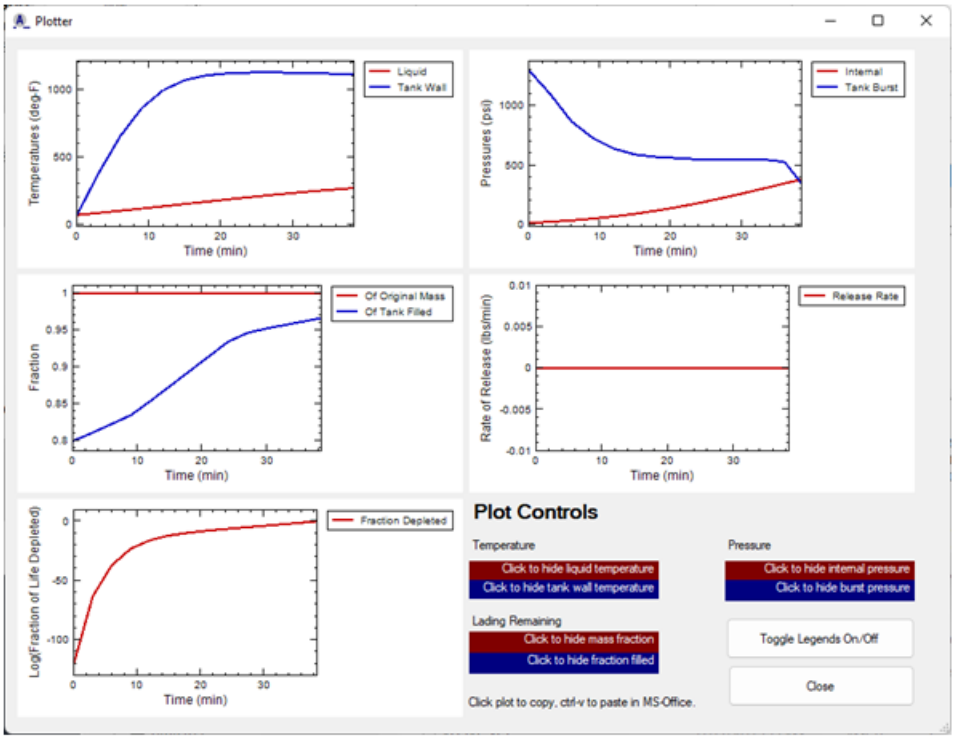

Figure 10.5: Plotting capability that shows ”Fraction of Life Depleted” when the Larson-Miller failure model is used

10.2 Larson-Miller Model Theory

In this section, we describe the Larson-Miller failure model, which can be activated only by specifying a tank wall material using Advanced Strength Model, as described in the previous section.

High stress at an elevated temperature creates damage in materials that accumulates over time. The damage is due to the migration and production of microscopic defects, both of which occur at higher rates as stress and temperature is increased. As the damage accumulates, the material becomes weaker and it creeps under loading. Eventually, the damage can accumulate to such a high level that the material fails.

Creep is usually discussed using strain as a primary quantity of interest. During a creep-to-failure test, the material is loaded with a constant temperature and stress. Many metals respond by straining at three different rates in distinct stages as shown in Figure 10.6. The first stage is characterized by a strain rate that is relatively large. But this stage is short-lived and quickly gives way to a prolonged second stage where the strain rate is relatively small. The second stage ends by transitioning to a third stage that is relatively short-lived and is nonlinear. It is this third stage that ends relatively quickly and abruptly by failure of the material.

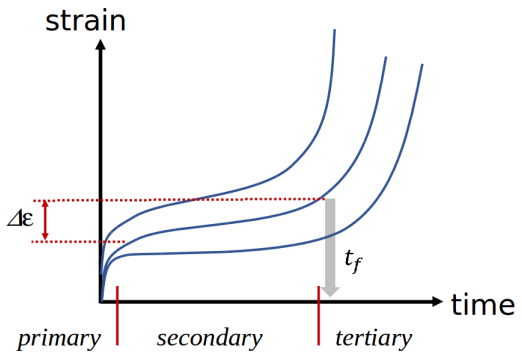

Figure 10.6: General behavior in a creep strain test. *Mechanical Behavior of Materials, Marc Meyers and exclusive focus of phenomenological Krishan Chawla, Cambridge University Press, 2009*

Figure 10.6 is not to scale. In reality, the second stage is usually much larger than the other two, on the order of a thousand times greater. Thus it is often the exclusive focus of phenomenological failure modeling for engineering applications. The strain rate during that second stage is referred to using different terms including the "secondary strain rate", the "steady-state strain rate", and the "minimum strain rate". All of these terms are correct and appropriate. Here, the term "secondary strain rate" will be used, and the variable will be denoted as $\dot{\epsilon}_{ss}$.

In deriving the Larson-Miller phenomenological failure model, it is assumed that the phenomena giving rise to the secondary strain can be modeled using the Arrhenius equation. The Arrhenius equation is empirical but has been found to accurately model several phenomena such as diffusion and reactions where temperature plays a key role. Insofar as the accumulation of damage that leads to ductile failure is like a diffusion process on the macroscopic scale, e.g., the diffusion of voids, it is reasonable to assert that the Arrhenius equation may be a good candidate for a phenomenological model. Experimental data has proven that this assertion is valid.

Therefore, proceeding along those lines of reasoning, it is suggested that the secondary strain rate is governed by the following Arrhenius type equation

$$\dot{\epsilon}_{ss} = Ae^{-\Delta H/RT} \tag{10.1}$$

where

$$\begin{aligned} A &= \text{ a material constant,} \\ \Delta H &= \text{ the activation energy of the phenomenon, which here is creep,} \\ R &= \text{ the Universal Gas Constant, and} \\ T &= \text{ absolute temperature.} \end{aligned}$$

If one ignores the primary and tertiary phases and approximates the entire process as consisting only of the secondary phase, and if $\dot{\epsilon}_{ss}$ is considered to be a constant, in addition to the expression in Equation 10.1, we can express the time derivative as

$$\dot{\epsilon}_{ss} \approx \frac{\Delta\epsilon}{t_f}. \tag{10.2}$$

Equating the two expressions for $\dot{\epsilon}_{ss}$, the Arrhenius relation becomes

$$\frac{\Delta\epsilon}{t_f} = Ae^{-\Delta H/RT}. \tag{10.3}$$

Equation 10.3 can be solved for $\Delta H/R$ through straightforward algebraic manipulation. Doing so produces

$$\frac{\Delta H}{R} = T(\ln(A/\Delta\epsilon) + \ln(t_f)). \tag{10.4}$$

The first term inside the parentheses has been found to be nearly a constant for metals and we will name it C' for now. Thus

$$\Delta H/R = T(C' + \ln(t_f)). \tag{10.5}$$

Regarding the left-hand side, R is a constant and we assert that the activation energy is a function of stress alone. Thus the ratio on the left-hand side of the equation is considered to be a function of stress alone. We will name that value $LMP' = LMP'(\sigma)$ for now, and the meaning of that name will be made clear shortly. Thus, we write

$$LMP'(\sigma) = T(C' + \ln(t_f)). \tag{10.6}$$

The natural log may be converted to a base-ten logarithm using a scaling constant, which will be absorbed into C', renaming it to C, and is also absorbed into the left-hand side, renaming it to LMP . Thus we have

$$LMP(\sigma) = T(C + \log(t_f)). \tag{10.7}$$

$LMP(\sigma)$ is the Larson-Miller parameter, which is a function of stress, and C is a constant. It has been found that, by experience, $C = 20$ for most metals. In experiments that determine the Larson-Miller parameter, this assumption is often made at the outset, i.e., C is often not measured. Solving for t_f,

$$t_f(\sigma, T) = 10^{\frac{LMP(\sigma)}{T} - C}. \tag{10.8}$$

The Larson-Miller parameter is found by loading a material at a constant temperature and stress and then measuring the time to failure. In order to apply this value and the above relation in a transient situation, an assertion regarding the secondary strain rate is made. Specifically, it is asserted that while the secondary strain rate ($\dot{\epsilon}_{ss}$) is a constant in time for a fixed temperature and stress, it will change instantaneously to a new fixed value if the temperature and/or stress change, thus $\dot{\epsilon}_{ss} = \dot{\epsilon}_{ss}[\sigma(t), T(t)]$.

Using this assertion, the time at which failure occurs during a transient simulation can be determined by integrating $\dot{\epsilon}_{ss} = \dot{\epsilon}_{ss}[\sigma(t), T(t)]$ over time. When its time integral equals $\Delta\epsilon$, failure will occur. In other words, t_f is the solution to this equation:

$$\int_0^t \dot{\epsilon}_{ss}[\sigma(\tau), T(\tau)]d\tau = \Delta\epsilon \tag{10.9}$$

Care regarding the time variables is warranted. Here, the current time in the simulation is t, and note that it appears as the upper limit of the integral. Thus we are evaluating the integral from the beginning of the simulation up to the current time, t, in the simulation. The value of $\dot{\epsilon}_{ss}$ changes through the simulation, and that fact is represented by evaluating it at each time τ from zero up until t. When the integral's value at time t equals $\Delta\epsilon$, failure has occurred.

To evaluated the integral, first note that Equation 10.2, written more explicitly, is

$$\dot{\epsilon}_{ss} \approx \frac{\Delta\epsilon}{t_f[\sigma(t), T(t)]} \tag{10.10}$$

Using that in Equation 10.9,

$$\int_0^t \frac{\Delta\epsilon}{t_f[\sigma(\tau), T(\tau)]}d\tau = \Delta\epsilon \tag{10.11}$$

Recall that the ratio $A/\Delta\epsilon$ was considered a constant (specifically, $\log(A/\epsilon) = 20$ for most metals). Since A is considered a constant, then so must $\Delta\epsilon$, which means it cancels itself on both sides of the above equation. Thus, the failure condition becomes

$$\int_0^t \frac{1}{t_f[\sigma(\tau), T(\tau)]} d\tau = 1 \tag{10.12}$$

where t_f is known from experimental data, i.e., Equation 10.8.

During a simulation, the progress of the tank material toward failure is tracked by evaluating the above integral at each time step. To avoid having to evaluate the entire integral from $t = 0$ up to the current time in the simulation, for each and every time step, we instead build the integral up, step by step, by adding to its value from the previous time step.

To be clear on that point, let us label each time as time step "j", such that the time at time step j is t_j. Since AFFTAC's time steps are a constant during a simulation, $t_j = j\Delta t$, where Δt is the size of the time step. We define what we will call the "Life Used" as L, as the value of the above integral at time step j. We begin with $L = 0$ at the start of the simulation. Then, for each time step that follows, we update L using the rectangle rule for integration as

$$L \leftarrow L + \frac{1}{t_f[\sigma(t_j), T(t_j)]} \Delta t \tag{10.13}$$

When $L = 1$, we know that the integral condition in Equation 10.12 is satisfied and the tank will have failed at that time step.

In the Larson-Miller model, the tank is considered to be symmetric about a vertical plane passing through its axis. Using that symmetry, half of the tank is divided into 180 points, $i = 1, 2, ..., 180$, where each point is separated by one degree. Zero degrees represents the bottom of the tank and ninety degrees is at the top of the tank. Each of those 180 points experiences a different temperature history because of differences in TPS coverage and the fact that the liquid level can rise and fall. Thus each of those points have separate values for L. So we add a subscript to L, computing $L_i(t)$ for $i = 1, 2, 3, ..., 180$.

10.2.1 Burst Pressure for the Larson-Miller Failure Model

In the Basic Strength Model, a straightforward algebraic equation relates the material's temperature to its ultimate tensile strength. From that, using simple geometric considerations described in Chapter 14, the pressure inside the tank that will lead to bursting can be computed. Thus, when using the Basic Models, one of the outputs in AFFTAC is the burst pressure as a function of time. That pressure is plotted on the same plot as the tank internal pressure. When those two lines cross, the tank fails. That plot is therefore very valuable.

In the Larson-Miller model, the relationship between temperature and failure is more complex. It involves time and also the stress history. However, the idea of a "burst pressure" is still extremely valuable and so AFFTAC defines one for the Larson-Miller model to be as follows: "The Larson-Miller burst pressure is the pressure that would cause the tank, given its temperature-stress history and accumulated damage, to fail in one minute at current conditions."

To derive the equation for that pressure, we represent Equation 10.13 as a summation. Evaluated at time step $t_n = n\Delta t$, that sum is

$$S_n \equiv \sum_{i=1}^{n} \frac{\Delta t}{t_f(\sigma(t_i), T(t_i))} \tag{10.14}$$

We seek a stress, $\sigma(t_{n+1})$, such that $S_{n+1} = 1$ in 1 minute. Or,

$$S_{n+1} = S_n + \frac{1 \text{ min}}{t_f(\sigma(t_i), T(t_i))} = 1 \text{ (failure)} \tag{10.15}$$

Solving for t_f,

$$t_f(\sigma(t_i), T(t_i)) = \frac{1 \text{ min}}{1 - S_n} \tag{10.16}$$

This value can be used to solve for stress in a two-step process starting first with Equation 10.7, in which the above expression for is t_f inserted, producing

$$LMP(\sigma) = T \cdot \left[\log \left(\frac{1 \text{ min}}{1 - S_n} \right) + C \right] \tag{10.17}$$

This is the first step in computing the burst strength; it gives a value for the Larson-Miller parameter. The second step to finding the burst stress is to perform an inverse lookup, $\sigma = \sigma(LMP)$, of the experimental data or the curve fit to that experimental data. In other words, given the value of LMP from the above equation, the experimental data or curve fit is used to find the corresponding value of σ. Lastly, that value of tensile stress is converted to an internal pressure through geometric considerations described in chapter 14.

10.2.2 Ultimate Tensile Strength Data

As mentioned earlier in this chapter, the ultimate tensile strength (UTS) model is implemented in a way very similar to AFFTAC's Basic Strength Model. In the Advanced Strength Model's use of UTS, the input data is queried to determine the UTS of the tank at the highest temperature in the tank wall. Using that value, the internal pressure sustainable by the tank wall is computed. If the actual pressure inside the tank exceeds that computed pressure, failure occurs. The only difference between the Advanced Model and the Basic Model regarding UTS is that you can specify the UTS using polynomial or tabular entry whereas the Basic version uses hard-coded equations. The Basic Model is retained in AFFTAC to maintain backward compatibility and for providing benchmark calculations against which the more general failure models can be compared. Both the UTS model and the Larson-Miller failure model, which are contained in the Advanced Strength Model, can be run simultaneously during a simulation. As mentioned above, when the Larson-Miller and the UTS models are both active, AFFTAC outputs the minimum burst strength of their predictions at each time step.

Chapter 11

AFFTAC's Basic PRD Model

11.1 What Distinguishes Basic from Advanced PRD Models

There are essentially two aspects to modeling a PRD. One aspect is determining how much of the PRD is open, i.e., how much the PRD's cross-sectional flow area is available for lading release. The other is using that area to compute the physics for lading (liquid and/or vapor) flow through the PRD. AFFTAC's Basic and Advanced Models both use the same physics models for flow, once the fraction open is known. What distingishes AFFTAC's Basic and Advanced Models is how the area for the PRD is computed.

The term "fraction open", a number that varies between zero and one, is used to describe the open-close state of the PRD in AFFTAC. The fraction open value is multipled by the valve's cross-sectonal flow area to compute the actual flow area available at any point in time. AFFTAC's Basic PRD Model has a very limited model for describing the open-close behavior of a PRD, whereas the Advanced PRD Model has multiple options.

Thus, when using the Basic PRD Model, you need only provide a handful of values, and so those values are included directly with the Analysis you are planning to run. They are entered in the **Edit Tank Car Properties** window, which is the second of the four windows encountered when editing an analysis. When using the Advanced PRD Model, there can be many more values and so, like with ladings and other advanced models in AFFTAC, they are gathered together as a "Resource" and referred to by a single name in setting up the Analysis. Figure 11.1 shows the **Edit Tank Car Properties** window in two configurations, using the Basic PRD Model and the Advanced PRD Model.

11.2 Essential Ideas in the Basic Open-Close Model

The Basic PRD Model accommodates two different types of pressure relief devices: Pressure relief valves (PRVs), which can open and close repeatedly, and frangible disks which, once burst open, remain open. The frangible disk model is very simple, being that once the designated pressure for the disk is exceeded, the fraction open is set to one and remains at that value for the remainder of the simulation. So here we focus on PRVs.

The Basic Model for PRVs is captured in Figure 11.2, which shows the fraction open as a function of pressure. In this Basic Model, the valve is assumed to be spring loaded, remaining closed until the pressure reaches a "Start-to-Discharge" pressure. As pressure increases beyond that pressure, the valve opens more until it is fully opened, i.e., with a fraction open value equal to one.

As lading is released and the pressure differential decreases, the valve's spring begins to close it again. There are two paths that the valve can follow when closing. If the valve is fully open and the pressure drops below the full open pressure ($F_{\text{full\_open}} \times P_s$), the valve will begin to close an amount that is proportional to the difference between the full open pressure and a reference closing pressure ($F_{\text{elbow}} \times P_s$). The fraction open at F_{elbow} is f_{elbow}. Once $F_{\text{elbow}} P_s$ is reached, the valve will become more sensitive; the rate of closure with respect to the

pressure increases until it is fully closed at $F_{\text{full\_close}} \times P_s$. That path is marked “A”. The other path, marked “B”, is followed if the pressure begins to drop before the valve is fully open.

When using AFFTAC’s Basic PRD Model, the values $F_{\text{full\_open}}$, F_{closure}, F_{elbow}, and f_{elbow} are hard-coded. They are shown in Table 11.1. So, to be clear, the only adjustable parameter for the open-close behavior of a valve in the Basic PRD Model is the Start-to-Discharge pressure. If your valve’s open-close behavior cannot be modeled with that single parameter, in combination with Figure 11.2, you should consider using the Advanced PRD Model, which is described next.

Open-Close Modeling Values used in Default Model	
$F_{\text{full\_open}}$	1.03
F_{closure}	0.82
F_{elbow}	0.88
f_{elbow}	0.85

Table 11.1: Default parameters for valve opening and closing model

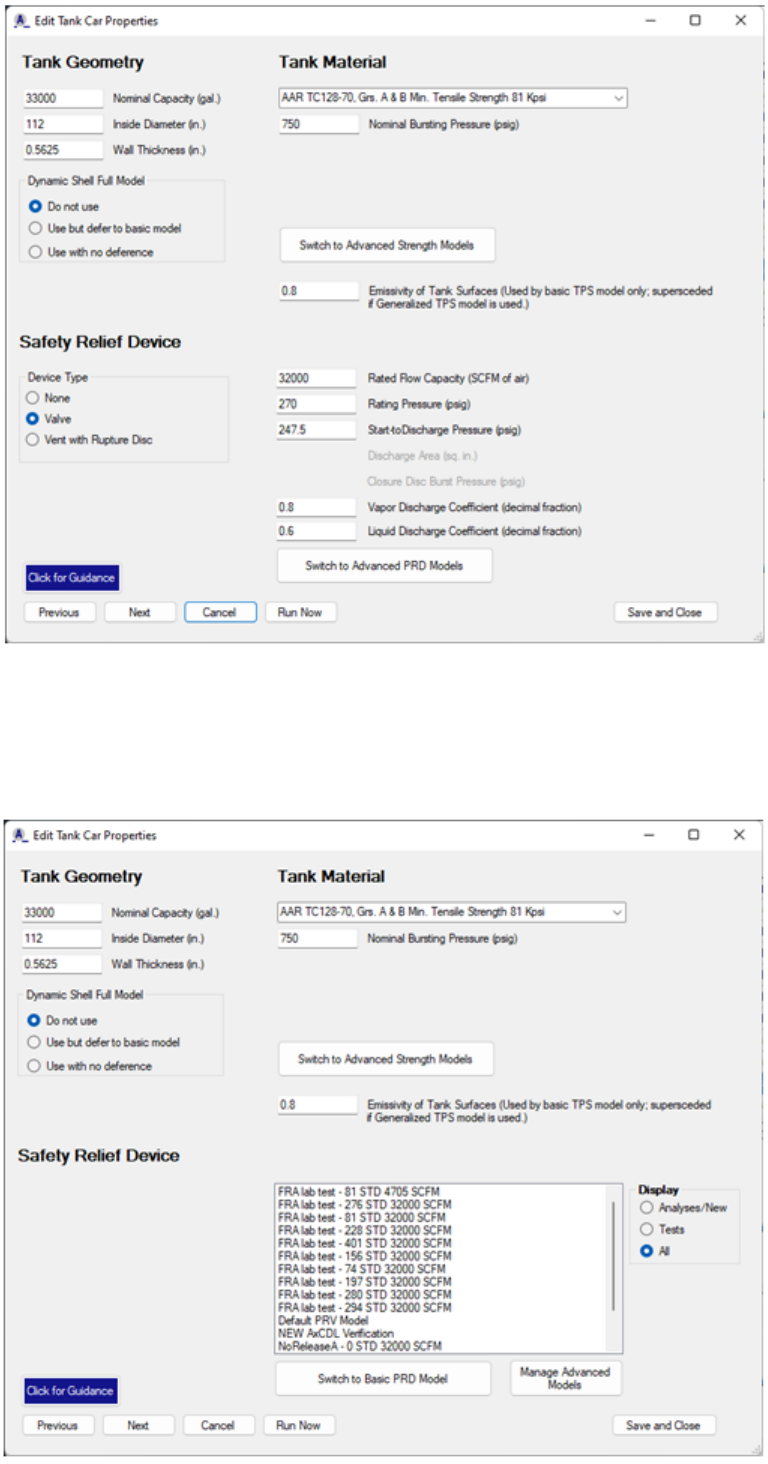

Figure 11.1: The Edit Tank Car Properties window shown in two modes in the bottom portion of the window. On the left is the Default PRV Model. On the right, is the PRD Database mode, which gives access to the Standard PRV Model and the Generalized PRV Model.

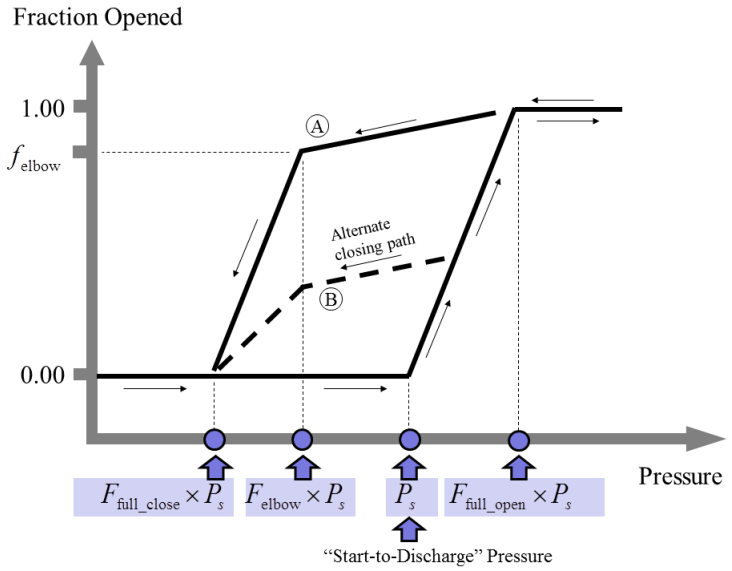

Figure 11.2: Model for the spring-loaded pressure relief valve

Chapter 12

AFFTAC's Advanced PRD Model

If you use AFFTAC's Advanced PRD Model for the open-close behavior of a pressure relief device (PRD), you have much more freedom in specifying how the fraction open changes with pressure. One option is to stay with the essential ideas of the Basic PRD Model, as shown in Figure 11.2 but utilize the freedom to adjust the key points on that figure's paths to represent different types of PRVs. In the Advanced PRD Model, the "Standard Path" shown in Figure 11.2 can be modified by adjusting the positions of each endpoint.

In an experimental and validation exercise described in the *AFFTAC Verification and Validation Testing* document, values for the parameters in Figure 11.2 as well as areas and coefficients of liquid discharge were determined and used to establish a set of of PRVs released with AFFTAC as part of the Advanced PRD Resource list. Those values are shown in Table 12.1. AFFTAC is shipped with these entries. However, you can edit and expand this list as needed. Very important details regarding how these values were obtained are documented thoroughly in *AFFTAC Verification and Validation Testing*.

AFFTAC Database Entry	Measured Start-to-Discharge (psig)	Multipliers for Open-Close Model			Fraction Open At Descent (Point "A")
		Full Open	Descent	Closed	
FRA lab test - 81 STD 4705 SCFM	81	1.01	0.69	0.69	0.94
FRA lab test - 276 STD 32000 SCFM	276	1.03	0.71	0.69	0.95
FRA lab test - 81 STD 32000 SCFM	81	1.09	1.07	0.91	1.00
FRA lab test - 228 STD 32000 SCFM	228	1.11	0.89	0.82	0.54
FRA lab test - 401 STD 32000 SCFM	401	1.05	0.94	0.91	1.00
FRA lab test - 156 STD 32000 SCFM	156	1.10	1.04	0.85	1.00
FRA lab test - 74 STD 32000 SCFM	74	1.12	1.03	0.81	0.99
FRA lab test - 197 STD 32000 SCFM	197	1.03	0.87	0.71	1.00
FRA lab test - 280 STD 32000 SCFM	280	1.00	0.86	0.54	1.00
FRA lab test - 294 STD 32000 SCFM	294	1.00	0.86	0.85	0.94

Table 12.1: Results of the model calibration exercise for the valve opening and closing model

If the shape of the Standard Path is in Figure 11.2 is not sufficiently flexible to represent your PRD, e.g., you need more line segments, you can create your own set of paths to represent the PRD open-close behavior. You can create what is called a “Generalized Path,” where you create new and different types of relationships between pressure, pressure history, and the fraction open value. These relationships are specified using multiple line segments, like those in Figure 11.2, except you have more freedom in their number, shape, size, relationships, and generality.

For example, you can create multiple segments that resemble a curvilinear relationship between pressure and fraction open. You can specify the direction of pressure change for which each segment is applicable. You can also specify what other segment should be used when a pressure reversal occurs. Lastly, the type of behavior represented by the dotted line in Figure 11.2, i.e., where the path used when one of the paths is abandoned upon a pressure reversal, can be specified using “templates” in your Generalized Path. Multiple templates and multiple instances of hysteresis are accommodated. More instructions on setting up a Generalized Path is provided later in this chapter and also by the tutorial in section 18.

12.1 Managing Advanced PRD Model Resources

From the list in the lower part of the window that was shown in Figure 11.1, you can select a PRD for your analysis. You can also edit the list of Advanced PRD Models by clicking the **Manage Advanced Models** button. When you do, the window in Figure 12.1 appears in which you can create new, edit, or delete PRDs.

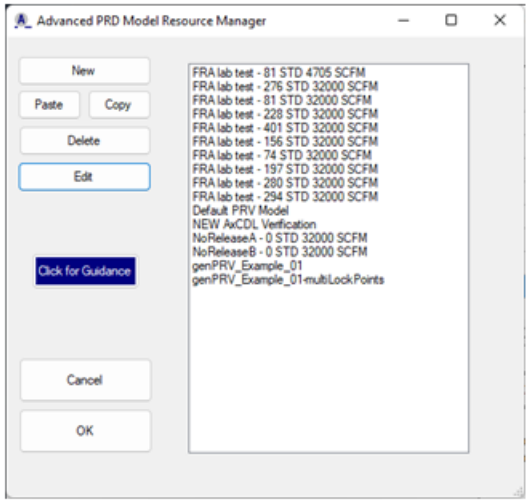

Figure 12.1: PRD Resource Manager

To edit an individual Advanced PRD Model, either double click on its name or highlight it and click the **Edit** button. When you do, a window that resembles the ones shown in Figure 12.2 will appear. As Figure 12.2 indicates, there are three basic modes for the PRD setup. The mode represented in the top part of Figure 12.2 is for a PRV that uses the Standard PRV Model for open-close behavior. The mode represented in the middle of Figure 12.2 is for a vent with a rupture disk. And the mode represented in the bottom of Figure 12.2 is for a PRV whose open-close behavior is modeled using a Generalized Path.

Because the physics of the flow models are the same for the Advanced PRD Model, the window for an Advanced PRD Model also receives as input the vapor flow rating and flow rating pressure. However, there is more flexibility

regarding the relationship between the experimental vapor flow data and the experimental data obtained for liquid/two-phase flow. In the Advacned PRD Model, you have the freedom to specify the area explicitly for a PRV, allow AFFTAC to estimate the area using vapor flow data, and also specify area times the coefficient of liquid discharge for the liquid discharge model.

AFFTAC's method of area estimation, based on the volumetric vapor flow data, is discussed in Appendix E. Once the value for area is computed, it can be used by AFFTAC in the two-phase liquid flow model, along with the coefficient of liquid discharge that you provide. However, for liquid flow, if you only have data for the product of the valve area and the liquid discharge coefficient, you can have AFFTAC use that combined value instead.

A key point to note is that in all flow calculations, the same value of area is ultimately used. So, if you choose to input the area of a PRV manually, it will override the area computed internally and, in so doing, override the vapor flow test data that you specify.

12.1.1 Entries Specific to the PRVs

As discussed above, you must specify a valve open-close model for PRVs, and there are two options for doing that. The Standard PRV model is the choice represented by the top of Figure 12.2. With that choice, you can enter the parameters directly on top of a graphic that shows the nonlinear and hysteresis open-close behavior of the PRV as discussed in Figure 11.2. The primary quantity of interest for the open-close behavior is the start-to-discharge pressure, which is entered on the left-hand side of the window. In the plot, that value is referred to as "P_{Start}". The valve begins to open at P_{Start} and is fully open at a value greater than P_{Start}. That value is 1.01 in the upper window in Figure 12.2, but you are free to enter whatever value is appropriate for the valve you are modeling. If the pressure decreases at any time after the PRV is open, the closing path is different than the opening path. If it is fully open when the pressure decreases, it follows the upper curve shown in Figure 12.2. If it is not yet fully open, it follows the lower curve. The control points that define the closing paths are all inputs that you are free to specify. Again, this is discussed more fully in section 11.2.

A second option available for PRVs is to specify a customized relationship between pressure, pressure history, and the fraction that the valve is open. That option is accessed by clicking the **Generalized** option as shown in the bottom of Figure 12.2. The specifics of the Generalized PRV Model are entered by clicking the **Edit Generalized Path** button. The Generalized PRV Model is rather complex is so a separate section is devoted to it. See section 12.2 later in this chapter.

12.1.2 Entries Specific to Vents with Rupture Disks

For a vent with a rupture disk, the graph of open-close behavior is not present. Instead, the only value of relevance is the start-to-discharge value, which is when the rupture vent bursts.

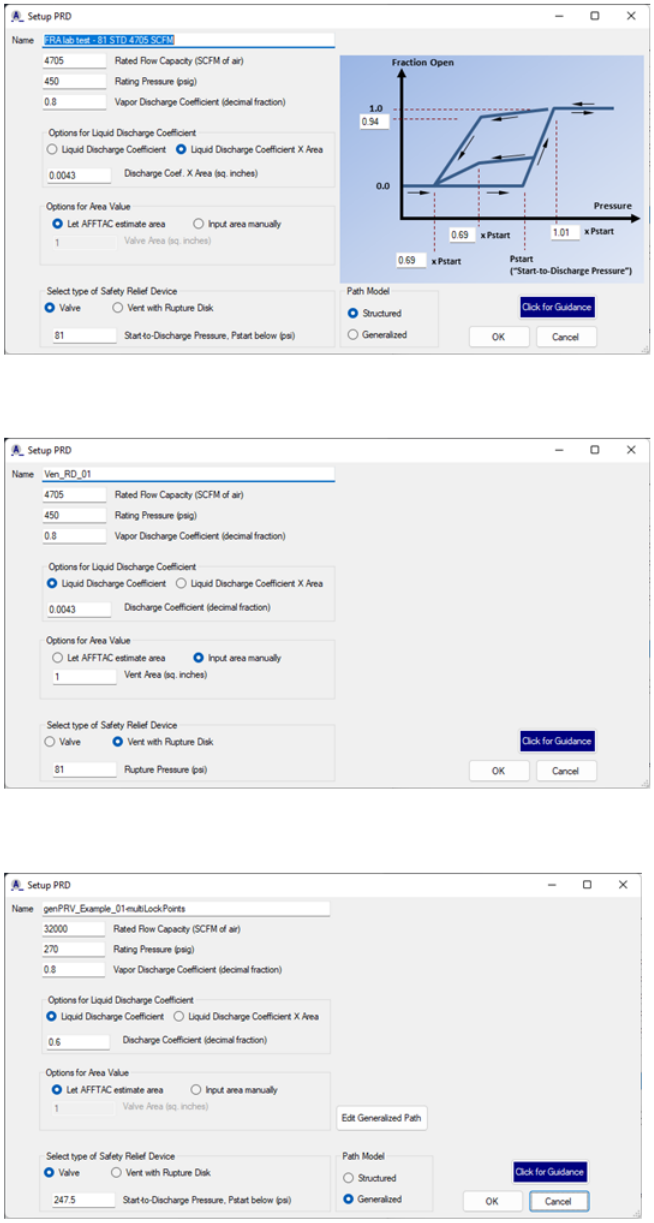

Figure 12.2: Three edit modes for a PRD Database entry. **Upper:** PRV using the Standard PRV Model, **Middle:** Frangible Disk, **Lower:** PRV using the Generalized PRV Model.

12.2 Specifying a Fully Customized Open-Close Path

You can create a fully customized open-close path by selecting the **Generalized** button in the **PRD Setup** Window, i.e., the mode shown in the bottom of Figure 12.2. Once in that mode, clicking the button the **Edit Generalized Path** displays the **Generalized PRV Editing** window shown in Figure 12.3. In this window, you can enter multiple and complex piece-wise linear curves that represent a PRV's open-close behavior, specifically, its fraction open as a function of pressure and pressure history. Before describing the operation of this window, however, the concepts and terminology in the Generalized PRV Model are described first.

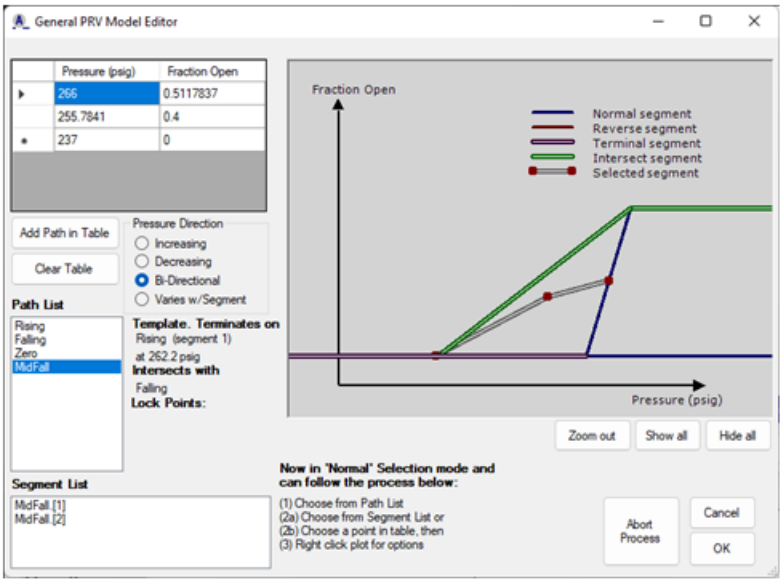

Figure 12.3: Appearance of the Generalized PRV Model Editing Window in use.

12.2.1 A Simple Bi-Directional Path

Figure 12.4 shows a very simple PRV open-close model that can be set up as a Generalized Path. It is a sequence of line segments, which we will continue to formally call "segments", that relate the fraction open of the valve to pressure. Together, the "segments" form what we call a "path". In this simple model, each segment applies regardless of the pressure direction. In other words, whether the pressure is increasing or decreasing does not come into play for this rather simple instance of the model. So the path for this example is called a "bi-directional" path.

12.2.2 Reverse Segments and Templates

PRVs can exhibit hysteresis. Shown in Figure 12.5 is a more complex example for a PRV exhibiting hysteresis. There are two paths specified. The black dotted line is the path for when the PRV is opening under increasing pressure and the orange solid line is for when the PRV is closing under decreasing pressure. In the software, the paths are named and segments on the paths are automatically given sequential integer ID numbers, i.e., 1, 2, 3,... etc. by AFFTAC.

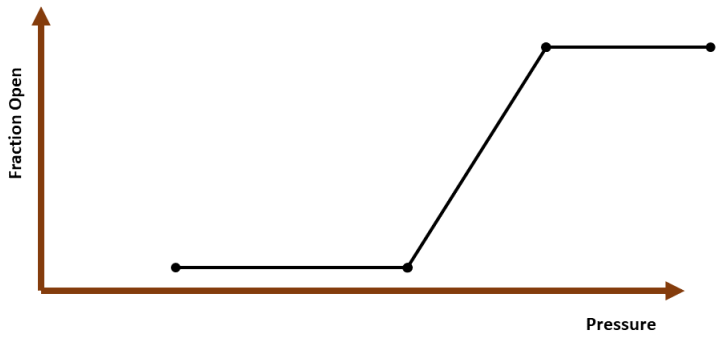

Figure 12.4: Simple open-close model expressed as a Generalized Path.

The labels in the figure are for instructional purposes here and are intended to stand for these ideas:

ZO → Zero fraction open, valve opening
ZC → Zero fraction open, valve closing
TP → Fully open, i.e., “Top” segment, valve opening
TC → Fully open, i.e., “Top” segment, valve closing
A → Ascending toward opening
D → Descending during closing

The simplified example shown in Figure 12.5 prompts some questions, for example, what happens when the pressure direction reverses while on the black dashed line? Is the action different when on segments “ZO”, “TO”, or “A”?

Let us consider a reversal while on segment “TO” first. As the figure shows, the model switches from “TO” to “TC”. While that switch makes intuitive sense, in the Generalized PRV Model, you must specify that there is a relationship between “TO” and “TC”. In the General PRV Model language, “TC” is a “reverse segment” for “TO”, or in other words, “TO” has a reverse segment, which is “TC”. There is nothing special about the behavior of a reverse segment. Rather, its relationship to another segment is what matters. The “reverse segment” is the segment to which the algorithm switches when leaving another segment because of a pressure reversal.

Now let us consider a reversal while on segment “ZO”. In the model shown in Figure 12.5, the lowest part of the black dashed line, “ZO”, can accommodate any direction in pressure. It is a bi-directional segment. So for that segment, it is not necessary to specify a reverse segment. The same is true for “TC”. “ZC” needs “ZO” as a reverse segment. As a user you must specify these relationships; the complexity is a consequence of the model being so general.

Now let us consider a pressure reversal while on segment “A” - the question is illustrated in Figure 12.6. To handle that situation, we use a “template”, which is illustrated in Figure 12.7. In Figure 12.7, a user-specified template is shown as a maroon path descending toward the left from the ascending black dashed line, which is for increasing pressure. The template is not an actual path because, clearly, the odds of the pressure beginning to decrease at the template’s point of intersection with the ascending black dashed line is practically zero. Rather, it serves

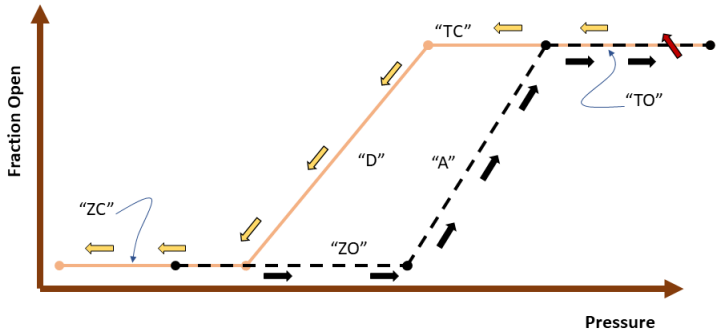

Figure 12.5: Illustration of simple pressure reversal hysteresis on a General Path on overlaying segments.

as an example path that is used to generate an actual path upon pressure reversal, where that pressure reversal might occur at any point along the ascending black dashed line. The path shown in gray could be one such actual path generated from the template. Although not an actual path, a template is specified using actual pressure and fraction open values, just as it appears in Figure 12.7. Note that templates and the paths generated from them are automatically bi-directional in pressure.

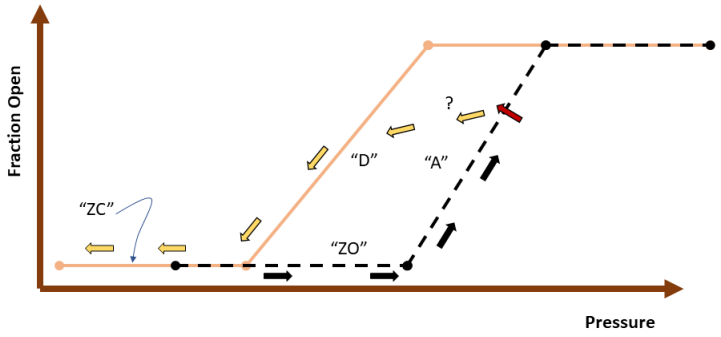

Figure 12.6: Reversal when there is no overlaying segment for the opposing direction.

To see how a template would function during a simulation, follow the pressure path in Figure 12.8. Pressure starts at the bottom left-most black arrow, transfers from "ZO" to "A" and continues to ascend upwards along "A" until it reverses direction, as shown by the red arrow. At that point, the maroon template is scaled geometrically so that it maintains its same shape but is applied to the pressure value at which the pressure reversal begins, i.e., the

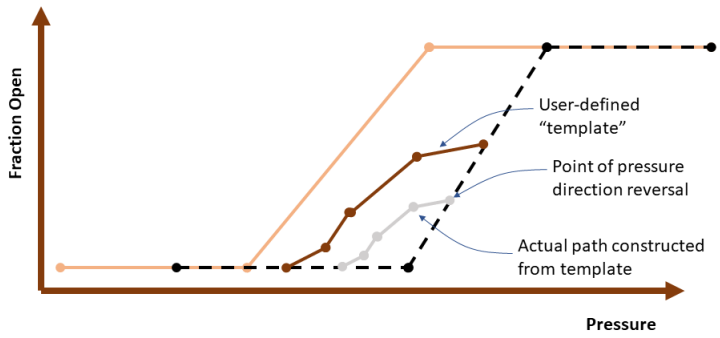

Figure 12.7: Basic concepts of a “template”.

pressure at the red arrow. As the pressure continues decreasing to the left indicated by the gold arrows, it stays on the temporary gray path created from the template until it reaches its termination point, i.e., which is where it hits segment “ZO”. Note that, when specifying a template, it is necessary to identify the termination path, and the pressure at which it terminates.

Figure 12.9 shows multiple examples of actual paths that can be created from a template during a simulation. Note again that all paths generated from the template are bi-directional in pressure. Also, notice the top gray path, which is an actual path that intersects with another non-template path. When specifying a template, you have the option of specifying a non-template path with which it might intersect. When a template-generated temporary path intersects with that non-template path, the non-template path takes over. That is the situation illustrated in Figure 12.10.

12.2.3 Templates with Lock Points

In the preceding section, the template was scaled geometrically to create an actual set of paths, based on where the pressure reversal took place along the ascending black dashed segment. Other than the intersection situation, which was illustrated in Figure 12.10, the actual segments created from a template are exactly the same shape. It may be, however, that you need to distort the scaling of the template when creating actual segments during the simulation. In particular, it may be that there are certain key pressure points along the template that should remain constant during the scaling, or an endpoint that is not allowed to move. Here those are called “lock points”.

Figure 12.11 illustrates two types of lock points, which are only specified on templates. The light blue circle represents a lock point where both pressure and fraction open are fixed during scaling of the template. The green circle represents a lock point that can move vertically but cannot move left or right, i.e., it is locked in pressure. The gray path in the figure represents the actual path created dynamically during a simulation. Notice that its terminal point on the lower black dashed line is at the same location as the template’s. Likewise, notice its middle point is at the same pressure as the green point. Those two aspects are due to the two lock points.

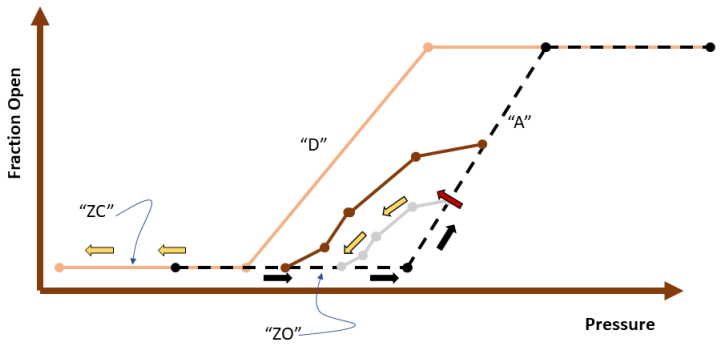

Figure 12.8: Example of a template in use, where an actual path is generated by scaling the template geometrically.

12.3 Operation of the Generalized PRV Model Editor

To reach the Generalized PRV Model editor, access the PRV Resource either through the **Main Window** menu items **Resources - Advanced PRD Models**, or through the analysis editing sequence. Choose or create the PRV in the usual way and then double-click to edit it. Doing so will display a window like those shown in Figure 12.2. In the lower right part of that window, choose **Generalized**. When you do, the **Edit Generalized Path** button will appear. Click it to access the Generalized PRV Model editor.

There are four main operational sections in the General PRV Model editor, as shown in Figure 12.12:

Section 1 (Enter Points): In this table, you manually enter points that constitute the endpoints of segments like those discussed in the previous section. You may enter any number of points, i.e., segments. Each adjacent pair of points comprise one segment in the path. When you select a previously entered path in Section 2 (below), it is displayed in this table. Once it is displayed, you can select a point by clicking on it in the table. You can also edit the values in the table to adjust the path.

Section 2 (Select Path): Previously entered paths are displayed in this list box. When you click on an entry in this list, it is highlighted in the plot section (Section 4). Also, the points comprising its segments are displayed in Section 1's table, and information about each segment is displayed in Section 3. Segments for each path are numbered in an ascending order, 1, 2, 3,..., where "ascending" here does not mean pressure direction but, rather, the order in which they appear in Section 1's table. By double-clicking on a path, you are allowed to perform detailed manual editing on it; this feature is particularly valuable for templates. Lastly, right-clicking on an individual path gives you the option of showing it or hiding it in the plot (Section 4). Using the show/hide option for individual paths, in combination with the **Show All** and **Hide All** buttons in Section 4 can greatly simplify visualization of the model and simplify operations on it.

Section 3 (Select Segment): If a path is selected in Section 2, its segments are displayed in this list. Information about pressure direction applicability, reverse segments, and templates are also displayed for each segment in the selected path. By clicking on a segment in this list, it is selected and highlighted in Section 4's plot.

Section 4 (Plot and Perform Actions): This section displays the paths graphically. Also, as the buttons indicate,

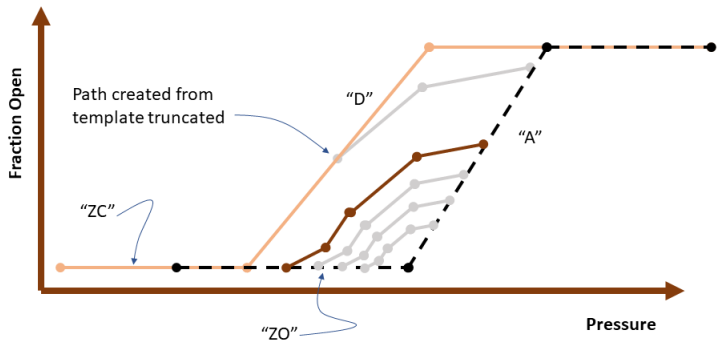

Figure 12.9: Multiple examples of actual paths that might be generated by a template during a simulation, including one path that intersects with another path.

all paths can be hidden or shown. Individual paths can be hidden or shown by right clicking them in Section 2. Key operations for the model development are accessed through a right click in Section 4's plot area. This right click operation in Section 4 is very important because it provides some of the key operations, especially pressure direction applicability, the designation of reverse segments, and the establishing of templates.

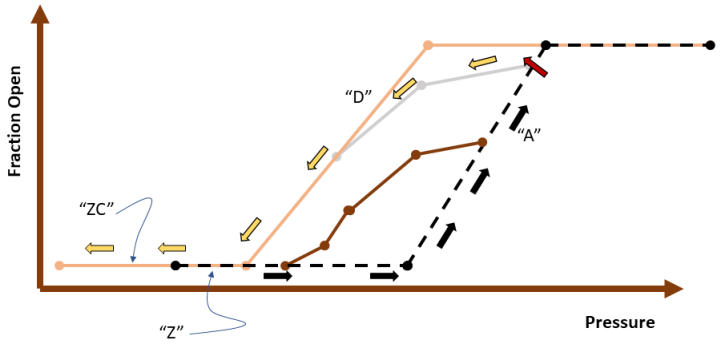

Figure 12.10: A template-generated path, which intersects with a non-template path in use. Notice that the non-template path (the gold path, segment "D") takes over upon intersection.

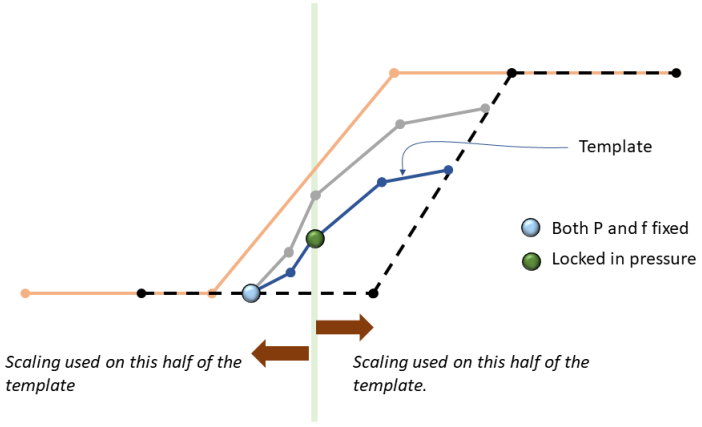

Figure 12.11: Use and effect of "lock points".

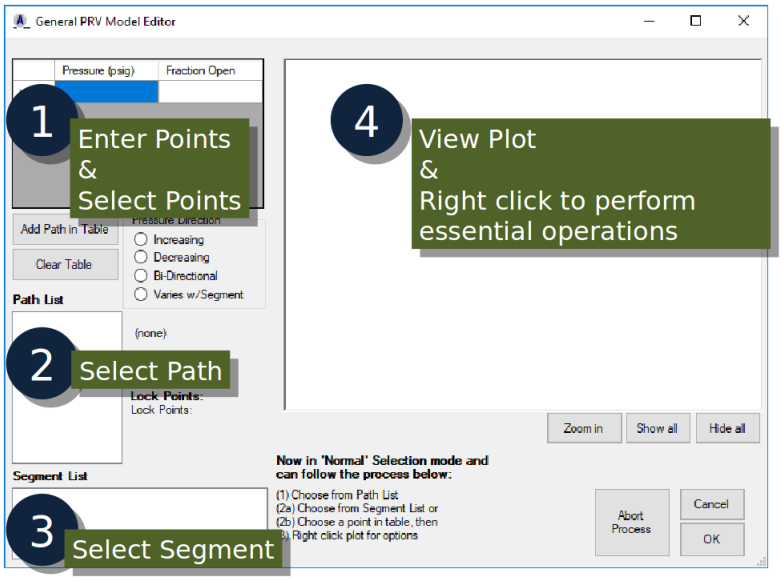

Figure 12.12: Basic layout of the Generalized PRV editing window.

Chapter 13

Modeling Flow Physics through a Relief Device

13.1 Required Input Values

As mentioned in Section 11.1, AFFTAC's Basic PRD Model and Advanced PRD Model both use the same physics models for flow of lading through the PRD. What distinguishes them is their models for the extent to which the PRD is open. Thus, they have the same input values for modeling the flow physics of a PRD. Those values are required for any PRD and are summarized in Table 13.1. The values in Table 13.1 are combined with some of the lading's thermodynamic properties, which also govern how the lading flows through the PRD. A more thorough understanding of the PRD input values and the role of the thermodynamic properties are provided in this chapter.

13.2 Summary of Flow Scenarios

There are four different scenarios in which the tank car can lose lading through the PRD. They are illustrated in Figure 13.1 and summarized in Table 13.2. In the two cases where vapor alone is being ejected, the classical model for choked vapor flow, described in the next subsection is used. In the two cases where liquid is being ejected, the Bernoulli equation is applied. But the possibility that some of the liquid might evaporate during that process could result in two-phase flow, which is also accommodated. In that case, a two-phase isentropic, inviscid flow model is used.

The flow models for choked flow and two-phase flow are discussed in the following subsections. A summary of the mass transport scenarios is tabulated below. The *Programmer's Guide to the Computational Module's Unit Tests* document describes some of the subtleties and provides more information on the flow models; see Section 2.1 of this manual.

As mentioned above, AFFTAC has the ability to estimate the discharge area of the PRD. The choked flow model, which is used for vapor discharge, is also used for that purpose. Therefore, the choked flow model is described first. Then the liquid and two-phase discharge models, which require information about area, are described.

13.2.1 Choked Flow Model

If the total pressure within the tank is greater than 27.0 psia, 12.3 psig, the flow of vapor through the relief device can be modeled as choked flow. The value of 12.3 psig is the pressure required to sustain choked flow. The classical equation for choked flow of a compressible gas flow through a nozzle is therefore used. That model is derived in detail in Appendix C and is

$$w = 144 C_{DV} A_v P \sqrt{\frac{g\gamma}{ZRT}\left[\frac{2}{\gamma+1}\right]^{(\gamma+1)/(\gamma-1)}} \tag{13.1}$$

Input Value	Applies To	Description
Rated Flow Capacity	Valves	This value describes the amount of air vapor that the PRV can discharge when tested at a specific pressure, which is the "Rating Pressure."
Rating Pressure	Valves	This is the pressure at which the PRV was tested to determine its rated flow capacity.
Vapor Discharge Coefficient	Valves and Vents	This is a coefficient used to make the flow model more accurate for modeling vapor flow. Because of various obstructions and geometries unique to each PRD, this coefficient is specific to a PRD type.
Liquid Discharge Coefficient	Valves and Vents	This coefficient has the same meaning as the Vapor Discharge coefficient but is for liquid discharge.
Discharge Area	Vents	This is the area through which the lading flows when a vent is the PRD. Note that for a valve, the area is estimated from the rated flow capacity whereas for vents it is entered directly. This aspect is different and is generalized in the Advanced PRD Model.
Closure Disk Burst Pressure	Vents	This is the analog of the start-to-discharge pressure for valves. The difference is that for a vent, once it ruptures, it never closes.

Table 13.1: Parameters used in modeling the physics of lading (vapor or liquid) flow through PRDs

where

$$
\begin{aligned}
w &= \text{mass flow rate } \left[\frac{\text{lbm}}{\text{sec}}\right] \\
A_v &= \text{minimum cross-sectional area of the valve } \left[\text{ft}^2\right] \\
C_{DV} &= \text{valve discharge coefficient} \\
P &= \text{upstream gas pressure (psia)} \\
T &= \text{upstream gas temperature (absolute) [R]} \\
g &= \text{gravitational constant } \frac{\text{ft}}{\text{sec}^2} \\
Z &= \text{gas compressibility factor} \\
R &= \text{gas constant, equal to 1,545/(molecular weight) ft/deg-R} \\
\gamma &= \text{ratio of specific heats}
\end{aligned}
$$

Most of the terms in the above equation are constants and are therefore separated into a single value. Specifically, the constant V_{con} is defined as follows:

$$V_{con} \equiv 144\sqrt{\frac{g\gamma}{R}\left[\frac{2}{\gamma+1}\right]^{(\gamma+1)/(\gamma-1)}} \tag{13.2}$$

Tank Contents	Flowing Out	Supporting Model
Liquid and Vapor	Vapor	Choked Flow or Low-Speed Flow
Liquid and Vapor	Liquid	Two-Phase Flow
Liquid	Liquid	Liquid or Two-Phase Flow
Vapor	Vapor	Choked Flow or Low-Speed Flow

Table 13.2: Models used for PRD flow scenarios.

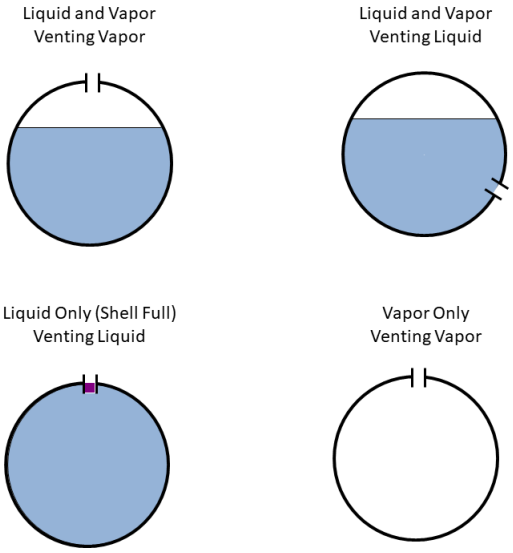

Figure 13.1: Illustration of the four different scenarios for lading release

so that the first equation for the mass flow rate may be written

$$w = V_{con} \frac{C_{DV} A_v p}{\sqrt{ZT}} \tag{13.3}$$

The above equation is used for each constituent in the vapor, where p becomes the constituent's partial pressure, p_i. The effect of the padding gas on the mass flow rate becomes negligible after a short period of time, because its mass is small compared to that of the lading.

In this model and the ones that follow, the above equation is multiplied by the "fraction open", which varies between zero and unity. The fraction open parameter is used to model the opening and closing of valves and has a model of its own, and is the distinguishing feature of AFFTAC's Basic PRD Model and its Advanced PRD Model. See Section 11.2 and Chapter 12 for extensive discussion on how to model the fraction open of PRVs in AFFTAC.

13.2.2 Estimation of the PRD's Area using the Choked Flow Model

The choked flow model can be used in AFFTAC to compute the minimum cross-sectional area of the PRD. It uses experimental data entered by the user, specifically, the "rated flow capacity", "rating pressure", and "coefficient of vapor discharge" as described in Table 13.1. It is assumed that the experimental data was obtained using air at room temperature. For air under those conditions, Z = 1.0, $\gamma = 1.4$, R = 53.3 ft-lbf/lbm-deg-R, T = 519.7 deg-R (60 deg-F). Also, in those conditions, the density of air is 0.0763 $\left[\frac{\text{lbm}}{\text{ft}^3}\right]$, which is a required value because the rated flow

capacity is given in cubic feet per minute. Substituting those values into Equation 13.3 the above equation produces the following estimate for the valve area which appears in this form in the Computational Module:

$$A_v = \frac{m_r}{C_{DV} p_s 2644} \tag{13.4}$$

However, there is a non-trival amount of units conversion embedded in this equation. See Appendix E for the derivation.

13.2.3 Low Speed Vapor Flow

If the total pressure within the tank is greater than atmospheric pressure (14.7 psia), but less than 12.3 psig, the flow can no longer be considered choked. In these cases, the amount of vapor flow produced during a choked condition is computed and then scaled downward accordingly.

13.2.4 Two-Phase Flow

When liquid escapes through the pressure relief device, its pressure and temperature drops, possibly leading to the creation of some vapor from the liquid state. The resulting situation is known as "two-phase flow" and can occur any time liquid is being ejected.

The model for two-phase flow assumes that the flow is inviscid, which means that the Bernoulli equation can be applied along any streamline. The streamline that flows through the middle of the relief device is chosen for the analysis. For any two points, 1 and 2, on the streamline, the Bernoulli equation states that

$$V_2^2(p_2) = V_1^2 + 2g \int_{p_1}^{p_2} \frac{dp}{p} \tag{13.5}$$

where V is the speed at those points and p is the pressure. Since the pressure is a function of temperature, the above integral may be rewritten as

$$V_2^2(p_2(T)) = V_1^2 + 2g \int_{p(T_1)}^{p(T_2)} \left(\frac{dp}{dT}\right) \frac{dT}{\rho(T)} \tag{13.6}$$

For this analysis, Point 1 is assumed to be located far from the opening so that, when there is no padding gas present, V_1 can be assumed to be zero. When padding gas is present, the saturated condition of the liquid flow through the valve will be reached after the fluid has been given some velocity. In this circumstance, the initial velocity is approximated as

$$V_1 = \sqrt{\frac{2gp}{\rho}} \tag{13.7}$$

In either case, V_1 is known and so is $p(T_1)$, which is the bulk pressure inside the tank.

For any value T_2, which corresponds to some unknown position along the streamline, the above integral can be used to compute the speed $V_2(p_2)$ at a second point. The objective is to find the temperature T_2 that corresponds to the point along the streamline where the cross-sectional area of the flow is a minimum. When that point is found, it is used to compute the mass flow rate.

Point 2 is found using the above integral with the help of an additional constraint, which is that the entropy of the liquid-vapor mixture is assumed to be constant. The integral form of the Bernoulli equation, plus the constraint of isentropy provides the theoretical backbone of the algorithm to compute two-phase flow through the relief device. The integral in Equation 13.6 is approximated by this summation:

$$V_2^2 = V_1^2 + 2g \sum_{i=1}^{?} \frac{1}{\rho(T_1 + i\Delta T)} \frac{dp}{dT} \Delta T \tag{13.8}$$

where "?" denotes the to-be-determined upper limit of the integration/summation. The summation is not carried out at once, but instead in a step-by-step fashion. Because of the temperature-pressure relationship, each addition of a term in the summation represents a small step along the streamline. At each step, the specific entropies (recall $\Delta S = \Delta Q/T$) of the liquid and vapor are computed as follows:

$$\text{Liquid State: } S_L(T) = S_{L1} - c_{p-liq}\frac{T - T_1}{(T + T_1)/2}$$
$$\text{Vapor State: } S_V(T) = S_L(T) + \frac{H_v}{(T + T_1)/2} \tag{13.9}$$

Where c_{p-liq} is the liquid's specific heat and H_v is the heat of vaporization. Based on the assumption of isentropy, the

$$\text{Combined total entropy: } S(T) = \lambda S_L(T) + (1 - \lambda)S_V(T) \tag{13.10}$$

must remain constant; λ is the mass fraction of the liquid, which can change. Therefore requiring

$$S(T) = \lambda S_L(T_i) + (1 - \lambda)S_V(T_i) \tag{13.11}$$

at each step allows the ratio λ to be computed at each step. With the value obtained for $V(T_i)$ and the ratio λ , which allows for the density to be computed, the cross-sectional area at step i can be computed.

Calculations proceed for $i = 1, 2, ...,$ at each step computing λ and the cross-sectional area. When the cross-sectional area reaches a minimum value, the computations are stopped. That cross-sectional area is used with the speed and density computed at that point to provide the estimate for the mass flow rate for the two-phase flow.

However, as with the other flow models, e.g., the choked vapor flow model, if the PRD is a valve, the resulting cross-sectional area is multiplied by the "fraction open" parameter to represent the opening and closing of the valve. The model for the fraction open parameter is provided in a later section.

For alternative wording describing this model, you might also find it helpful to consult the chapter on PRV flow model validation in the *AFFTAC Verification and Validation Testing* document. See Section 2.1 of this manual for important information on that topic.

13.2.5 Liquid Ejection in the Shell Full Condition

AFFTAC provides two different models for the shell full condition. Each are explained in the subsections below. A discussion of how the models compare and how to choose which one to use, is presented after that.

Basic Model

The shell full condition occurs when the tank is completely full of liquid. As the liquid continues to heat and expand, the volume it would occupy if unconstrained by the tank would exceed the volume of the tank. In that scenario, the Basic Shell Full Model assumes all of the excess liquid is ejected during the current time step. From that assumption, the Basic Model computes the flow rate over the time step that would be required to accomplish the expulsion of that excess volume. And from that flow rate, it computes the pressure inside the tank that would be required to accomplish said flow. Details for those computations follow.

The specific volume, which is specified as a function of temperature by the user, is used to compute the expansion that would occur when heated if the liquid were completely unconstrained. The volume of the tank is subtracted from that volume and divided by the time step length to determine a flow rate. Then, the Bernoulli equation is used to provide an estimate of the pressure required to expel that amount during the time step. For this situation, which is depicted in Figure 13.2, the Bernoulli equation is

$$\frac{1}{2}\rho V_s^2 = g(p_c - p_s), \tag{13.12}$$

where the velocity V_s is related to the mass flow rate through the following relationship [1]

$$V_s = \frac{\text{Mass Flow Rate (lbs/sec)}}{\text{Liquid Discharge Coefficient} \times \text{Device Opening Area} \times \text{Density}(\text{lbs}/\text{ft}^3)} \tag{13.13}$$

all of which are known, p_c is the upstream pressure, and p_s is the terminal pressure on exit. The value of p_s is taken to be the saturated vapor pressure or the atmospheric pressure, whichever is higher. [2] Once p_c is computed, it is used to determine what type of flow conditions exist. The final form of the equation used to compute the pressure required to produce sufficient lading ejection is

$$\hat{p}_{com}\left[\frac{\text{lbf}}{\text{ft}^2}\right] = \hat{p}_{min}\left[\frac{\text{lbf}}{\text{ft}^2}\right] + \frac{1}{64.4 v_{liq}}\left(\frac{Q_{liq}}{720 \cdot C_{DL} \cdot A_{areq}}\right)^2 \left[\frac{\text{lbf}}{\text{ft}^2}\right] \tag{13.14}$$

where

$\hat{p}_{min}$ Taken to either atmospheric pressure or the lading vapor pressure, whichever is less

Q_{liq} The amount of lading that must be ejected

A_{areq} The area of the pressure relief device

C_{DL} The liquid discharge coefficient

The hard-coded numbers in the above equation are to handle units and mass-to-volume conversion. A thorough derivation of that equation is given in Appendix F.

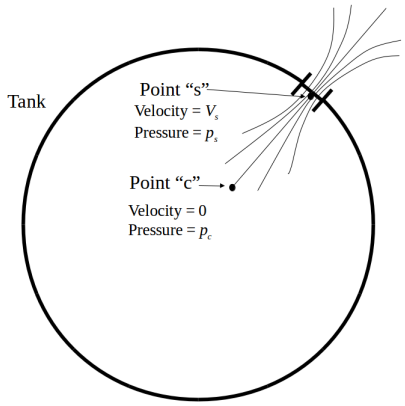

Figure 13.2: Configuration representing the expulsion of liquid due to thermal expansion while in the shell full condition

In addition to determining the pressure required to expell the lading, the model attempts to determine if any *additional* lading is expelled during the current time step. In one case, if p_s is not sufficiently high, the flow through the relief device is assumed to be in the liquid phase. It is assumed that the device will accommodate the amount of mass flow, but no more than that will leave. Therefore, the tank will remain shell full having expelled exactly the amount that is due to thermal expansion. This situation occurs for a vent if $p_s < p_{atm}$ (atmospheric pressure) and as a result, the total pressure inside the tank is set to p_{atm}. Likewise, this situation occurs for a valve if $p_s < P_{\text{close}}$ (valve closing pressure) and as a result, the total pressure in the tank is set to P_{close}.

If p_s is sufficiently high (greater than p_{atm} for a vent or greater than P_{close} for a valve) and the tank is sufficiently rolled over, it is assumed that two-phase flow occurs. In this situation, the two-phase flow model discussed previously

[1] See Appendix C for a discussion on the use of the liquid and vapor discharge coefficients.

[2] Consideration of two-phase flow effects for high vapor pressure ladings might result in a slightly lower tank pressure, but the difference would be small.

is invoked to determine the mass flow rate. If, in the case of an upright car, enough lading can be expelled in the vapor phase so that the tank will not be shell full at the end of the time step, the tank is no longer considered to be shell full and a logical flag in the program is set to record that fact. Otherwise, the simulation continues cconsidering the tank to be shell full.

13.2.6 Dynamic Shell Full Model

An alternative to the Basic Shell Full Model's method for computing the internal pressure is the Dynamic Shell Full Model, which is a direct mechanical simulation of the stress balance between the liquid, when compressed by the tank, and the tank when expanded by the liquid.

To begin developing the ideas of the model, we write down the volume of the tank when it has been expanded due to thermal expansion, elastic stress, and creep (if included). That equation is developed in chapter 14. We repeat that equation (Equation 14.16) here, for convenience:

$$V_{Te}(p_g) = V_0(1 + \epsilon_c(p_g) + \epsilon_{creep})^2 \left(1 + \epsilon_a(p_g)\right) \left(\frac{1 + \alpha T}{1 + \alpha T_o}\right)^3 \tag{13.15}$$

Again, this equation is derived in the aforementioned chapter. But for now, we simply recognize that the internal gauge pressure inside the tank, p_g, generates circumferential strain ϵ_c and axial strain ϵ_a, which result in a volume change beyond V_o, which is the tank's original volume. In the Dynamic Shell Full Model, the above equation will become part of an algorithm that seeks a value for p_g such that $V_{Te}(p_g)$ is equal to the volume of the liquid, which in turn will also be compressed by that same pressure. The liquid compression is considered next.

The volume that the liquid would take on naturally, if unconstrained, is obtained by multiplying its mass, m, by its specific volume $v(T)$, which is a thermodynamic property entered by the user. So, the unconstrained volume of the liquid would be

$$V_l = mv(T) \tag{13.16}$$

When $V_l > V_{Te}$, the liquid will exert pressure on the tank and vice-versa. The liquid's bulk modulus K relates a volume change ΔV in the liquid to the pressure required to produce that change. Its definition is,

$$K = -V_l \frac{\Delta p}{\Delta V_l} \tag{13.17}$$

Thus, using K, we have a way to compute the effect of the pressure on the volume change for the liquid. Rearranging Equation 13.17,

$$\Delta p = -\frac{\Delta V_l}{V_l} K \tag{13.18}$$

where we take $\Delta p = p - 0 = p$. Requiring that the liquid fit into the volume, V_{Te}, accommodated by the tank means that the volume change asked of the liquid in order to fit inside the tank is

$$\Delta V = V_{Te} - V_l = V_{Te} - mv(T) \tag{13.19}$$

Using that result in Equation 13.18, produces

$$p = -\left(\frac{V_{Te} - mv(T)}{mv(T)}\right) K \tag{13.20}$$

or, by rearranging it,

$$V_{Te} = mv(T)\left(1 - \frac{p}{K}\right) \tag{13.21}$$

Expressing absolute pressure, p using gauge and atmospheric pressure while also recalling that V_{Te} is a function of gauge pressure produces the following from Equation 13.21:

$$V_{Te}(p_g) = mv(T)\left(1 - \frac{p_g + p_{atm}}{K}\right) \tag{13.22}$$

Equation 13.22 represents the balance between the pressure contained by the tank and the pressure generated by the liquid. The strength of the tank is represented by E embedded in the expression for V_{Te} in Equation 13.15 while the liquid's resistance to compression is represented by K. Given the temperature, T, and the various material and geometric properties (E, K, r, and t_w), the nonlinear equation above can be solved for p_g to determine the compromise pressure reached by the liquid and tank in compromising with each other.

As with the Basic Shell Full Model, the Bernoulli equation is then used determine the liquid flow rate:

$$p + \frac{1}{2}\rho(0)^2 = p_{atm} + \frac{1}{2}\rho U^2 \tag{13.23}$$

The left-hand-side of the above equation is on the inside of the tank, where the velocity is zero, while the right-hand-side is at the exit. Rearranging, and using the definition of gauge pressure as well as the fact that $v(T) = 1/\rho$,

$$U = \sqrt{2v(T)p_g} \tag{13.24}$$

Dividing by specific volume (which is the same as multiplying by density), multiplying by the area of the PRV and its coefficient of liquid discharge converts the velocity above to mass flow rate, i.e.,

$$\dot{m} = \sqrt{\frac{2p_g}{v(T)}} A_{PRV} C_{DL} \tag{13.25}$$

Equation 13.25 can be integrated in time to give the mass of the liquid during the shell-full venting scenario. In this model, the value for $\dot{m}$ is therefore based on the mechanical interaction of the tank wall with the liquid, as opposed to the Basic Shell Full Model where $\dot{m}$ is computed by simply assuming the difference in the tank's and liquid's volume is expelled during each time step. The other caveats and flow models described for the Basic Shell Full Model are still considered when using the Dynamic Shell Full Model.

Dynamic Shell Full Model versus the Basic Shell Full Model

Initial studies have shown that the two models produce roughly the same pressures and flow rates. However, the Basic Shell Full Model exhibits spurious oscillations in release rate. The Dynamic Shell Full Model does not exhibit oscillations, but if the time steps are not chosen to be small enough, the Dynamic Shell Full Model appears to under-predict tank life. It is recommended that you try both models and compare them. Be sure to decrease the time step to ensure you have a converged solution in both cases.

Chapter 14

Models for Internal Pressure, Stress, and Strain

14.1 Modeling Pressure Inside the Tank

The pressure of the vapor lading, when present, is computed using the partial pressures of the vapor's constituents. For ladings that are a pure substance, the total vapor pressure is the sum of the vaporized lading's pressure plus that of the padding gas, if present. For a binary solution, it is the sum of the partial pressures of the solution's vaporized constituents plus the pressure of the padding gas.

When the quantity of liquid in the tank is very small, the remaining vapor is treated as an ideal gas. The temperature from the previous time step is used, thereby immediately allowing the computation of the vapor pressure p_i.

When the quantity of liquid in the tank is not small, the vapor is assumed to be saturated. The partial pressures of the lading's constituents are computed using pressure-versus-temperature data that you enter in tabular form in the Ladings Resource. That data is queried through quadratic interpolation during the simulation.

It is assumed that the padding gas first achieves an initial state of equilibrium before the fire event, but after that no further mass exchange occurs between the padding gas in the vapor and the liquid lading, which is to say that the padding gas is assumed to never diffuse into or out of the liquid, regardless of the pressure. Once the relief device has opened, the padding gas pressure is calculated from the mass of the padding gas remaining in the tank and its temperature.

Aside:

The assumption described above is believed to have little or no impact on the simulation results. The primary reason for it is the little likelihood that equilibrium conditions could ever be attained during the course of the fire. There would not be sufficient time for the effect of the padding gas' partial pressure to be communicated to all portions of the liquid within the tank for the gas to be absorbed or liberated quickly enough.
Additionally, the assumption is believed to produce a conservative estimate for the padding gas pressure even though it has counteracting impacts. Specifically, during the initial stages of heating, allowing mass exchange to maintain equilibrium would cause there to be an increase in the amount of gas in the liquid phase caused by the initial expansion of the liquid phase due to heating. That dissolution into the liquid phase would lead to a decrease in the padding gas' partial pressure. However, counteracting that effect is the fact that, if mass exchange were allowed, then after the initial opening of the safety relief device, the decrease in pressure would lead to liberation of the padding gas from the liquid phase, causing an increase in vapor pressure and an increased flow rate through the valve.
Therefore, no mass exchange of the padding gas between the vapor and liquid phases would on the one hand delay the time at which the relief device opens, but on the other hand increase the pressure after the lading begins to flow through it. To some extent, these effects would probably counteract each other. Regardless, when the space occupied by the vapor reaches approximately 10%, the effect of the padding gas becomes insignificant on the prediction of flow through the relief device.

As mentioned above, when the amount of liquid is small, the pressure of the padding gas is computed using the ideal gas law, still holding to the assumption of no mass exchange between the liquid and vapor phases. The user's inputs for the padding gas' initial pressure, initial volume occupied by the vapor, and initial temperature are used in conjunction with the current volume and current temperature to compute the current pressure. The embodiment of this law is expressed in:

$$p_{pad}(t) = p_{pad}(0) \times \frac{1 - f(0)}{1 - f(t)} \times \frac{T_{lading}(t)}{T_{lading}(0)} \times \frac{w_{pad}(t)}{w_{pad}(0)} \tag{14.1}$$

where $p_{pad}(t)$ is the pressure of the padding gas at time, t, $f(t)$ is the fraction of the tank filled with liquid at time, t, and $w(t)$ is the weight of the padding gas at time, t. In all cases, the padding gas pressure is never allowed to be negative. The proprietary *Programmer's Guide to the Computational Module's Unit Tests* contains more information. See Section 2.1 of this manual regarding that document.

14.2 Modeling Tank Deformation

The volume of the tank becomes an important factor in the shell full condition, i.e., the situation in which the tank is completely filled with liquid. The shell full condition can occur as an initial condition, but can also occur due to the thermal expansion of the liquid. In the shell full situation, the physics for the tank stress and tank-lading interaction change significantly. See, for example, section 13.2.6.

The volume of the tank changes due to three factors: (1) Thermal expansion, (2) Elastic strain, and (3) Creep. The first two are recoverable. In other words, if the temperature is returned to the tank's initial temperature and the internal pressure is eliminated, the contribution of those two effects disappear. The third is not recoverable. Also, the first two are always included in an AFFTAC calculation, whereas the third is included only if the user selects it through the Advanced Strength Model. The ideas behind these three effects are developed below.

14.2.1 Thermal Strain

A linear thermal expansion law is used as the basis for the thermal strain computation. It is that

$$L(T) = L_{ref}\left[1 + \alpha(T - T_{ref})\right] \tag{14.2}$$

where $L(T)$ is the length of an object as a function temperature T, L_{ref} is the length at a reference temperature T_{ref}, and α is the coefficient of thermal expansion. The ratio of lengths at two different temperatures is therefore

$$\frac{L(T_2)}{L(T_1)} = \frac{1 + \alpha(T_2 - T_{ref})}{1 + \alpha(T_1 - T_{ref})} \tag{14.3}$$

T_{ref} can be taken to be zero with no loss of generality. Therefore, the relationship reduces to

$$\frac{L_2}{L_1} = \frac{1 + \alpha T_2}{1 + \alpha T_1} \tag{14.4}$$

If T_1 is taken to be the initial temperature of the tank, then the above ratio represents the ratio of the hot length to the cool length, i.e., the thermal strain,

$$R_T(T) = \frac{1 + \alpha T}{1 + \alpha T_{init}} \tag{14.5}$$

14.2.2 Elastic Strain

The tank can also expand due to internal stresses imposed by the pressure building up inside. As shown in Figure 14.1, the pressure differential represented as p in the figure is balanced by the circumferential stress inside the tank wall. Through geometrical considerations, the following stress balance in the radial direction can be written:

$$2\sigma_c t_w \frac{\Delta\theta}{2} = p \cdot r \frac{\Delta\theta}{2} \tag{14.6}$$

Canceling terms and using half the diameter ($d/2$) instead of radius, r, produces

$$\sigma_c = \frac{p \cdot d}{2t_w} \tag{14.7}$$

In a similar way, the axial strain can be related to the internal pressure by writing a stress balance in the axial direction. Referring to Figure 14.2, the balance of stresses requires that

$$(\pi r^2)p = \sigma_a t_w (2\pi r) \tag{14.8}$$

In terms of diameter,

$$\sigma_a = \frac{dp}{4t_w} \tag{14.9}$$

The axial and circumferential stresses derived above are related to the corresponding strains through Hooke's law of elasticity

$$\epsilon_c = \frac{\sigma_c}{E} - \nu\frac{\sigma_a}{E} \tag{14.10}$$

$$\epsilon_a = \frac{\sigma_a}{E} - \nu\frac{\sigma_c}{E} \tag{14.11}$$

where E is Young's modulus and ν is Poisson's ratio.

The thermal strain, circumferential strain, and axial strain all contribute to a change in volume of the tank car. The thermal strain acts in all three directions and so the change in volume depends on it to the third power. The circumferential strain will act only on the circular cross section and so the change in volume depends on it to the second power. The axial strain only acts in one direction. Therefore, the new volume is due to elastic and thermal strain is modeled as

$$V_T(p_g) = V_0\left(1 + \sigma_c(p_g)\right)^2\left(1 + \epsilon_a(p_g)\right)\left(\frac{1 + \alpha T}{1 + \alpha T_o}\right)^3 \tag{14.12}$$

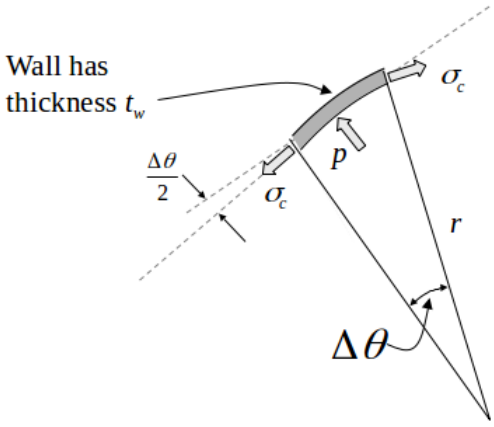

Figure 14.1: Circumferential stress in the tank wall and its relationship to the pressure differential

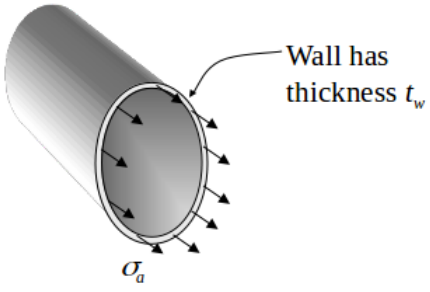

Figure 14.2: Axial stress in the tank wall

14.2.3 Creep Strain

Creep strain differs from the previous two strains already discussed because it is not recoverable. It grows over time during the simulation and never decreases. In this section, we describe how AFFTAC computes the accumulated creep strain by expanding upon the ideas of the Larson-Miller model covered in chapter 10.

During the type of experimental testing that is performed to determine the Larson-Miller parameter used in chapter 10, note may also be made of the creep strain that occurs just before failure. Here, we call that the "creep failure strain," and we consider it to be a function of temperature. Note that while $\Delta\epsilon$ in the Larson-Miller model (e.g., in Figure 10.6) is considered a constant, the actual creep failure strain is not a constant. Rather, it is a function of temperature because it includes the initial and tertiary phases of creep, which are not part of the Larson-Miller model.

To make use of creep failure strain data, we assign a new, additional role to the Life Used function, which was developed in chapter 10. Shown in Figure 14.3 is a typical plot for the Life Used during an AFFTAC simulation. The sudden rise from near zero to unity is related to the fact that both the Larson-Miller parameter, which is a function of stress, and temperature appear as exponent terms on the number 10 in the equation for time to failure, t_f (see Equation 10.8). Thus, once the pressure-temperature combination reaches a critical value, t_f shortens significantly and, being in the denominator of Equation 10.12, causes a sudden and drastic increase from near zero to near unity. We use $L(t)$ as a surrogate function with which to model the accumulation of the creep strain by asserting that

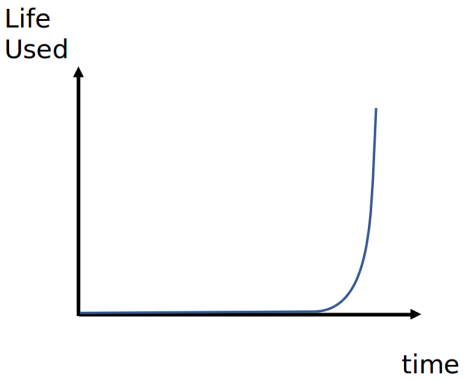

Figure 14.3: General trajectory for the "Life Used" value during an AFFTAC simulation.

$$\epsilon_{creep}(t) = L(t) \cdot \epsilon_f\left(T(t)\right) \tag{14.13}$$

where $\epsilon_{creep}(t)$ is the permanent strain due to creep and $\epsilon_f(T)$ is the experimentally measured creep strain at failure. This value of creep strain may then be added to the elastic strain when computing the tank's volume change. There are some choices to be made, however, regarding how that strain is added.

To begin that discussion, we must refer to Equation 14.12, where the volume of the tank car is computed in a way that considers the elastic deformation as well as the thermal expansion. That equation is based on the notion that the end caps do not restrict the volumetric expansion. Specifically, the change in radius, which is refected by the

$$(1 + \epsilon_c)^2 \tag{14.14}$$

term, is used to impact the circular cross section for the entire length of the tank. Doing so is an approximation, because it ignores the restriction of circumferential expansion that would be imposed by the end caps. This approximation is one we will bear in mind when considering how and where to add creep strain to elastic strain.

A second point to consider is how the creep strain is computed. In the preceding section, stress (σ) is used but there is no mention of which stress it represents. Since hoop stress is larger than axial stress, hoop stress had always been used in AFFTAC to determine if failure occurs. That same vein of reasoning was used when implementing the Larson-Miller model, specifically, $\sigma = \sigma_c$. Thus the resulting creep strain would also be in the circumferential direction.

It would be possible to implement a second computation for the Life Used value, specifically for the axial direction, say $L_a(t)$, which would be based on axial stress, and use that to compute an axial creep strain. However, there may be reasons why computing that strain and adding it to the axial elastic strain may be non-conservative. One of those reasons is end cap effects.

As mentioned above, the elastic volume expansion models the impact of hoop strain uniformly down the length of the tank, without considering the restriction that might be imposed by the end caps. In the case of creep strain, which will be much larger, it might be prudent to refrain from making that same uniform application because the impact of the end caps might be even more severe. And yet, it is difficult to know how to curtail the impact of creep strain in

the circumferential direction as the end caps are approached. Thus, a compromise is to not apply creep in the axial direction, but only in the circumferential direction, yet do so uniformly.

Lastly, like the Life Used quantity, $L_i(t)$, creep strain (ϵ_{creep}) is a function of position around the circumference of the tank. Thus we introduce a subscript for it as well so that $\epsilon_{creep_i}(t)$ is the creep strain at point i (i degrees from the bottom of the tank). It is anticipated that the top part of the tank, the part exposed to vapor and which therefore gets much hotter, will have a more rapidly progressing $L_i(t)$ and $\epsilon_{creep_i}(t)$. It would likely be an observable deformation in the curvature in the top part of the tank. Meanwhile, in the lower part of the tank, the temperature will be much lower so that the values for $L_i(t)$ and ϵ_{creep_i} will be much smaller. So, creep strain will be non-uniform around the circular cross-section of the tank.

Moreover, the deformation caused by creep would also be subject to the same restraints imposed by the end caps. Thus, not only would the creep strain be non-uniform around a circular cross section, it would be non-uniform along the axis of the tank. Outside of a 3D model of the tank wall, it is difficult to know how to properly treat this non-uniformity in creep strain along the axis, and also around the circumference. In AFFTAC, the creep strain around the circumference is averaged, and that average circumferential creep strain is added to the elastic circumferential strain in the volume calculation, i.e., it is applied uniformly along the axis. This treatment is consistent with the elastic strain treatment, except that it is not also added to the axial strain, as a compromise for the fact that the constraint imposed by the end caps might be quite significant.

So, in summary, a single circumferential creep strain is computed as

$$\overline{\epsilon}_{creep} = \frac{1}{180}\sum_{i=1}^{180}\epsilon_{creep_i}(t) \tag{14.15}$$

Therefore, including the creep strain in Equation 14.12 gives us this approximation for the tank volume:

$$V_T(p_g) = V_0\left(1+\epsilon_c(p_g)+\overline{\epsilon}_{creep}\right)^2\left(1+\epsilon_a(p_g)\right)\left(\frac{1+\alpha T}{1+\alpha T_o}\right)^3 \tag{14.16}$$

Chapter 15

Numerics

Some of the core conservation models in AFFTAC manifest themselves as first order ordinary differential equations. For example, Equation 5.13, which is the transient equation for the lading temperature, is such an equation. AFFTAC uses a step-wise transient approach known as the Forward Euler method with nonlinear lagging to solve that transient equation, as well as the other transient heat and mass conservation equations. In the Forward Euler method, the time derivative is estimated as follows, for example:

$$\frac{dT_{lading}}{dt} \approx \frac{T_{lading}^{new} - T_{lading}^{old}}{\Delta t} \tag{15.1}$$

By substituting this approximate derivative, an equation for T_{lading}^{new} is obtained. That equation uses values of the other temperatures from the previous time step, e.g., T_{lading}^{old}. The overall conceptual flow chart of the AFFTAC computations shown in Figure 3.1, illustrates the presence of the Forward Euler method.

15.1 Dampening

The advantages and disadvantages of the Forward Euler method have been clearly discussed in the literature. The advantages are that it eliminates the need to solve nonlinear equations. Specifically, at each time step, the previous time step's solution is used to extrapolate forward in time, also described in chapter 3. The disadvantage is that if the time step is too large, the extrapolation can cause the solution to overshoot acceptable bounds and be unstable.

As a simple example of this phenomenon, consider two stacked blocks of wood, A and B, where A is hotter than B. Because A is hotter, heat flux will flow from it to B. The amount of heat flux is proportional to their temperature difference. So, in reality, as B warms up and A cools off, the heat flux falls off to zero. In a Forward Euler scheme, the initial temperature difference would be used to compute an initial flux between them. That flux would be multiplied by a time step and used to extrapolate the temperatures at the end of the time step. If the time step is not too big, the result will be that B is a little warmer and A is a little cooler. In that case, the method works fine. But if the time step is too big, the initial flux will be extrapolated out in time too long, causing B to actually become warmer than A, and A cooler than B.

This scenario is unstable and causes the simulation to fail catastrophically. One approach to solving this problem is to continue to use a larger time step but arbitrarily reduce the result obtained. The effect is to dampen the transient behavior. Although there clearly are errors associated with this approach, often an appropriate dampening factor can be used that causes the solution to be stable. Although the transient solution will be in error, the steady state solution will still be correct, unless nonlinear effects play a dominant role.

AFFTAC makes heavy use of this approach. It is manifested in the source code as a weighted average between the previous time step's solution for, say, temperature, and the prediction for the temperature at the new time step,

e.g.,

$$T^{new} = \alpha T^{old} - (1 - \alpha)\hat{T}^{new} \tag{15.2}$$

where $\hat{T}^{new}$ is the value predicted without dampening. Typically, $0.25 < \alpha < 0.5$. In addition to the thermal solution values, dampening is also used for the auxiliary models. For example, in computing the change in volume due to thermal expansion and the pressure differential, the new value for the volume is dampened using $\alpha = 1/3$.

15.2 Overshoot

A problem similar to the instability problem discussed above is that of overshoot. For example, during the choked flow computations, if the resulting pressure after discharge during the time step would be less than atmospheric in the case of a vent, or less than the valve closing pressure in the case of a safety relief valve, the out-flows are arbitrarily reduced. This compensation is required because of the consequences due to the finite time step, which may not be sufficiently accurate for rapidly changing conditions. The effect is significant only as the shell full condition is approached.

Chapter 16

Tutorial 1: A Simple Analysis

To begin this tutorial, start the AFFTAC GUI. When you do, the **Main Window** should appear, where the Analyses are displayed. In its distributed version, AFFTAC comes preloaded with several regression tests, including the example problems in [14]. For this tutorial, one of these example problems (Example 1.1) will be recreated from scratch.

Click **New** in AFFTAC's **Main Window**. Doing so will create a new entry at the bottom of the list of Analyses and will display the first of the four editing windows. In this first window select the **Standard Pool Fire** option and enter 100 for the **Length of the Simulation** entry. Leave zero as the entry for the rollover angle. When you are finished making those adjustments, the window should look like that shown in Figure 16.1.

When it does, click **Next**. Doing so displays the **Edit Tank Car Properties** window. Enter the following information:

Nominal Capacity:	33000
Inside Diameter:	112
Wall Thickness:	0.5625

Then select "AAR TC128-70, Grs. A & B Min. Tensile Strength 81 Kpsi" from the pull-down arrow. Enter the following data for the material:

Nominal Burst Strength:	750
Tensile Strength:	81000
Emissivity:	0.8

Select **Do not use** for the Dynamic Shell Full model entry area. In the lower half of the window, select the **Valve** option under **Device Type for the Safety Relief Device** option and enter the following information:

Rated Flow Capacity:	32000
Rating Pressure:	270
Start-to-Discharge Pressure:	247.5
Vapor Discharge Coefficient:	0.8
Liquid Discharge Coefficient:	0.6

When you have finished making these entries, the window should look like that shown in Figure 16.2. When it does, click **Next**. Doing so will leave you in the **Select TPS Model** window.

For this tutorial, highlight "Example 1", which is a pre-loaded TPS type. To see the data describing the insulation named "Example 1," double click on it. Doing so displays the window shown in Figure 16.3. The "Example 1"

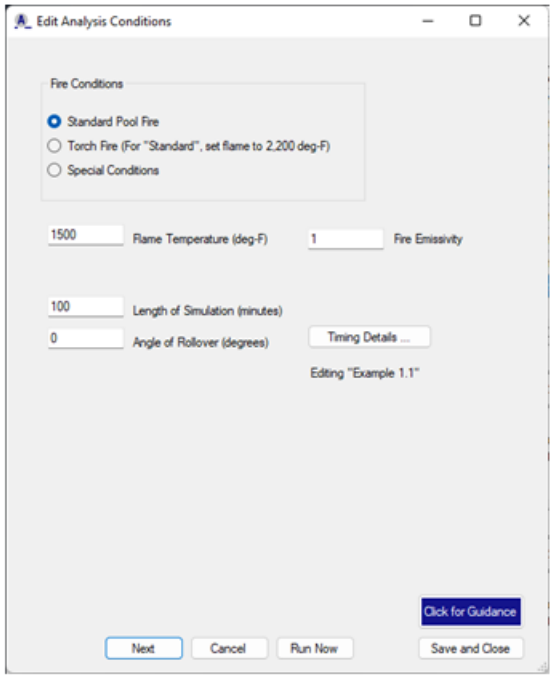

Figure 16.1: Analysis conditions for Tutorial 1

insulation type is a temperature-independent thermal protection system that is constant in time. The value of the conductance is 5.4 $\left[\frac{\text{BTU}}{\text{hr}\cdot\text{ft}^2\cdot\text{R}}\right]$.

Now, click **OK** to return to the **Select TPS Model** window. To add or delete TPS types, the Basic TPS Resources can be accessed by clicking the **Manage Basic TPS Models** button in the **Select TPS Model** window. It can also be accessed through the **Main Window** under the **Resources-Basic TPS Models** menu option.

Highlight "Example 1" in the **Select TPS Model** window, select **Consider Discontinuities**, and enter 234 for the value. Then click **Next**, which will display the fourth in the series of four editing windows. Select the lading named "Butane" and enter the following data:

Fraction of Tank Filled:	0.96
Initial Temperature:	60.

The Ladings Resource can be accessed through the **Manage Ladings** button, or the menu option **Resources-Ladings** in the **Main Window**.

The inputs you have provided in the past three windows may be reviewed using the **Previous** and **Next** buttons that are shown at the bottom of each of the four editing windows. Clicking **Cancel** would erase these changes and return you to the **Main Window**. At this point, the **Setup Lading** window should look like that shown in Figure 16.4.

When it does, click **Run Now**, which will execute the analysis and return you to the **Main Window**. To review the input as echoed by the Computational Module, scroll through the information in the middle pane of the **Main Window**.

In the left pane of the **Main Window**, look at the list of analyses. Notice that this analysis is listed at the bottom.

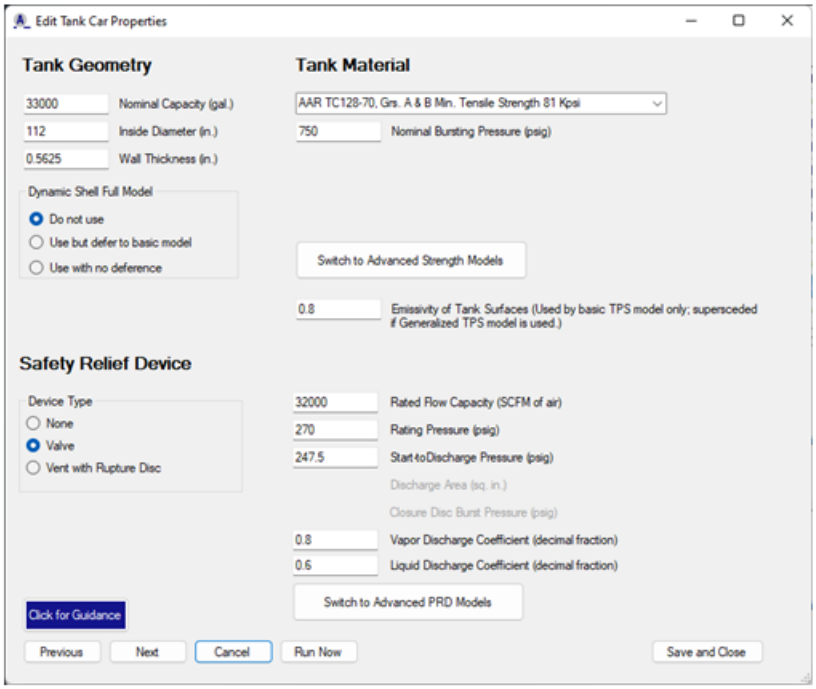

Figure 16.2: Tank car properties for Tutorial 1

In the lower part of the **Main Window**, click the **Edit Admin Data** button. Enter the following information:

Job Number:	My First Tutorial
Customer:	N/A

Click **OK** and then you can save the analysis and print the results.

Note that the default information for your name and your company name may be defined through the **Main Window**, under the menu option Options-User Information.

In the **Main Window** click the **Plot Displayed Results** button. Doing so displays the plot window shown in Figure 16.5. These plots can be cut and pasted into other Microsoft Office applications.

Then, back in the **Main Window**, select the menu item **File-Write to PDF**, which will produce a PDF file containing the simulation setup and the results.

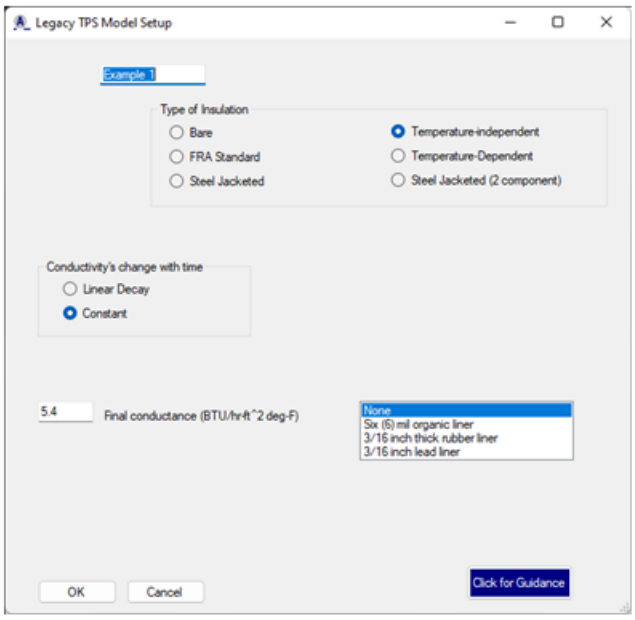

Figure 16.3: Basic TPS Model for Tutorial 1

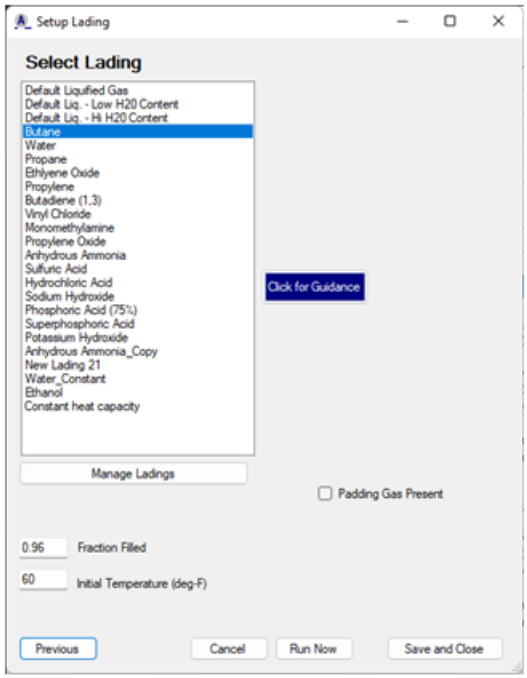

Figure 16.4: Lading setup for Tutorial 1

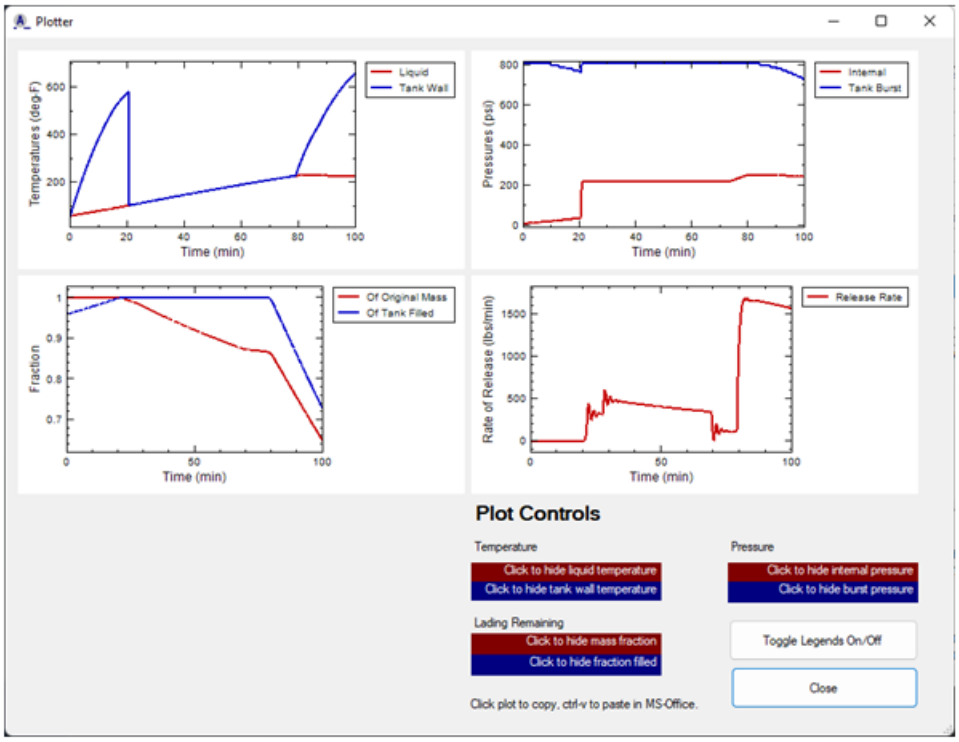

Figure 16.5: Graphical results for Tutorial 1

Chapter 17

Tutorial 2: Adding a Lading

In this tutorial, you will be guided through the process of adding a new lading to the Ladings Resource. Run the AFFTAC GUI and, once in the **Main Window**, select the menu option **Resources-Ladings**. Upon doing so, a window like that shown in Figure 17.1 will appear. In that window are listed the various ladings that are already contained in the Resource.

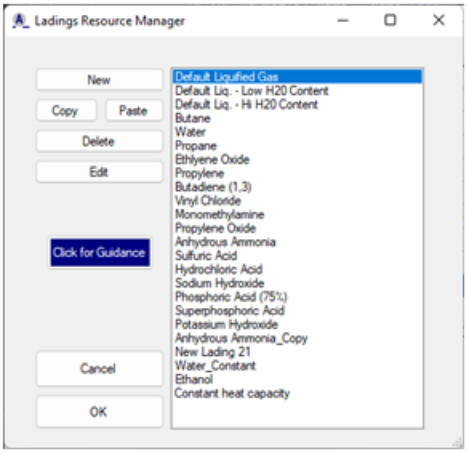

Figure 17.1: Ladings Resource

Click **New**. When you do, a new lading is added to the list and is displayed as the last entry. This new lading is merely a placeholder. It does not yet have any real data associated with it. To provide the necessary data, highlight it and click the **Edit** button.

Doing so displays the window shown in Figure 17.2. In this window, the various properties required by the AFFTAC Computational Module are displayed. First, type in the name “My Lading” in the **Name** entry box. Next, make sure that the **Pure Substance** button is selected. Note that if **Solution** is selected (try it) there are some properties that require values for both the solvent and solute, and some values are required at two concentration levels.

Now it will be demonstrated how to provide the data for one of the properties. Click on the **Edit Table** button next to the **Specific Heat** label. When you do, the window shown in Figure 17.3 appears.

Although there are values supplied in that window, they are not to be taken as legitimate, but rather, placeholders to demonstrate how the window should look once data is entered. For now, click the menu option **Edit-Clear Table**, which will remove these entries and prepare the table for fresh data.

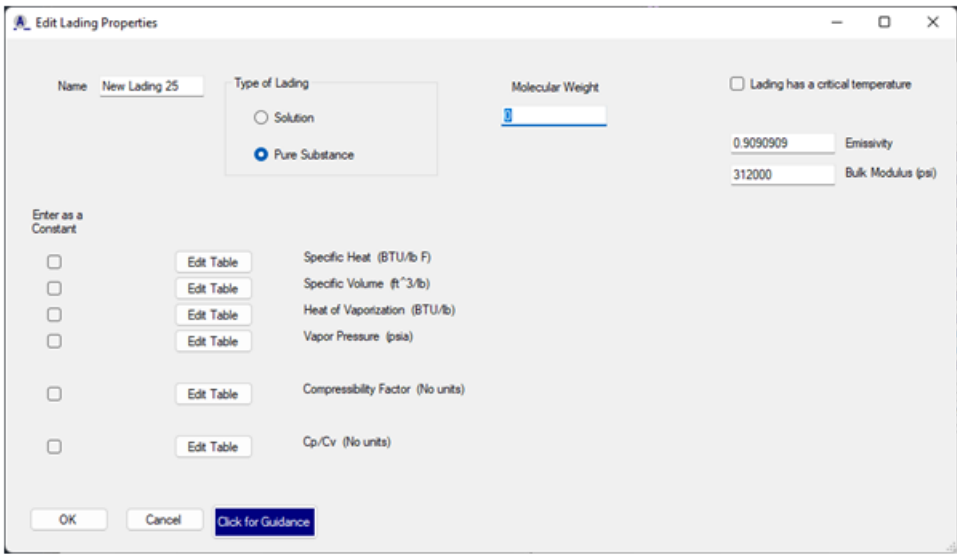

Figure 17.2: Configuration of Edit Lading Properties window for Tutorial 2

After you have cleared the placeholder data, click on the left cell, in the temperature column. Using the numeric keypad on your keyboard, type the value 30 and press ENTER. Next type 120 and press ENTER. Repeat this process to enter 210 and 260 (do not press ENTER after 260).

Now, click on the top right cell, under the Cp column. Type 0.5546 and press ENTER. Type 0.5946 and press ENTER again. Continue, entering 0.7141 and 0.9619 (do not press ENTER after 0.9619).

You may edit the data by clicking directly over the cell you wish to change. You can also copy, cut, and paste rows using the menu options. When you are finished, the window should look like that shown in Figure 17.4.

Once the data has been entered correctly, click **OK**. This same process may be repeated for all of the properties listed. Note that the current version of the Computational Module has certain requirements regarding the number of data points that should be provided for each property. If those requirements are not met, the AFFTAC GUI will inform you when you click **OK** in the **Edit Lading** window.

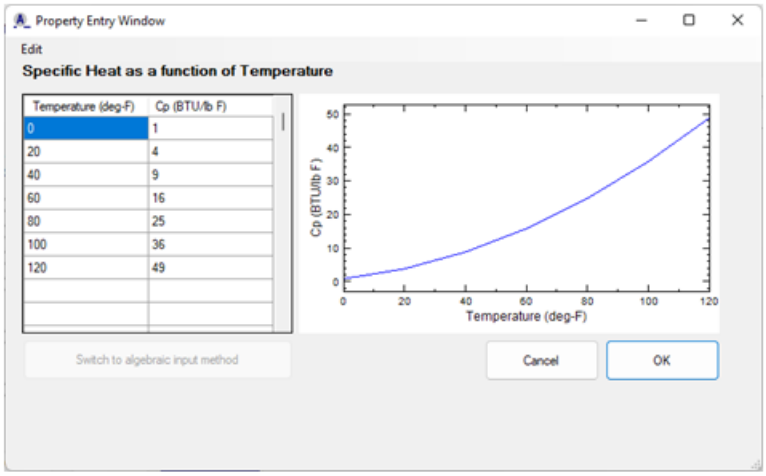

Figure 17.3: **Property Entry** window for specific heat

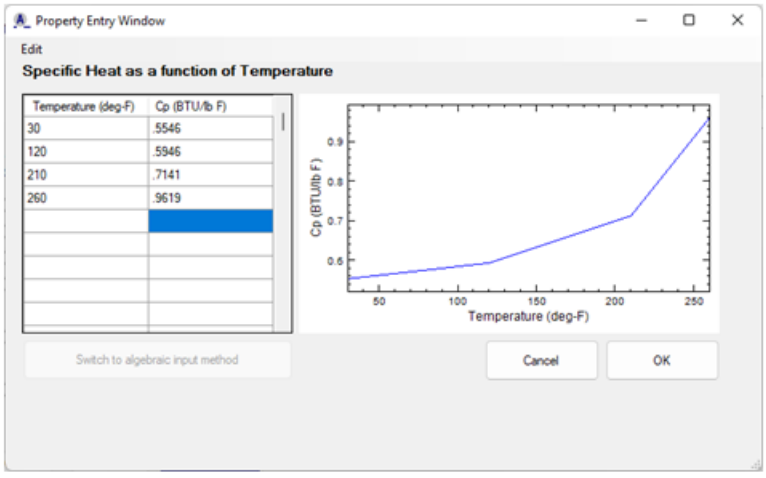

Figure 17.4: Specific volume for Tutorial 2

Chapter 18

Tutorial 3: Creating a Customized PRV Open-Close Model

In this tutorial, you will be guided through the process of making a general open-close model for a PRV. To begin, select the menu option **Resources-Advanced PRDs** from the **Main Window**. The PRD Resource Manager will appear. Click **New**. When you do, a new PRD will be added to the bottom of the list. Double click that new entry. When you do, the **Setup PRD** window will appear with default values, like that shown in Figure 18.1.

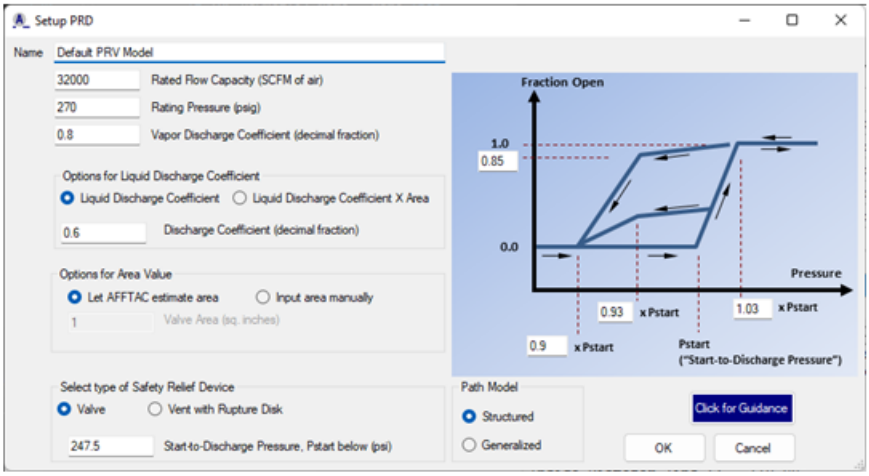

Figure 18.1: PRD Setup Window with default values.

Click **Generalized** under **Path Model**. When you do, the plot will disappear and will be replaced with a button labeled **Edit Generalized Path**. Click that button. When you do, the Generalized **PRV Model Editor** will appear, like that shown in Figure 18.2.

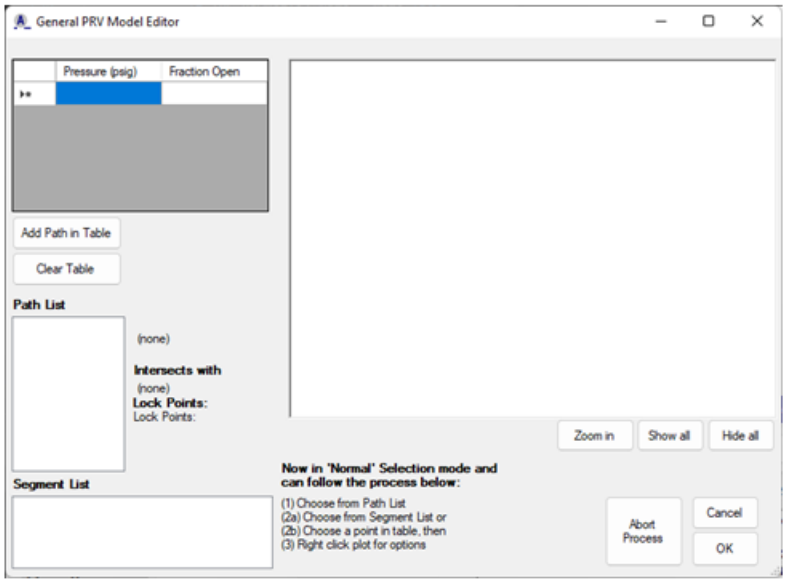

Figure 18.2: **Generalized PRV Editor** window as it initially appears.

In the top-left portion of that window, enter these numbers:

Pressure (psig)	Fraction Open
0	0
262.2	0
269.625	1
500.	1

Select **Increasing for the Pressure Direction**, and then click **Add Path in Table**. When you do, AFFTAC will prompt you for a path name. Enter “Rising” and click **OK**. When you do, the path will appear in the **Path List** and will be plotted, as shown in Figure 18.3 (top). Click **Zoom in**. AFFTAC will zoom in on where the PRV is most active, as shown Figure 18.3 (bottom).

Note: You must enter the initial path, i.e., that path on which the PRV starts the simulation, first. Notice that the first path entered above starts at a low pressure, which will be where the simulation starts.

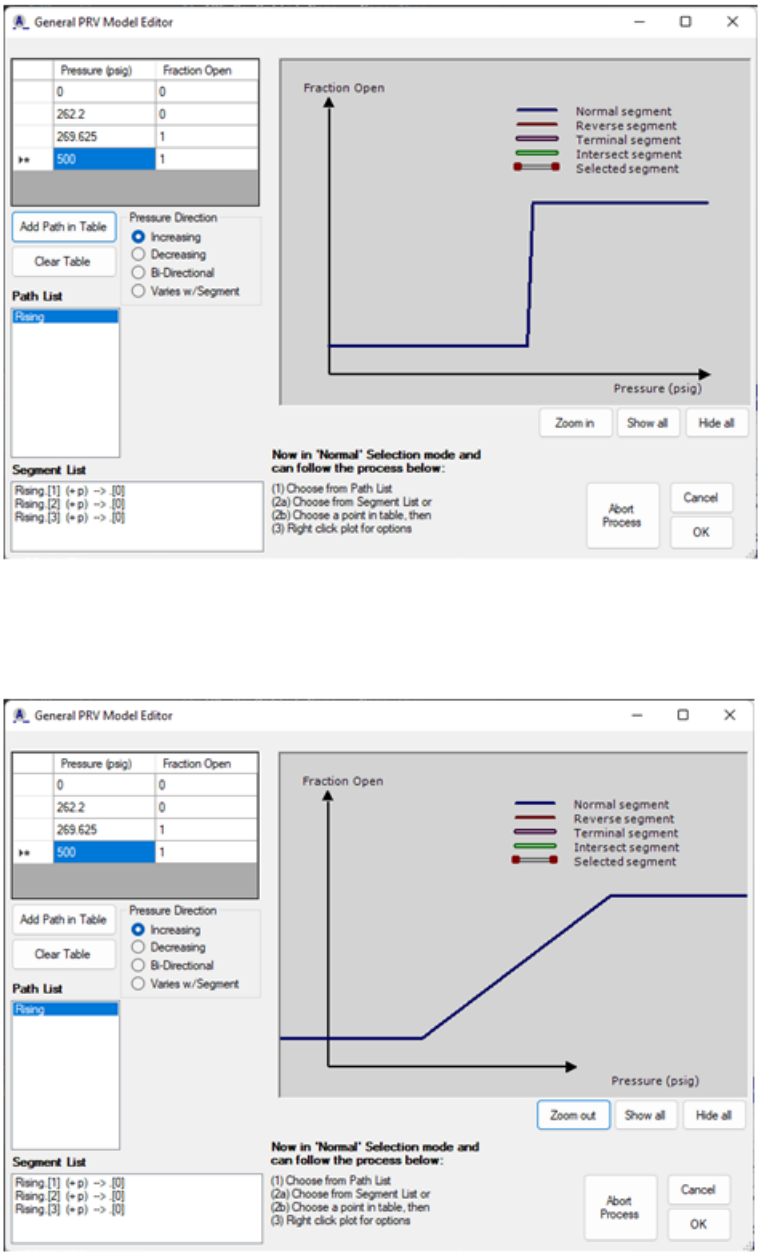

Figure 18.3: **General PRV Model Editor** with one path entered. **Upper:** Not zoomed in. **Lower:** Zoomed in to the region of PRV action.

You will now enter a second path. Click **Clear Table**, and enter these new values:

Pressure (psig)	Fraction Open
500	1
269.625	1
237.45	0
0	0

Select **Decreasing for the Pressure Direction** and then click **Add Path in Table**. For the name, enter "Falling" and click **OK** in the **Query** window. If the plot is not zoomed in, click the **Zoom in** button. Select "Rising" in the **Path List**. Once that path is selected, select the middle segment in the **Segment List**, i.e., click "`Rising.[2] (+p) --> .[0]`" in the lower left part of the window. Your window should look like that shown in Figure 18.4.

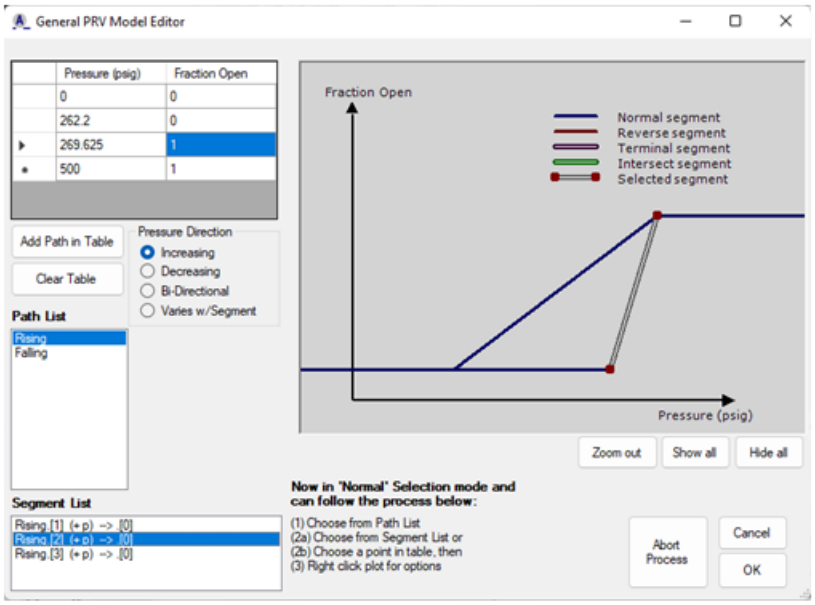

Figure 18.4: **PRD Setup** window with the Falling path selected and highlighted in the plot (Zoomed in).

With "Rising's" middle segment selected, move your mouse to the plot area and right click. From the right-click menu that appears, select **Launch template from this segment**. AFFTAC will prompt you for a name for the path (which will be a template path). Enter "MidFall" and click **OK**.

Next, AFFTAC will ask you to select a terminal segment, i.e., the segment on a path you have already established where the template should terminate. You will select the first segment in the "Rising" path. To do that, click "Rising's" lowest, horizontal segment on the plot. When you do, the window will look like that in Figure 18.5 (top). If it does, answer **Yes** when AFFTAC asks you if that is the path you wanted. Otherwise, try again. AFFTAC will, prompt you for the pressure at which it should terminate on that segment. Enter "252" and click **OK**. Next AFFTAC will ask you to select a path with which the template might intersect. On the plot, select the "Falling" path. Doing so will cause the window to look like the one in Figure 18.5 (bottom). If it does, click **Yes** when prompted. Otherwise try again.

Once finished, highlight “MidFall” in the **Path List**. Doing show should make your window look like that in Figure 18.6 (top). With “MidFall” still as the selected path, click its only segment in the **Segment List**. Then, carefully position your mouse at the half-way point of the highlighted segment in the plot. Holding your mouse there, right click and select **Insert point**. A point will be added approximately where your mouse was. Click “MidFall” in the **Path List** to refresh the table, and manually edit the location of your new point to be at pressure = 259., fraction open = 0.5. Select “MidFall” again in the **Path List**. Your window should look like that in Figure 18.6 (bottom).

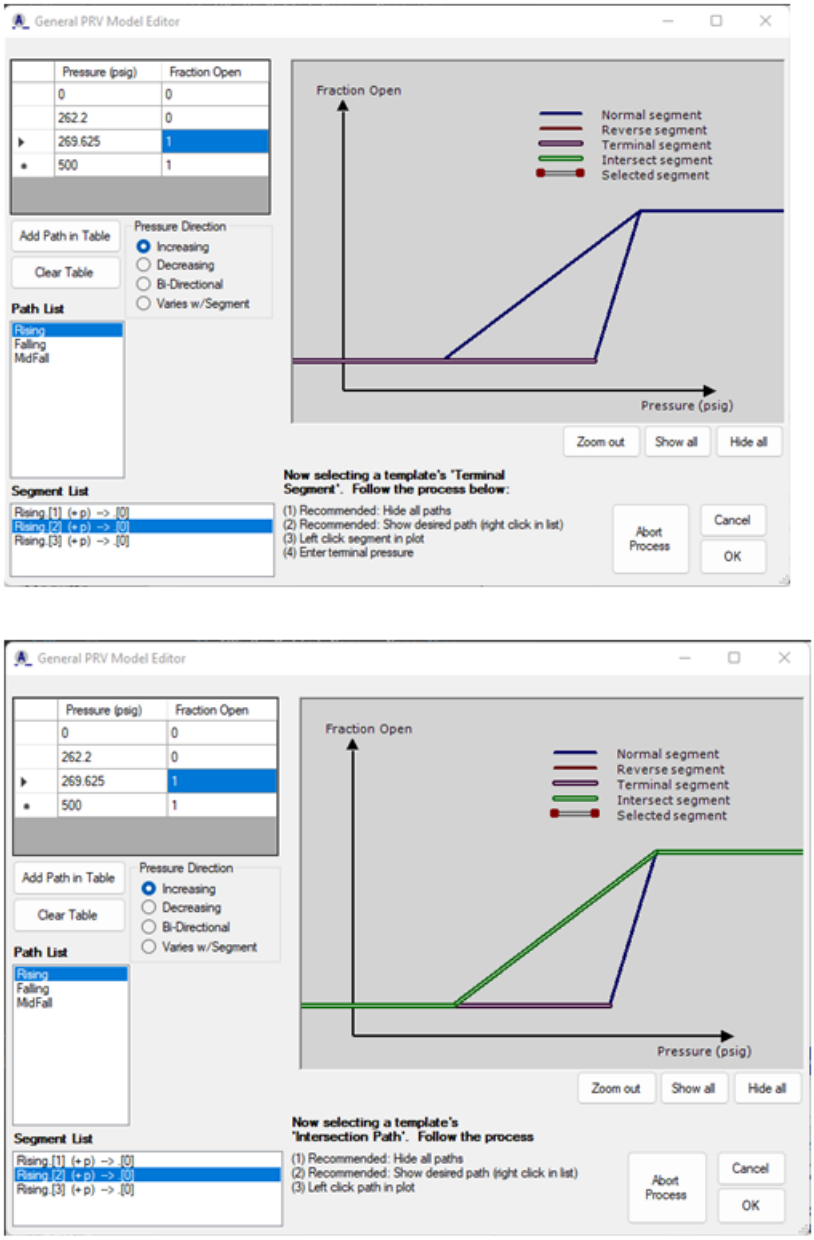

Figure 18.5: PRD Setup Window with the, **Upper:** First correct terminal paths selected for the template, and **Lower:** The second correct terminal path selected.

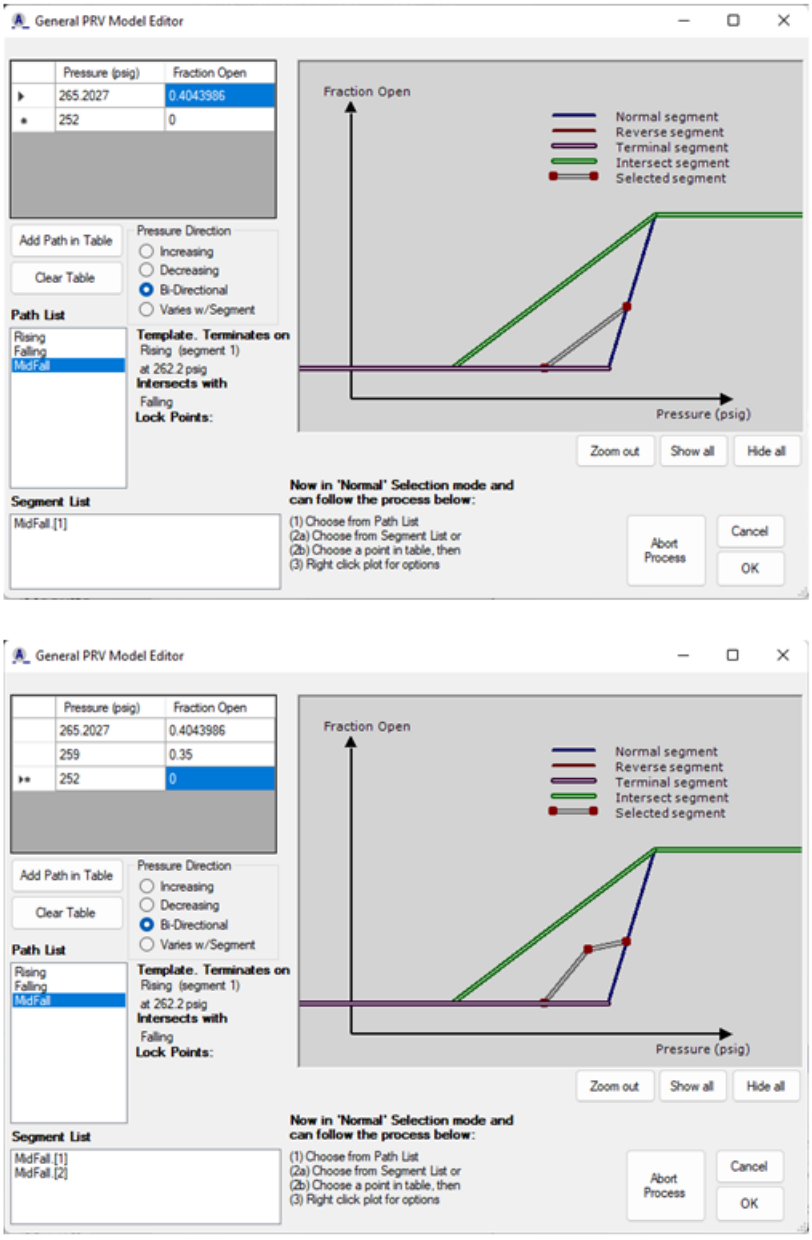

Figure 18.6: **Upper: Generalized PRV Model Editor** with correct intersection path for the template. **Lower: Generalized PRV Model Editor** after adding a point to "MidFall."

With “MidFall” still highlighted, click on its last point in the table. Doing so will make your window look like that in Figure 18.7 (top). With that point highlighted, right click in the plot area and select **Make lock point (both)**. Execute a similar process for “MidFall’s” middle point: (1) Click on the middle point in the table, (2) Right click in the plot window, selecting **Make lock point (pressure)**. Selecting “MidFall” in the **Path List** then makes the window appear like that shown in Figure 18.7 (bottom).

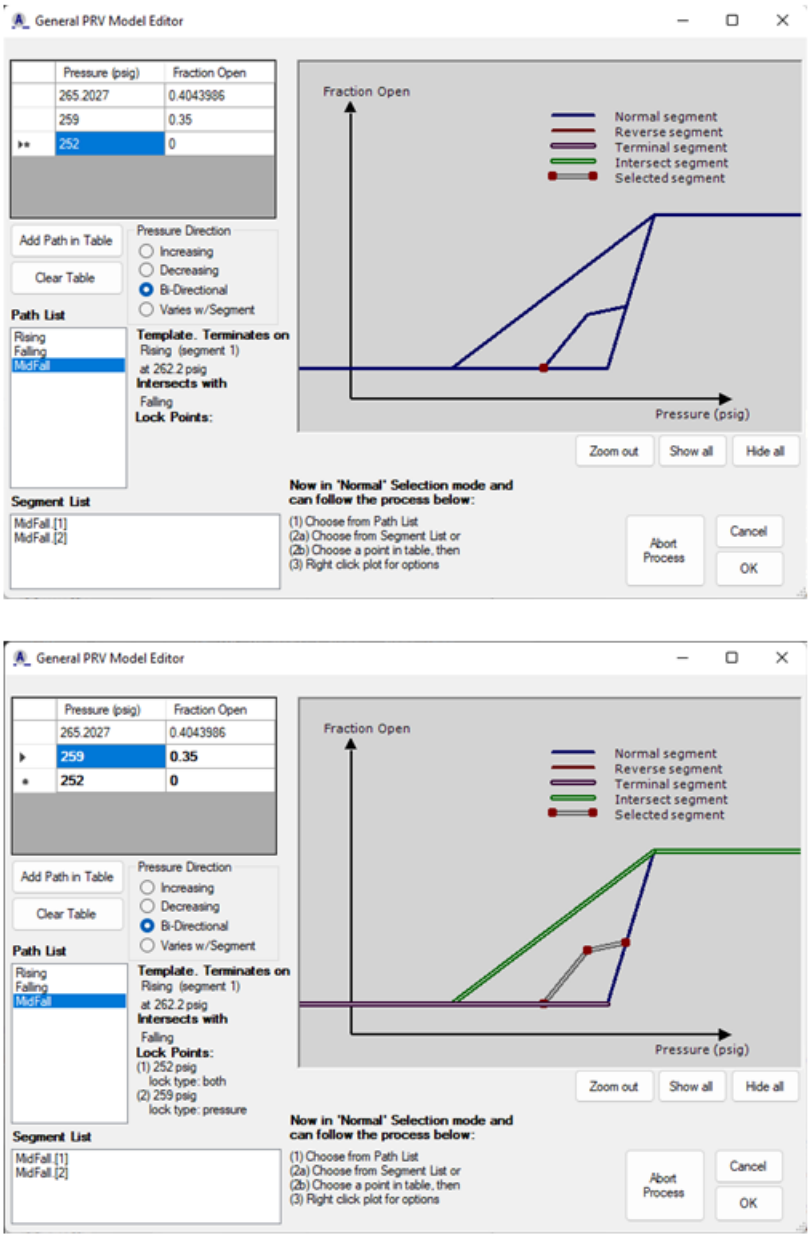

Figure 18.7: **Upper: Generalized PRV Model Editor**, having specified the two endpoints in the “MidFall” template as lock points. **Lower:** Same as the top figure, but after having also specified the middle point in the “MidFall” template as a pressure lock point.

Notice the information on the lock points. You may double-click “MidFall” in the Path List to manually edit its entries. That manual editing window is shown in Figure 18.8.

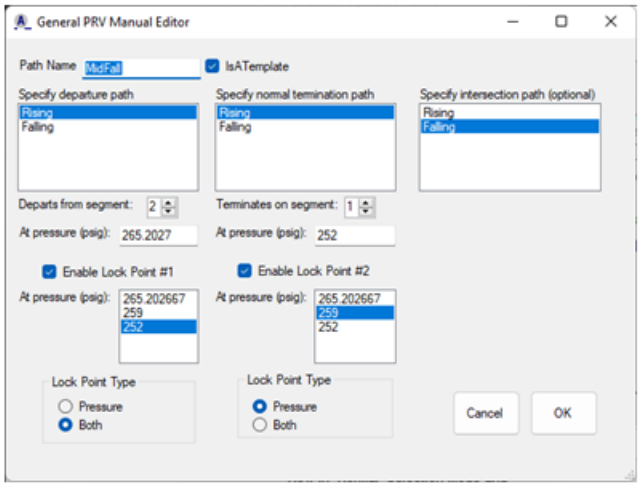

Figure 18.8: Generalized PRV Model Editor, showing “MidFall’s” lock points.

Lastly, instruct AFFTAC about pressure reversals. We will instruct AFFTAC to change from “Rising’s” last segment (fully open) to Falling’s first segment (also fully open) upon a pressure reversal. To do that:

1. Select “Rising” in the **Path List**.
2. Select its last segment in the **Segment List**.
3. In the plot area, right click and select the option **Specify reverse segment**.
4. Click **Hide all**.
5. In the Path List, right-click “Falling” and select **Show** in graphic.
6. In the plot area, select its highest, horizontal segment, i.e., its fully open segment. It will change to red.
7. If the highest, horizontal segment is selected, answer **Yes** to AFFTAC’s query.

Click **Show all** and then select “Rising” in the **Path List**. Your window should look like the one in Figure 18.9. Notice in the Segment List that “Rising’s” middle segment is for increasing pressure only, signified by the (+p). Upon a pressure reversal, the model will switch to the “MidFall” path, which is a template. However, on “Rising’s” third segment, also for increasing pressure only, the model will switch to “Falling’s” first segment upon a pressure reversal.

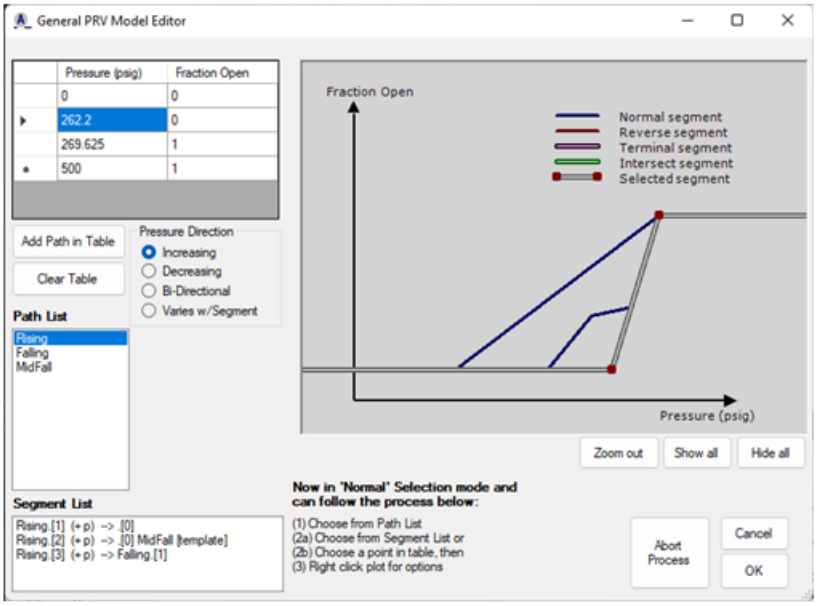

Figure 18.9: General PRV Model Editor after having added the first reversal segment for path “Rising.”

Now, perform a similar process for “Falling’s” fully closed segment. First, click **Show all**. Then:

1. Select “Falling” in the **Path List**.
2. Select its last segment in the **Segment List**.
3. In the plot area, right click and select the option **Specify reverse segment**.
4. Click **Hide all**.
5. In the **Path List**, right-click “Rising” and select **Show in graphic**.
6. In the plot area, select its lowest, horizontal segment. It will change to red.
7. If the lowest (i.e., fully closed) segment is selected, answer **Yes** to AFFTAC’s query.

Once you have finished with this process, click **OK**, and continue to proceed out of the PRD editing process.

Bibliography

[1] *ASME Handbook on Certification of Capacity of Pressure Relief Devices, Section VIII - Division I*.

[2] *International Critical Tables of Numerical Data, Physics, Chemistry and Technology, Volume III*.

[3] Specifications for tank cars. Technical report, Association of American Railroads, Mechanical Division.

[4] Report on a study of metal specimens removed from tank car tanks involved in a derailment and explosions at laurel, mississippi. Technical Report MR-453, Association of American Railroads, July 1969.

[5] Design guidelines for the selection and use of stainless steel. Technical report, AISI Committee of Stainless Steel Producers, 1977.

[6] *Properties and Selection: Irons and Steels, Metals handbook, Ninth Edition, Volume 1*. 1979.

[7] *Properties and Selection: Non-Ferous Alloys and Pure Metals, Metals Handbook, Ninth Edition, Volume 2*. 1979.

[8] Macriss. R. A. Liquid and vapor phase enthalpy of monomethlamine. *Journal of Chemical and Engineering Data*, 12(1):28–33, January 1967.

[9] W. Braker and A. L. Mossman. *The Matheson Unabridged Gas Data Book*. 1974.

[10] Alan J. Chapman. *Heat Transfer Fourth Edition*. Macmillan Publishing Company, New York, 1984.

[11] R. W. Gallant. Physical properties of hydrocarbons, part 12, c2-c4 oxides. *Hydrocarbon Processing*, 46(3):143–150, March 1967.

[12] R. W. Gallant. *Physical Properties of Hydrocarbons, Volume 1*. Gulf Publishing Co., Houston, Texas, 1968.

[13] M. R. Johnson. Temperatures, pressures and liquid levels of tank cars engulfed in fires, volume 1, results of parameteric analyses and volume ii description of analytic procedure. Technical Report DOT/FRA/OR&D-84/08.II, Federal Railroad Administration, June 1984.

[14] Milton Johnson. Tank car thermal analysis, volume i, user's manual for analysis program (final report) for the u.s. department of transportation, federal railroad administration, office of research and development, washington, d.c. 20590. Technical Report DOT/FRA/ORD-98/09A, IIT Research Institute, Chicago, IL 60616, November 1998.

[15] Milton Johnson. Tank car thermal analysis, volume ii, technical documentation report for analysis program (final report), for the u.s. department of transportation, federal railroad administration, office of research and development, washington, d.c. 20590. Technical Report DOT/FRA/ORD-98/09B, IIT Research Institute, Chicago, IL 60616, November 1998.

[16] Kirk and Othermer. *Encyclopedia of Chemical Technology, 3rd edition*. Interscience Publishers, John Wiley & Sons.

[17] W. H. McAdams. *Heat Transmission, 2nd Edition*, pages 133–141, 294–337. McGraw-Hill Book Company, 1942.

[18] Irving H Shames. *Mechanics of Fluids, Second Edition*. McGraw-Hill, Inc., New York, 1982.

[19] A. V. Slack, editor. *Phosphoric Acid*. Marcel Depper, Inc., New York, 1968.

[20] Anderson Townsend, W., J. C., Zook, and G. Cowgill. Comparison of thermally coated and uninsulated rail tank cars filled with lpg subjected to a fire environment. Technical Report FRA-OR&D 75-32, Federal Railroad Administration Report, December 1974.

[21] Bryan Trostel. Pressure relief valve testing for us dept. of transportation. Technical Report 10RN-CE10015 Rev. 1, November 2010.

Appendix A

Details of the Lading Model

AFFTAC's lading model handles ladings consisting of pure substances, which consist of one species, and ladings that are binary solutions, which consist of two pure species, a solute and a solvent. The purpose of the lading model is to provide the following thermodynamic properties during the simulation:

1. Specific heat, C_p,
2. Specific volume, C_v,
3. Heat of vaporization, H_f,
4. Vapor pressure, V_p,
5. Compressibility factor, Z, and
6. Ratio of specific heats, γ.

For a pure substance comprised of only one species (or "constituent") the above properties are represented as a function of temperature, T. Specifically, you enter the above values in AFFTAC as tables where one column is T and the other is the thermodynamic property listed above (see the tutorial in chapter 17). The model then interpolates on T to provide the needed property. For binary solutions, the above properties are modeled as a function of temperature *and* concentration. To describe this aspect, more careful definition of terms is needed.

The terms "solute" and "solvent" are two key terms. Ultimately, from a modeling standpoint, there is no difference in their role; neither has a physical impact that is greater than the other. But typically, the solute is the substance of interest, e.g., hydrochloric acid, and the solute is something that dilutes it, i.e., water. The only thing that matters here is that you, as a user, must be consistent regarding how you enter the data for a binary solution with respect to specifying the concentration. The term "concentration" (c) in the user interface refers to the mass fraction of the *solute* (the species of interest), not the solvent. So when you enter the initial concentration of a binary solution, you are entering the mass fraction of the solute. The mass fraction of the *solvent*, which you are not asked to enter, is automatically computed internally as $1 - c$.

As indicated above, the lading model performs a simple tabular lookup for the thermodynamic properties listed above as a function of temperature for a pure substance. For a binary solution, the model provides those values as function of temperature and concentration (c) of the solute, i.e., it provides

1. Specific heat, $C_p(T, c)$,
2. Specific volume, $C_v(T, c)$,
3. Heat of vaporization, $H_f(T, c)$,

4. Vapor pressure, $V_p(T, c)$,
5. Compressibility factor, $Z(T, c)$, and
6. Ratio of specific heats, $\gamma(T, c)$.

The binary mixture model uses different approaches for the different properties, above. For specific heat, specific volume, and heat of vaporization, the user enters temperature-dependent tables that represent the composite mixture's property as a whole, at two different (solute) concentrations. The current solute concentration at any time during the simulation is then used to interpolate between those two tables. In contrast to that, for the compressibility factor and ratio of specific heats, the user enters temperature-dependent tables for the solute and solvent *separately*, as pure species. Those values are combined in a weighted sum where solute concentration is used to compute the weights. The vapor pressure computation uses a combination of these two approaches. A detailed explanation for V_p follows next.

We start with a summary of what tables are required of the user:

1. Temperature-dependent specific heat tables for the mixture at low (c_l) and high (c_h) solute concentrations, $C_{p-c_l}(T)$ and $C_{p-c_h}(T)$
2. Temperature-dependent specific volume tables for the mixture at low and high solute concentrations, $C_{v-c_l}(T)$ and $C_{v-c_l}(T)$
3. Temperature-dependent heat of vaporization tables for the mixture at low and high solute concentrations, $H_{f-c_l}(T)$ and $H_{f-c_l}(T)$
4. For vapor pressure:
   (a) Of the solute at low and high solute concentrations, $V_{p-solute-c_l}(T)$ and $V_{p-solute-c_h}(T)$
   (b) Of the solvent at low and high solute concentrations, $V_{p-solvent-c_l}(T)$ and $V_{p-solvent-c_h}(T)$
5. Compressibility factor for the solute and solvent as a pure species, $Z_{solute}(T)$ and $Z_{solvent}(T)$
6. Ratio of specific heats for the solute and solvent as a pure species, $\gamma_{solute}(T)$ and $\gamma_{solvent}(T)$

The first three properties are computed for the composite mixture by interpolating the temperature-dependent low- and high-concentration tables, and then interpolating those two resulting values using concentration. Mathematically, for specific heat, the operation is as follows:

Given current temperature T and solute concentration c, find $C_p(T, c)$:

1. Interpolate on T from the low-concentration table, i.e., evaluate $C_{p-c_l}(T)$
2. Interpolate on T from the high-concentration table, i.e., evaluate $C_{p-c_h}(T)$
3. Compute $C_p(T, c)$ by interpolating on c between $C_{p-c_l}(T)$ and $C_{p-c_h}(T)$

Linear interpolation is used in the last step, thus the above three steps may be written succinctly as

$$C_p(T, c) = C_{p-c_l}(T) + (c - c_l) \cdot \frac{C_{p-c_h}(T) - C_{p-c_l}(T)}{c_h - c_l}$$

This same procedure is used for specific volume and heat of vaporization, e.g.,

$$C_v(T,c) = C_{v-c_l}(T) + (c - c_l) \cdot \frac{C_{v-c_h}(T) - C_{v-c_l}}{c_h - c_l}$$
$$H_f(T,c) = H_{f-c_l}(T) + (c - c_l) \cdot \frac{H_{f-c_h}(T) - H_{f-c_l}}{c_h - c_l}$$

i.e, the identical process as for C_p.

The last two properties (Z and γ) are computed for the solute and solvent separately and then combined using the solute and solvent mass fractions as weight factors. Note that these two properties are provided as tables for the solute and solvent as pure species by the user, and so a single temperature interpolation is performed and the results combined using c. Mathematically,

$$Z_(T,c) = cZ_{solute}(T) + (1-c)Z_{solvent}(T)$$
$$\gamma_(T,c) = c\gamma_{solute}(T) + (1-c)\gamma_{solvent}(T)$$

Vapor pressure combines the two approaches discussed above. In the end, it is also computed as a mass fraction weighting of the solute's and solvent's properties, i.e.,

$$V_p(T,c) = cV_{p-solute}(T,c) + (1-c)V_{p-solvent}(T,c) \tag{A.1}$$

However, the method of obtaining the solute and solvent vapor pressure values in the above equatioin are analogous to the C_p, C_v and H_f calculations. Specifically, they are computed via linear interpolation on temperature first, and then on concentration second. To be clear, they are computed as follows:

$$V_{p-solute}(T,c) = V_{p-solute-c_l}(T) + (c - c_l) \cdot \frac{V_{p-solute-c_h}(T) - V_{p-solute-c_l}(T)}{c_h - c_l}$$
$$V_{p-solvent}(T,c) = V_{p-solvent-c_l}(T) + (c - c_l) \cdot \frac{V_{p-solvent-c_h}(T) - V_{p-solvent-c_l}(T)}{c_h - c_l}$$

Substituting the linear interpolation for $V_{p-solute}(T,c)$ and $V_{p-solvent}(T)$ into Equation A.1, yields

$$V_p(T,c) = c\left[V_{p-solute-c_l}(T) + (c - c_l) \cdot \frac{V_{p-solute-c_h}(T) - V_{p-solute-c_l}(T)}{c_h - c_l}\right]$$
$$+(1-c)\left[V_{p-solvent-c_l}(T) + (c - c_l) \cdot \frac{V_{p-solvent-c_h}(T) - V_{p-solvent-c_l}(T)}{c_h - c_l}\right] \tag{A.2}$$

Note here the quadratic dependence on c. If one were to multiply out all the terms, two c^2 terms would emerge. Thus the lading model is quadratic in c.

But this quadratic dependence on concentration is tied to another important aspect of the lading model, which is that the solute's and solvent's contributions to vapor pressure does not necessarily monotonically decrease to zero as their presence in the binary solution diminishes. If their original temperature-based tables at low- and high-concentration are not constructed carefully, their contributions to vapor pressure can go negative. Care in constructing those tables should be exercised to avoid that situation.

Appendix B

Default Ladings

Originally written by Milton Johnson, Ph.D.
Minor nomenclature adaptations by Scott Runnels, Ph.D.

The use of default values for the thermal properties is not recommended. If at all possible, a search for the thermal properties of a lading should be conducted and the values that are obtained entered into the AFFTAC Ladings Resource. If this is not feasible, then the default lading templates may be used, keeping in mind the following guidelines that have been followed to estimate their thermal properties. These guidelines do not apply to tank cars transporting cryogenic liquids, compressed gases such as helium, or slurries/products, such as liquid sulfur, which solidify upon heating. If the product being considered is a solution, it should be treated as though it were a substance for the purpose of obtaining default values and the following guidelines should be used.

B.1 Vapor Pressure

The test pressure of the tank car class authorized to transport a product is often an indication of the vapor pressure of the product. Therefore, two sets of values for default vapor pressure data are provided, one for products that would be shipped in non-pressure cars having a test pressure of 100 psi and the other for products that must be shipped in pressure tank cars having a test pressure of 300 psi or greater. Some products that have low vapor pressures, e.g. products classified as poison by inhalation, must be shipped in pressure tank cars even though they may have low vapor pressures. This is done to require the use of a stronger tank car providing added safety in the shipment of the product. The suggested vapor pressures given below could be substantially over estimated for those ladings.

Assuming that liquefied gases are shipped in pressure cars and liquids are shipped in non-pressure cars, the vapor pressure property values are estimated as shown in Table B.1.

Temperature (deg-F)	Vapor Pressure (psia)
60	5
150	40
240	125

Table B.1: Liquids (non-pressure cars)

Some products, such as bromine, chlorine and hydrogen cyanide, must be shipped in tank cars having a test pressure of 500 psi or greater. This is done not because they have high vapor pressures, but to insure they are shipped in stronger, safer cars. The vapor pressures given in Table B.2 for pressure tank cars would be conservative for these products.

Temperature (deg-F)	Vapor Pressure (psia)
60	140
120	300
180	570

Table B.2: Liquified gasses (pressure cars)

B.2 Specific Heat

There is a wide range of values for the specific heat of the liquid for products shipped in tank cars. Values can range from over 1.00 BTU/lb-oF, for solutions containing a large percentage of water, to as low as 0.10 BTU/lb-deg-F for bromine at about 200 deg-F. Also, for most products the specific heat tends to rise with increasing temperature, but for some products (e.g. bromine) it decreases. This makes it difficult to suggest default properties for specific heat that are conservative, but not overly conservative. Since the specific heat of the liquid determines the rate of temperature increase of the product with a given heat input, it is obvious that lower values for this parameter will lead to more conservative analyses. The default values in Table B.3 are suggested, although they may not always lead to conservative results.

Temperature (deg-F)	Specific Heat (BTU/lb-deg-F)
60	0.40
300	0.70

Table B.3: Specific heat

B.3 Specific Volume

It is assumed that the density of the product is known. The specific volume is simply the inverse of this value expressed in $\left[\frac{ft^3}{lbm}\right]$. Since the density of materials tend to decrease with increasing temperature, the specific volume will increase with increasing temperature.

Again, there is a considerable variation of this rate of increase among products shipped in tank cars making it difficult to suggest default properties. Values range from an increase in specific volume of 13 percent for chlorosulfonic acid in the temperature range from 50 to 302 deg-F to a 70 percent increase for hydrogen fluoride in the same temperature range. The rate of increase in specific volume with temperature is an important parameter when the tank car becomes shell full and liquid is being expelled through the valve, a larger valve capacity for liquid flow being required when the rate of increase is higher. Tentative values are suggested in Tables B.4 and B.5.

Temperature (deg-F)	Percentage increase in Specific Volume from Ambient Value
60	Ambient Value
180	10%
300	30%

Table B.4: Specific volume for liquids (non-pressure cars) or Liquefied Gases Containing at least 50% water heat

Temperature (deg-F)	Percentage increase in Specific Volume from Ambient Value
60	Ambient Value
150	20%
240	50%

Table B.5: Specific volumes for liquefied gasses (pressure cars)

B.4 Heat of Vaporization

There is also considerable variation in the heat of vaporization among products shipped in tank cars ranging from about 1000 BTU/lb for solutions containing a high percentage of water to less than 100 BTU/lb, for products such as bromine, methyltrichlorosilane, titanium tetrachloride and phosphorus trichloride. Other factors being equal, a lower heat of vaporization will result in the generation of greater volume of vaporized product requiring a larger capacity pressure relief valve. The heat of vaporization decreases with increasing temperature. The default values in Table B.6 are suggested although they may not be conservative in all cases. If the product is a solution containing at least 50 percent water as the solvent, the values Table B.7 are suggested.

Temperature (deg-F)	Heat of Vaporization BTU/lb
60	300
240	100

Table B.6: Heat of vaporization without 50% water as solvent.

Temperature (deg-F)	Heat of Vaporization BTU/lb
60	800
240	300

Table B.7: Heat of vaporization for a solution containing at least 50% water as solvent.

B.5 Compressibility Factor

This parameter does not have a major influence on the calculations. A default value of 0.9 is suggested for the compressibility factor of product vapor. It would be entered into the program at two values for temperature (e.g. 60 and 300 deg-F).

B.6 Ratio of Specific Heats

This parameter does not have a major influence on the calculations. A default value of 1.1 is suggested for the ratio of specific heats of product vapor. It would be entered into the program at two values for temperature (e.g. 60 and 300 deg-F).

Appendix C

Choked Vapor Flow Derivation and Area Estimation Method

The primary reference for these derivations is given in [1].

C.1 Applications of the First Law of Thermodynamics

C.1.1 Application to Quasi-Static Process

In this section, thermodynamic relationships are derived that describe intrinsic responses of the fluid, without consideration of a system. To derive these relationships, consider fluid in a quasi-static process, where pressure, p, is uniform. The differential form of the First Law of Thermodynamics (hereafter, "First Law") reduces to

$$dq - dw = du \tag{C.1}$$

where u is the internal energy of the fluid, q is the heat transferred into the fluid, and w is the work done by the fluid.

If this process is adiabatic, reversible (isentropic), $dq = 0$. Also, fluid alone can only do work intrinsically through expansion, so $dw = pdv$, where dv is the infinitesimal change in volume. Therefore, the First Law for the fluid is

$$du = -pdv \tag{C.2}$$

The specific heat at constant volume, c_v, is defined as

$$c_v \equiv du/dT \tag{C.3}$$

or

$$du = c_v dT \tag{C.4}$$

so that

$$c_v dT = -pdv. \tag{C.5}$$

Returning to Equation C.3 and adding pdv to both sides,

$$du + pdv + vdp = vdp \tag{C.6}$$

which means that

$$d(u + pv) = vdp \tag{C.7}$$

or

$$dh = vdp \tag{C.8}$$

where $h = u + pv$ is enthalpy. The specific heat at constant pressure, c_p, is defined as

$$c_p \equiv dh/dT \tag{C.9}$$

or

$$dh = c_p dT \tag{C.10}$$

so that

$$c_p dT = vdp. \tag{C.11}$$

Divide Equation C.11 by Equation C.5, to get

$$c_p/c_v = -vdp/pdv. \tag{C.12}$$

Rearrange,

$$-(c_p dv)/(c_v v) = -dp/p, \tag{C.13}$$

and define the ratio of specific heats as $k = c_p/c_v$, so that

$$-kdv/v = dp/p. \tag{C.14}$$

Assume a constant ratio (k) of specific heats, and integrate:

$$-\int k\frac{dv}{v} = \int \frac{dp}{p} \tag{C.15}$$

$$pv^k = \text{constant}. \tag{C.16}$$

The above equation means that the product of pressure and specific volume is everywhere constant in the quasi-static process. Introducing "i" to denote an inlet and "o" to denote and outlet, the above equation implies that

$$p_i v_i^k = p_o v_o^k \tag{C.17}$$

$$\frac{p_i}{p_o} = \left(\frac{v_o}{v_i}\right)^k \tag{C.18}$$

For an ideal gas, $pv = RT$ so that the above equation may be written as

$$\frac{T_i v_o}{T_o v_i} = \left(\frac{v_o}{v_i}\right)^k \tag{C.19}$$

or

$$\frac{T_i}{T_o} = \left(\frac{v_o}{v_i}\right)^{k-1} \tag{C.20}$$

The ideal gas law, $pv = RT$, can be applied again, to produce

$$\frac{T_i}{T_o} = \left(\frac{RT_o/p_o}{RT_i/p_i}\right)^{k-1} = \left(\frac{T_o p_i}{T_i p_o}\right)^{k-1} \tag{C.21}$$

Manipulation of the above equation results in

$$\frac{T_i}{T_o} = \left(\frac{p_i}{p_o}\right)^{(k-1)/k} \tag{C.22}$$

C.1.2 Application to a Control Volume

The differential form of the First Law of Thermodynamics for a system ("First Law") is as follows,

$$dQ - dW = dE \tag{C.23}$$

where

$$\begin{aligned} Q &= \text{heat transferred in to the system} \\ W &= \text{work done by the system} \\ E &= \text{energy in the system} \end{aligned} \tag{C.24}$$

The right-hand side has to do with the state of the fluid in the system. Since fluid can move through the system, it is helpful to highlight that fact when writing the First Law as time derivatives. In particular, the energy time derivative must be a "substantial" derivative (i.e., follows the substance, which is the fluid). Capital "D" is used for that purpose, and the time-derivative form of the First Law may be written as

$$\frac{dQ}{dt} - \frac{dW}{dt} = \frac{DE}{Dt} \tag{C.25}$$

It is necessary at this point to more firmly establish the notion of a control volume, which will be denoted here by Ω. The Reynolds Transport Theorem accounts for the fact that the substance (fluid) flows through the control volume. In taking the flow into account, the First Law, which is meant to apply to a system, can be made to handle the situation where fluid flows through the system. The derivation of the Reynold's Transport Theorem can be made from geometrical considerations and can be applied to any material state variable. For energy, it is stated as follows:

$$\frac{DE}{Dt} = \int_{\partial\Omega} e\rho \mathbf{V} \cdot \hat{\mathbf{n}} dA + \frac{\partial}{\partial t} \int_{\Omega} e\rho d\nu \tag{C.26}$$

where $\partial\Omega$ is the boundary of Ω, e is the material-intensive energy, $\mathbf{V}$ is the velocity vector at the boundary, and $\hat{\mathbf{n}}$ is the outward normal at the boundary.

For steady-state flow, the second term on the right-hand side is zero. Using the resulting expression for DE/Dt in the First Law,

$$\frac{dQ}{dt} - \frac{dW}{dt} = \int_{\partial\Omega} e\rho \mathbf{V} \cdot \hat{\mathbf{n}} dA. \tag{C.27}$$

It is helpful to separate the work term on the left-hand side into two parts:

$$\frac{dW}{dt} = \frac{dW_s}{dt} + \int_{\partial\Omega} \mathbf{T} \cdot \mathbf{V} dA = \text{"Shaft work rate"} + \text{"Flow work rate"} \tag{C.28}$$

where $\mathbf{T}$ is the stress tensor. The product of $\mathbf{T}$ and $\mathbf{V}$ represent stress through a distance, per time. When integrated over an area, it represents the rate of work done by the fluid.

The first term is the rate of work done on the fluid by moving parts inside the control volume (e.g., a fan). For flow through the pressure relief device, there are no moving parts that do any appreciable work on the fluid, so the "shaft work rate" is zero, which leaves only the flow work rate, so that

$$\frac{dW}{dt} = \int_{\partial\Omega} \mathbf{T} \cdot \mathbf{V} dA. \tag{C.29}$$

In flow through the pressure relief device, it is assumed the flow is frictionless, so the only stress at the surface is normal stress. In other words,

$$T = p\hat{\mathbf{n}} \tag{C.30}$$

So, the flow work rate is

$$\frac{dW}{dt} = \int_{\partial\Omega} \mathbf{T} \cdot \mathbf{V} dA = \int_{\partial\Omega} p\mathbf{V} \cdot \hat{\mathbf{n}} dA \tag{C.31}$$

Substituting this expression for the work term on the left-hand side of the First Law produces the following form of the First Law:

$$\frac{dQ}{dt} - \int_{\partial\Omega} p\mathbf{V} \cdot \hat{\mathbf{n}} dA = \int_{\partial\Omega} e\rho\mathbf{V} \cdot \hat{\mathbf{n}} dA \tag{C.32}$$

In the release of vapor through the safety relief device, the flow is sufficiently fast to completely neglect any heat exchanged between the fluid and the valve. Hence, the flow is adiabatic/isentropic and so the dQ/dt term is zero, so that the First Law becomes

$$-\int_{\partial\Omega} p\mathbf{V} \cdot \hat{\mathbf{n}} dA = \int_{\partial\Omega} e\rho\mathbf{V} \cdot \hat{\mathbf{n}} dA \tag{C.33}$$

The term on the left-hand side can be combined with the term on the right-hand side by inserting $\rho\nu$, which is unity. Doing so produces

$$-\int_{\partial\Omega} p\nu\rho\mathbf{V} \cdot \hat{\mathbf{n}} dA = \int_{\partial\Omega} e\rho\mathbf{V} \cdot \hat{\mathbf{n}} dA \tag{C.34}$$

Then, combining the two integrals,

$$\int_{\partial\Omega} p\left(e + p\nu\right)\mathbf{V} \cdot \hat{\mathbf{n}} dA = 0 \tag{C.35}$$

The energy of the material is comprised of kinetic, gravitational potential, and internal energy. In other words,

$$e = \frac{V^2}{2} + gz + u \tag{C.36}$$

where g is the acceleration due to gravity, z is the height above a datum, and u is the internal energy. Inserting this expression for energy into the preceding equation produces the following form of the First Law:

$$\int_{\partial\Omega} \rho\left(\frac{V^2}{2} + gz + u + pv\right)\mathbf{V} \cdot \hat{\mathbf{n}} dA = 0 \tag{C.37}$$

In flow through the pressure relief device, there is no appreciable altitude change. Therefore, the total surface integral of gz can be neglected. And so the First Law becomes

$$\int_{\partial\Omega} \rho\left(\frac{V^2}{2} + u + pv\right)\mathbf{V} \cdot \hat{\mathbf{n}} dA = 0 \tag{C.38}$$

Using enthalpy, which is defined as $h = u + pv$, the First Law can be expressed as

$$\int_{\partial\Omega} \rho\left(\frac{V^2}{2} + h\right)\mathbf{V} \cdot \hat{\mathbf{n}} dA = 0 \tag{C.39}$$

At this point, the surface integral can be simplified in two ways:

1. In the present application, the surface area is comprised of only one inlet and one outlet. The areas for the inlet and outlet are A_i and A_o, respectively.

2. An approximation is made concerning the direction of the flow at the inlet and outlet. It is assumed that the flow is normal to the control volume (A_i and A_o), which means that the dot product between velocity and the surface normal vector is simply the magnitude of the velocity ($\mathbf{V}$).

Under these assumptions,

$$\left(\frac{V_o^2}{2} + h_o\right)\rho_o A_o V_o = \left(\frac{V_i^2}{2} + h_i\right)\rho_i A_i V_i \tag{C.40}$$

The products of density, area, and velocity that appear on both sides of the above equation are expressions of mass flow rate. Conservation of mass therefore means that these two products must be equal and therefore cancel. And so the First Law becomes,

$$\frac{V_o^2}{2} + h_o = \frac{V_i^2}{2} + h_i \tag{C.41}$$

The control volume for this application is chosen to be such that the velocity at the inlet is very small, i.e., such that V_i^2 is negligible. Under that assumption, the First Law is

$$\frac{V_o^2}{2} + h_o = h_i \tag{C.42}$$

Next, it is assumed that the specific heats are constant, i.e., that

$$c_p \equiv \frac{dh}{dT} \tag{C.43}$$

is a constant. With c_p being a constant, the above equation may be integrated such that

$$h - h_d = c_p(T - T_d) \tag{C.44}$$

Here, (h_d, T_d) is an arbitrary datum. Substituting this expression into the First Law produces

$$\frac{V_o^2}{2} + c_p(T_o - T_d) = c_p(T_i - T_d) \tag{C.45}$$

The T_d terms cancel, and thus

$$\frac{V_o^2}{2} + c_p T_o = c_p T_i \tag{C.46}$$

Dividing by T_o,

$$\frac{V_o^2}{2T_o} + c_p = c_p\frac{T_i}{T_o} \tag{C.47}$$

and then by c_p,

$$\frac{V_o^2}{2c_p T_o} + 1 = T_i/T_o \tag{C.48}$$

In Appendix D, it is shown that for an ideal gas, $c_p = \left(\frac{k}{k-1}\right)R$. Using that fact, the First Law becomes

$$\frac{V_o^2}{kRT_o}\frac{(k-1)}{2} + 1 = \frac{T_i}{T_o} \tag{C.49}$$

Also, for an ideal gas, $c^2 = kRT$, and this term appears in the above equation. Therefore, the ratio $\frac{V_o^2}{kRT_o} = \frac{V_o^2}{c^2} = M^2$, where M is the Mach number (the ratio of flow speed to the speed of sound). The First Law in terms of M is

$$M^2\frac{(k-1)}{2} + 1 = \frac{T_i}{T_o} \tag{C.50}$$

Inverting the above equation,

$$\frac{T_o}{T_i} = \frac{1}{1 + M^2\frac{(k-1)}{2}} \tag{C.51}$$

Using Equation C.22, the First Law may be written as

$$\left(\frac{p_o}{p_i}\right)^{(k-1)/k} = \frac{1}{1+\frac{(k-1)}{2}M^2} \tag{C.52}$$

or

$$\frac{p_o}{p_i} = \frac{1}{\left(1+\frac{(k-1)}{2}M^2\right)^{k/k-1}} \tag{C.53}$$

C.2 Mass Flow for an Ideal Gas

The mass flow rate is

$$G = \rho V A \tag{C.54}$$

where

$$\begin{aligned} \rho &= \text{density} \\ V &= \text{average velocity} \\ A &= \text{area of flow} \end{aligned} \tag{C.55}$$

For an ideal gas,

$$\rho = p/RT \tag{C.56}$$

where

$$\begin{aligned} p &= \text{pressure} \\ R &= \text{gas constant} \end{aligned} \tag{C.57}$$

By substitution of the ideal gas law into the mass flow rate equation,

$$G = \frac{p}{RT} V A \tag{C.58}$$

The following step is simple algebra. The RT term is split into two square roots and a form of unity (k/k) is introduced. The value k is the ratio of the vapor's specific heats, as was described in the previous subsection (Equations C.13-C.14).

$$G = pA\frac{V}{\sqrt{kRT}}\sqrt{\frac{k}{RT}} \tag{C.59}$$

For an ideal gas, the speed of sound, c, is

$$c = \sqrt{kRT}. \tag{C.60}$$

For an ideal gas the Mach number is

$$M = \frac{V}{c} = \frac{V}{\sqrt{kRT}} \tag{C.61}$$

The Mach number can therefore be used in the expression for the mass flow rate as follows:

$$G = pAM\sqrt{\frac{k}{RT}} \tag{C.62}$$

Introducing the subscript "o" for "outlet," the above equation may be used to express the mass flow rate at the outlet of a control volume,

$$G = p_o A M \sqrt{\frac{k}{RT_o}} \tag{C.63}$$

Into this equation, pressures and temperatures at the inlet (subscript "i") will be introduced in ratios that equal unity. Then the terms are rearranged:

$$G = p_o A M \sqrt{\frac{k}{RT_o}} \left(\sqrt{\frac{T_i}{T_i}} \frac{p_i}{p_i} \right) \tag{C.64}$$

or

$$G = \frac{p_o}{p_i} A M \sqrt{\frac{k}{R}} \sqrt{\frac{T_i}{T_o}} \frac{p_i}{\sqrt{T_i}} \tag{C.65}$$

Into this equation, the relationships derived earlier for p_o/p_i and T_o/T_i (Equations C.51 and C.53) are substituted:

$$G = \frac{MA}{\left(1 + \frac{(k-1)}{2} M^2\right)^{(k+1)/2(k-1)}} \sqrt{\frac{k}{R}} \frac{p_i}{\sqrt{T_i}} \tag{C.66}$$

For $M = 1$,

$$G|_{M=1} = p_i A \left(\frac{2}{(k+1)} \right)^{(k+1)/2(k-1)} \sqrt{\frac{k}{RT_i}} \tag{C.67}$$

Or, combining terms,

$$G|_{M=1} = p_i A \sqrt{\frac{k}{RT_i} \left(\frac{2}{k+1} \right)^{k+1/k-1}} \tag{C.68}$$

C.3 AFFTAC's Sub-Sonic Vapor Flow Model

If the pressure is not sufficiently high, then it is assumed choked flow has not occurred, and so $M < 1$. Therefore, the applicable equation is not Equation C.68, but rather its predecessor, Equation C.66. That eqeuation, modified to include the vapor discharge coefficient, results in

$$G_{\text{sub-sonic}} = \frac{M(AC_{Dc})}{\left(1 + \frac{(k-1)}{2} M^2\right)^{(k+1)/2(k-1)}} \sqrt{\frac{k}{R}} \frac{p_i}{\sqrt{T_i}} \tag{C.69}$$

However, it is noted here that AFFTAC instead uses a simplified linear model for sub-sonic flow. Specifically, AFFTAC computes the flow rate as if the flow is choked, and then linearly scales it according to pressure. This simplification in AFFTAC is probably unneeded, since the compact analytical form is readily available in Equation C.69.

Appendix D

Thermodynamic Identities for an Ideal Gas

By definition,

$$c_p = \frac{dh}{dT} = \frac{d}{dT}(u + pv) \tag{D.1}$$

For an ideal gas,

$$pv = RT \tag{D.2}$$

And so

$$c_p = \frac{d}{dT}(u + RT) = c_v + R \tag{D.3}$$

Therefore,

$$c_p - c_v = R \tag{D.4}$$

Dividing both sides by c_v,

$$\frac{c_p}{c_v} - 1 = \frac{R}{c_v} \tag{D.5}$$

The ratio of specific heats appears often and is defined here as k,

$$k \equiv \frac{c_p}{c_v} \tag{D.6}$$

Therefore, using this definition,

$$\begin{aligned} k - 1 &= \frac{R}{c_v} \\ &= \frac{Rk}{c_p} \end{aligned} \tag{D.7}$$

so that

$$c_p = \left(\frac{k}{k-1}\right) R \tag{D.8}$$

Appendix E

Derivation of the PRD Area Estimation Formula

In the initialization part of the AFFTAC Computational Module's main routine, the vapor discharge coefficient is used with the choked flow model to compute the area of the valve. The line in the code resembles this:

```
PRVarea = ValveFlowCapacity/(DischargeCoef_Vap*ValveFlowRatingPressure*2644.0);
```

Derivation of that line of code starts with Equation C.68, solved for A, and here labeled Equation E.1:

$$A = \frac{G_{exp}}{C_{Dv} p \sqrt{\frac{k}{ZRT_{exp}\left(\frac{2}{k+1}\right)^{(k+1)/(k-1)}}}} \tag{E.1}$$

With units,

$$A\left[\text{ft}^2\right] = \frac{G_{exp}\left[\frac{\text{lbm}}{\text{min}}\right]}{C_{Dv} p_{exp}\left[\frac{\text{lbf}}{\text{ft}^2}\right] \sqrt{\frac{k}{ZR\left[\frac{\text{lbf ft}}{\text{deg-R lbm}}\right] T_{exp}[\text{R}]}\left(\frac{2}{k+1}\right)^{(k+1)/(k-1)}}} \tag{E.2}$$

In the line of code shown above, pressure is in psi instead of the units given in Equation E.2, and volumetric flow rate is used instead of mass flow rate. Thus, the following substitutions are made into Equation E.2:

$$G_{exp}\left[\frac{\text{lbm}}{\text{min}}\right] = Q_{exp}\left(\frac{\text{ft}^3}{\text{min}}\right) \cdot \rho\left(\frac{\text{lbm}}{\text{ft}^3}\right) \cdot \frac{1}{60}\left(\frac{\text{min}}{\text{sec}}\right) = \frac{Q_{exp}\rho}{60}\left[\frac{\text{lbm}}{\text{sec}}\right] \tag{E.3}$$

and

$$p_{exp}\left(\frac{\text{lbf}}{\text{ft}^2}\right) = \hat{p}_{exp}\left(\frac{\text{lbf}}{\text{ft}^2}\right) \cdot 144\left(\frac{\text{in}^2}{\text{ft}^2}\right) = \hat{p}_{exp} \cdot 144\left(\frac{\text{lbf}}{\text{ft}^2}\right) \tag{E.4}$$

Making these substitutions,

$$A\left[\text{ft}^2\right] = \frac{\frac{Q_{exp}\rho\left[\frac{\text{ft}^3}{\text{min}}\right]}{60}}{C_{Dv}\hat{p}_{exp} \cdot 144\left[\frac{\text{lbf}}{\text{ft}^2}\right] \sqrt{\frac{k}{ZR\left[\frac{\text{lbf ft}}{\text{deg-R lbm}}\right] T_{exp}[\text{R}]}\left(\frac{2}{k+1}\right)^{(k+1)/(k-1)}}} \tag{E.5}$$

or

$$A\left[\text{ft}^2\right] = \frac{Q_{exp}\left[\frac{\text{lbm}}{\text{sec}}\right]}{C_{Dv}\hat{p}_{exp} \cdot \frac{60 \cdot 144}{\rho}\left[\frac{\text{lbf}}{\text{ft}^2}\right] \sqrt{\frac{k}{ZR\left[\frac{\text{lbf ft}}{\text{deg-R lbm}}\right] T_{exp}[\text{R}]}\left(\frac{2}{k+1}\right)^{(k+1)/(k-1)}}} \tag{E.6}$$

Now, the remaining units may be considered. First, inside the radical, the fact that

$$\frac{1 \cdot \text{lbf}}{1 \cdot \text{lbm}} = g \frac{\text{ft}}{\text{sec}^2} \tag{E.7}$$

is used. Making that substitution,

$$A\left[\text{ft}^2\right] = \frac{Q_{exp}\left[\frac{\text{lbm}}{\text{sec}}\right]}{C_{Dv}\hat{p}_{exp} \cdot \frac{60 \cdot 144}{\rho}\left[\frac{\text{lbf}}{\text{ft}^2}\right]\sqrt{\frac{k}{g\frac{\text{ft}}{\text{sec}^2}ZR\left[\frac{\text{lbf ft}}{\text{deg-R lbm}}\right]T_{exp}[\text{R}]}\left(\frac{2}{k+1}\right)^{(k+1)/(k-1)}}} \tag{E.8}$$

The Rankine units cancel, leaving ft^2/sec^2 in the denominator inside the radical. Bringing those units outside the radical results in

$$A\left[\text{ft}^2\right] = \frac{Q_{exp}\left[\frac{\text{lbm}}{\text{sec}}\right]}{C_{Dv}\hat{p}_{exp} \cdot \frac{60 \cdot 144}{\rho}\left[\frac{\text{lbf}}{\text{ft}^2}\right]\frac{\text{sec}}{\text{ft}}\sqrt{\frac{k}{gZRT_{exp}}\left(\frac{2}{k+1}\right)^{(k+1)/(k-1)}}} \tag{E.9}$$

Simplifying produces

$$A\left[\text{ft}^2\right] = \frac{Q_{exp}}{C_{Dv}\hat{p}_{exp} \cdot \frac{60 \cdot 144}{\rho}\sqrt{\frac{k}{gZRT_{exp}}\left(\frac{2}{k+1}\right)^{(k+1)/(k-1)}}}\left[\frac{\text{lbm}}{\text{lbf}}\right]\left[\frac{\text{ft}^3}{\text{sec}^2}\right] \tag{E.10}$$

Using again that

$$\frac{1 \cdot \text{lbm}}{1 \cdot \text{lbf}} = \frac{1}{g}\frac{\text{sec}^2}{\text{ft}} \tag{E.11}$$

results in

$$A\left[\text{ft}^2\right] = \frac{Q_{exp}}{C_{Dv}\hat{p}_{exp} \cdot \frac{60 \cdot 144}{\rho}\sqrt{\frac{k}{gZRT_{exp}}\left(\frac{2}{k+1}\right)^{(k+1)/(k-1)}}}\left(\frac{1}{g}\right)\left[\frac{\text{lbm}}{\text{lbf}}\right]\left[\frac{\text{ft}^3}{\text{sec}^2}\right] \tag{E.12}$$

Pulling g inside the radical and coelescing units, produces

$$A\left[\text{ft}^2\right] = \frac{Q_{exp}}{C_{Dv}\hat{p}_{exp} \cdot \left\{\frac{60 \cdot 144}{\rho}\sqrt{\frac{gk}{ZRT_{exp}}\left(\frac{2}{k+1}\right)^{(k+1)/(k-1)}}\right\}}\left[\text{ft}^2\right] \tag{E.13}$$

The term in curly braces evaluates as follows:

$$\begin{aligned}\frac{60 \cdot 144}{\rho}\sqrt{\frac{gk}{ZRT_{exp}}\left(\frac{2}{k+1}\right)^{(k+1)/(k-1)}} &= \frac{60 \cdot 144}{0.0763}\sqrt{\frac{(32.2) \cdot (1.4)}{(1) \cdot (53.3533) \cdot (60+459)}\left(\frac{2}{1.4+1}\right)^{(1.4+1)/(1.4-1)}} \\ &= 2644\end{aligned} \tag{E.14}$$

which is what is used in the code, i.e., the line originally presented in this appendix, rewritten as

$$A\left[\text{ft}^2\right] = \frac{Q_{exp}}{C_{Dv}\hat{p}_{exp} \cdot 2644}\left[\text{ft}^2\right] \tag{E.15}$$

Appendix F

Derivation of the Basic Shell-Full Model for Pressure

When the Basic Shell Full model is used during a shell full condition, the pressure inside the tank is computed by assuming the amount of liquid to be discharged is known; it is asumed to be the volume that the liquid would fill if unconstrained by the tank minus the volume of the tank. The liquid discharge coefficient is used in that calculation. The line of code to compute the required pressure is shown below.

```
pcom = pmin +
(pow(reql/(720.0*DischargeCoef_Liq*areq),2))/(64.4*splq);
```

The volume to be expelled is computed as follows:

```
reql = 0.9*reql+0.1*(TotalMass*splq-TankVolume_cufeet)/delt.
```

Ignoring for the moment the 0.9-0.1 relxation factors, this equation may be rewritten as

$$\text{reql} = \frac{\text{TotalMass} \cdot v_{liq} - V_{tank}}{\Delta t} \tag{F.1}$$

Here, `reql` is the required liquid volumetric flow rate in a shell full condition. Renaming that variable to $Q_{liq}\left[\frac{\text{ft}^3}{\text{min}}\right]$, the `pcom` equation from the line of code above may be written as

$$p_{com} = p_{min} + \frac{\left(\frac{Q_{liq}}{720 \cdot C_{D_{liq}} \cdot A_{areq}}\right)^2}{64.4 \cdot v_{liq}} \tag{F.2}$$

The derivation of this equation starts with the Bernoulli equation,

$$p_{com} = p_{min} + \frac{1}{2}\rho_{liq} V^2 \tag{F.3}$$

With units, it is

$$p_{com}\left[\frac{\text{lbf}}{\text{ft}^2}\right] = p_{min}\left[\frac{\text{lbf}}{\text{ft}^2}\right] + \frac{1}{2}\rho_{liq}\left[\frac{\text{lbm}}{\text{ft}^3}\right] V^2 \left[\frac{\text{ft}}{\text{sec}}\right]^2 \tag{F.4}$$

The fact that

$$(1 \cdot \text{lbm}) = (1 \cdot \text{lbf})\frac{1}{g}\frac{\text{sec}^2}{\text{ft}} \tag{F.5}$$

may be substituted to produce

$$p_{com}\left[\frac{\text{lbf}}{\text{ft}^2}\right] = p_{min}\left[\frac{\text{lbf}}{\text{ft}^2}\right] + \frac{1}{2}\frac{\rho_{liq}}{g}\left(\frac{\text{lbf}}{\text{ft}^3}\cdot\frac{\text{sec}^2}{\text{ft}}\right)V^2\left[\frac{\text{ft}}{\text{sec}}\right]^2 \tag{F.6}$$

Coalescing units, leaves

$$p_{com}\left[\frac{\text{lbf}}{\text{ft}^2}\right] = p_{min}\left[\frac{\text{lbf}}{\text{ft}^2}\right] + \frac{1}{2}\frac{\rho_{liq}}{g}V^2\left[\frac{\text{lbf}}{\text{ft}^2}\right] \tag{F.7}$$

However, in the code, pressure is in psi, thus,

$$p_{com}\left[\frac{\text{lbf}}{\text{ft}^2}\right] = \hat{p}_{com}\left[\frac{\text{lbf}}{\text{in}^2}\right]\cdot 144\frac{\text{in}^2}{\text{ft}^2} = \hat{p}_{com}\cdot 144\left[\frac{\text{lbf}}{\text{ft}^2}\right] \tag{F.8}$$

is substituted to produce

$$\hat{p}_{com}\cdot 144\left[\frac{\text{lbf}}{\text{ft}^2}\right] = \hat{p}_{min}\cdot 144\left[\frac{\text{lbf}}{\text{ft}^2}\right] + \frac{1}{2}\frac{\rho_{liq}}{g}V^2\left[\frac{\text{lbf}}{\text{ft}^2}\right] \tag{F.9}$$

Dividing through by 144 and expressing 144 as 12 squared,

$$\hat{p}_{com}\left[\frac{\text{lbf}}{\text{ft}^2}\right] = \hat{p}_{min}\left[\frac{\text{lbf}}{\text{ft}^2}\right] + \frac{1}{2}\frac{\rho_{liq}}{g}\frac{V}{12}^2\left[\frac{\text{lbf}}{\text{ft}^2}\right] \tag{F.10}$$

Or, using specific volume instead while substituting $g = 32.2$,

$$\hat{p}_{com}\left[\frac{\text{lbf}}{\text{ft}^2}\right] = \hat{p}_{min}\left[\frac{\text{lbf}}{\text{ft}^2}\right] + \frac{\rho_{liq}}{64.4v_{liq}}\frac{V}{12}^2\left[\frac{\text{lbf}}{\text{ft}^2}\right] \tag{F.11}$$

The units of velocity, V, is ft/min. It is the required volumetric flow rate divided by the area and the liquid discharge coefficient, with factors to provide the appropriate conversion of units:

$$V\left[\frac{\text{ft}}{\text{sec}}\right] = \frac{Q_{liq}\left[\frac{\text{ft}^3}{\text{min}}\right]}{60\frac{\text{sec}}{\text{min}}\cdot C_{D_{liq}}\cdot A_{areaq}\left[\text{ft}^2\right]} = \frac{Q_{liq}}{60\cdot C_{D_{liq}}\cdot A_{areaq}}\left[\frac{\text{ft}}{\text{min}}\right] \tag{F.12}$$

Substituting that equation into Equation F.11 yields

$$\hat{p}_{com}\left[\frac{\text{lbf}}{\text{ft}^2}\right] = \hat{p}_{min}\left[\frac{\text{lbf}}{\text{ft}^2}\right] + \frac{1}{64.4v_{liq}}\left(\frac{Q_{liq}}{60\cdot 12\cdot\cdot C_{D_{liq}}\cdot A_{areaq}}\right)^2\left[\frac{\text{lbf}}{\text{ft}^2}\right] \tag{F.13}$$

or

$$\hat{p}_{com}\left[\frac{\text{lbf}}{\text{ft}^2}\right] = \hat{p}_{min}\left[\frac{\text{lbf}}{\text{ft}^2}\right] + \frac{1}{64.4v_{liq}}\left(\frac{Q_{liq}}{720\cdot C_{D_{liq}}\cdot A_{areaq}}\right)^2\left[\frac{\text{lbf}}{\text{ft}^2}\right] \tag{F.14}$$

which corresponds to the line of code originally cited,

```
pcom = pmin+( pow(reql/(720.0*DischargeCoef_Liq*areq),2)  ) /
            (64.4*splq);
```

Appendix G

Governing Equations for the Advanced TPS Model

G.1 Convection and Radiation Communication Areas

The assumptions in the introduction of chapter 8 mean that an equation can be written that describes the area of exposure between any two adjacent areas. We develop those equations here. To begin, A is the total area represented. Ac_i is the area of Layer i that is without voids while $A(1-c_i)$ is the area of Layer i that has voids. When considering the right-hand side of Layer i, the area that is exposed to layers beyond Layer $i+1$ is $Ac_i(1-c_{i+1})$. Here, the first c_i represents the non-void part of Layer i , where the $(1-c_{i+1})$ represents the part of Layer $i+1$ that is void. Through this area, $Ac_i(1-c_{i+1})$, Layer i can exchange heat and radiation with Layer $i+2$. But if Layer $i+2$ also has voids in it, Layer i will exchange heat with Layer $i+3$, and so on. For each layer j to the right of Layer i, the area of communication between i and j is reduced by the amount of coverage of the layers between them. In general, the communication area between the right side of Layer i and the left side of Layers $i+2$, $i+3$, etc. are as follows:

$$A_{R_iL_{i+2}} = Ac_i(1-c_{i+1})c_{i+2} \tag{G.1}$$

where $A_{R_iL_j}$ is the communication area between the right side of i and the left side of j. The communication area between i and the left side of $i+3$ is

$$A_{R_iL_{i+3}} = Ac_i(1-c_{i+1})(1-c_{i+2})c_{i+3} \tag{G.2}$$

Likewise, for i and $i+4$ it is

$$A_{R_iL_{i+4}} = Ac_i(1-c_{i+1})(1-c_{i+2})(1-c_{i+3})c_{i+4} \tag{G.3}$$

In general, the communication area between the right side of Layer i and the left side of Layer j $(j > i+1)$ is

$$A_{R_iL_j} = Ac_ic_j\Pi_{k=i+1}^{j-1}(1-c_k) \tag{G.4}$$

A similar exercise can be performed for the left side of Layer i and the right side of Layer $i-2$. Their communication area is

$$A_{L_iR_{i-2}} = Ac_i(1-c_{i-1})c_{i-2} \tag{G.5}$$

Likewise, for i and $i-3$,

$$A_{L_iR_{i-3}} = Ac_i(1-c_{i-1})(1-c_{i-2})c_{i-3} \tag{G.6}$$

And for Layer i-4, it is

$$A_{L_iR_{i-4}} = Ac_i(1-c_{i-1})(1-c_{i-2})(1-c_{i-3})c_{i-4} \tag{G.7}$$

So, in general, the communication area between the left side of Layer i and the right side of Layer j is

$$A_{L_iR_j} = Ac_ic_j\Pi_{k=j+1}^{i-1}(1-c_k) \tag{G.8}$$

G.2 Conduction Communication Areas

All areas, including the area in contact and the areas exposed to radiation and convective heat transfer, experience conduction. The areas over which each of the three temperatures exist may be computed by considering the fractional coverages as probabilities. For example, the probability at any point in the i interface of Layers i and $i+1$ being in contact is the product of the probability of there being material present on Layer i (c_i) with the probability of there being material present on Layer $i+1$ (c_i+1). Scaling this product by the total area considered yeilds the area of the region in contact, Ac_ic_{i+1}. In a similar fashion, the area over which T_{R_i} exists is the product of the probability that material in Layer i is present (c_i) with the probability that material in Layer $i+1$ is not present $(1-c_{i+1})$. In summary, the areas are as follows:

Temperature	Joint Probability at a Point	Scaled to Obtain Area	
T_i	c_ic_{i+1}	Ac_ic_{i+1}	(G.9)
T_{R_i}	$c_i(1-c_{i+1})$	$Ac_i(1-c_{i+1})$	(G.10)
T_{L_i}	$c_i(1-c_{i-1})$	$Ac_i(1-c_{i-1})$	(G.11)

Table G.1: Computing Areas of Contact and Exposure Using a Joint Probability Approach

To determine the communication areas between two areas, one multiplies the two joint probabilities together because doing so represents the probability of overlap. Table G.2 summarizes the results of this approach. The left column describes the two areas that are overlapping; the third column is the area of overlap. The "Nomenclature" column establishes a simpler notation that is used in subsequent equations. There are some subtleties to the notation. First, the area connecting T_i and T_{i-1}, is reversible, e.g., $A_{i,i-1} = A_{i-1,i}$. Using this fact, the $A_{i,i-1}$ variable can be used to represent other combinations. Substituting $i+1$ for i, $A_{i+1,i} = Ac_{i+1}^2c_{i+2}c_i = A_{i,i+1}$. Another subtlety is that the i index on L and R in $A_{L,R}$ is omitted since that conduction must occur on layer i. Likewise, the i subscript is omitted on R in $A_{i,R}$ since it that conduction must be $i+1$. And note that if the area connecting T_{i-1} and T_{R_i} is needed, $i-1$ can be substituted for i, giving the quantity $A_{i-1,R} = Ac_{i-1}c_i^2(1-c_{i+1})$. Finally, the i subscript on L is omitted in $A_{i,L}$ since that conduction must be on i. It is worthwhile to make special notation for how these values change at endpoints. Specifically, c_0 and c_{n+1} represent the "coverage" of the non-existent layers adjacent to the innermost and outermost layers, respectively. Hence, $c_0 = c_{n+1} = 0$. Thus, the above area values for these endpoints are:

G.3 Heat Balance Equations

G.3.1 Area in Contact

For generality, consider interface i, which is the interface between Layer i and Layer $i+1$. Since this area is in contact, conduction is the only mechanism for heat transfer. A heat balance on the interface states that the heat

Conduction Path Connecting	Joint Probability at a Point of Overlap Occurring	Scaled to Obtain Area	Nomenclature	
T_i and T_{i-1}	$c_i^2 c_{i+1} c_{i-1}$	$Ac_i^2 c_{i+1} c_{i-1}$	A_i	(G.12)
T_i and $T_{R_{i+1}}$	$c_i c_{i+1}^2 (1 - c_{i+2})$	$Ac_i c_{i+1}^2 (1 - c_{i+2})$	$A_{i,R}$	(G.13)
T_{L_i} and T_{R_i}	$c_i^2 (1 - c_{i+1})(1 - c_{i-1})$	$Ac_i^2 (1 - c_{i+1})(1 - c_{i-1})$	$A_{L,R}$	(G.14)
T_i and T_{L_i}	$c_i^2 c_{i+1} (1 - c_{i-1})$	$Ac_i^2 c_{i+1} (1 - c_{i-1})$	$A_{i,L}$	(G.15)

Table G.2: Computing Conduction Communication Areas Using a Joint Probability Approach

Area Value	$1 < i < n$	$i = 1$	$i = n$	
A_i	$Ac_i^2 c_{i+1} c_{i-1}$	0	0	(G.16)
$A_{i,R}$	$Ac_i c_{i+1}^2 (1 - c_{i+2})$	$Ac_i c_{i+1}^2 (1 - c_{i+2})$	0	(G.17)
$A_{L,R}$	$Ac_i^2 (1 - c_{i+1})(1 - c_{i-1})$	$Ac_i^2 (1 - c_{i+1})$	$Ac_i^2 (1 - c_{i-1})$	(G.18)
$A_{i,L}$	$Ac_i^2 c_{i+1} (1 - c_{i-1})$	$Ac_i^2 c_{i+1} (1 - c_{i-1})$	0	(G.19)

Table G.3: Endpoint values for area

flowing into it must equal the heat flowing out of it. That requirement is embodied in the following equation:

$$\frac{k_i}{w_i} A_i (T_i - T_{i-1}) + \frac{k_i}{w_i} A_{i,L} (T_i - T_{L_i}) + \frac{k_{i+1}}{w_{i+1}} A_{i+1} (T_i - T_{i+1}) + \frac{k_{i+1}}{w_{i+1}} A_{i,R} (T_i - T_{R_{i+1}}) = 0 \tag{G.20}$$

G.3.2 Right Side's Exposed Area

Consider again interface i, but this time, the part of that interface that is exposed due to a lack of coverage in Layer $i + 1$. Heat conduction still occurs to the left, but radiative and convective heat transfer occurs to the right. Again, a heat balance on the interface states that the heat flowing into it must equal the heat flowing out of it. That requirement is embodied in the following equation, where heat conduction to the left is represented in the first terms and radiative plus convective heat flow is represented in the last terms:

$$\frac{k_i}{w_i} A_{i-1,R} (T_{R_i} - T_{i-1}) + \frac{k_i}{w_i} A_{L,R} (T_{R_i} - T_{L_i}) + \sum_{k=i+1}^{n} A_{R_i L_k} h_{i,k} (T_{R_i} - T_{L_k}) + \sum_{k=i+1}^{n} A_{R_i L_k} \frac{\sigma \left(T_{R_i}^4 - T_{L_k}^4 \right)}{1/\epsilon_{R_i} + 1/\epsilon L_k + 1} = 0 \tag{G.21}$$

In the above equation, the radiative exchange is modeled as the exchange between two infinite parallel planes. Behind this choice are the assumptions that the distance separating them is small compared to the communication

area. Along with that assumption, the radiative and convective exchange between layers based on exposure of the walls surrounding the voids is neglected.

G.3.3 Left Side's Exposed Area

Now consider the layer on the right of interface i. Part of that layer will be exposed due to voids in Layer i. Analogous to the above equation, heat conduction will occur to the right, while radiative and convective heat transfer will occur to the left. The heat balance is in the following analogous equation:

$$\frac{k_i}{w_i}A_{i,L}(T_{L_i}-T_i)+\frac{k_i}{w_i}A_{L,R}(T_{L_i}-T_{R_i})+$$
$$\sum_{k=1}^{i-1}A_{L_iR_k}h_{i,k}(T_{L_i}-T_{R_k})+\sum_{k=1}^{i-1}A_{L_iR_k}\frac{\sigma\left(T_{L_i}^4-T_{R_k}^4\right)}{1/\epsilon_{L_i}+1/\epsilon_{R_k}+1}=0 \tag{G.22}$$

The same assumptions regarding radiative exchange for Equation G.21 apply here in an analogous way.

G.3.4 Boundary Conditions

Following the same methodology that is currently in AFFTAC, the following two boundary conditions are applied to the above equations:

1. Inner Boundary Known Temperature Condition: This condition is applied by setting $T_{L_1}=T_{known}$. Note that a requirement of the model is that the innermost and outermost layers have 100% coverage. The value of T_{known} is taken as the inner layer's inner temperature from the previous time-step. The process of using this old value is part of the current nonlinear lagging methodology in AFFTAC. So for Layer 1, Equations G.22 is replaced with
$$T_{L_1}=T_{known} \tag{G.23}$$

2. Outer Boundary Flux Condition: This condition replaces the conduction, radiation, and convection occuring towards the right for Layer n with a heat flux that is based on the flame temperature and outermost layer temperature. Thus, Equation G.21 for $i=n$ is replaced with
$$\frac{k_i}{w_i}A_{i-1,R}(T_{R_i}-T_{i-1})+\frac{k_i}{w_i}A_{L,R}(T_{R_i}-T_{L_i})+A\sigma(\epsilon_{R_n}T_{R_n}^4-\epsilon_f\epsilon_{R_n}fT_f^4)=0 \tag{G.24}$$
The factor f is a shape configuration factor as discussed in chapter 5. Also, it is noted that because there is 100% coverage on this outer surface, $T_n=T_{R_n}$. This equation replaces Equation G.22 for $i=n$.

3. Zero Coverage: Because no lateral conduction is built into the model, the model breaks down for small coverage values. However, the model recovers its accuracy in the limit of zero coverage by setting the conduction region temperatures equal to the radiating temperatures on the same surface (Equations G.25, below) and by setting the exposed area temperatures for the layer with zero coverage equal to their counterparts on the neighboring surfaces (Equations G.26, below).

   So when $c_i=0$ in place of the conduction equations, we have:
$$\begin{aligned}T_i-T_{L_{i+1}}&=0\\T_{i-1}-T_{R_{i-1}}&=0\end{aligned} \tag{G.25}$$
   And in place of the exposed areas' radiation and convection equations, we have
$$\begin{aligned}T_{L_i}-T_{R_{i-1}}&=0\\T_{R_i}-T_{L_{i+1}}&=0\end{aligned} \tag{G.26}$$

G.4 Angular Dependence

There are two ways in which the TPS model is in effect during an AFFTAC simulation. First, the TPS model is used to compute the updated outer surface temperature. In this situation, the interior boundary condition is applied as a known value and the outer surface temperature (T_1) is determined by solving the system of equations described above. Second, the TPS model is used in a heat balance equation for the innermost surface. In this second application, the inner surface temperature T_n is not known. But in this situation, the most recent value for T_{n-1} is used in with the thermal conductivity and thickness to compute the heat flux entering the innermost surface from the outside. This heat flux is balanced with the heat flux from the innermost surface to the vapor and liquid to compute T_n.

In the Advanced TPS Model, these two areas of application remain unchanged in principle. However, this model also admits the possibility that the coverage terms (c_i, above) may vary with angle. Specifically, the user is allowed to set up n_a segments of the tank car wherein the c_i array may have different values for each layer, i (see Figure G.1). Therefore, in the implemented algorithm, the coverage array has two subscripts, the first for the angle region and the second for the layer; for example, c_{ai} is the coverage for Layer i in angle region a.

The angular dependence of the TPS does not affect the assumption that the inner tank wall temperature adjacent to the liquid lading, which is equal to the liquid temperature, is uniform. However, it does affect the assumption that the inner tank wall temperature adjacent to the vapor lading is uniform. Rather, an array of innermost temperatures is introduced in AFFTAC; these values are determined using the procedure described in the first paragraph of this section. Likewise, an array of outermost temperatures for this region are introduced; these are determined using the procedure described in that same paragraph.

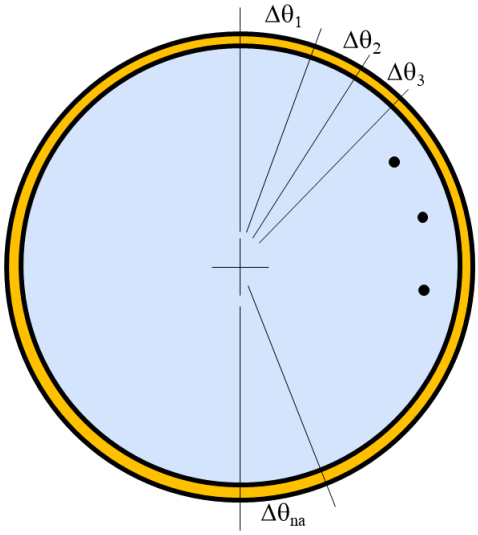

Figure G.1: Illustration of how the coverage values (c_i) can vary based on a user-specified number of angle bins.

G.5 Nonlinear Solver

Equation G.20-G.22 with boundary conditions Equation G.23-G.24 constitute $3n$ simultaneous nonlinear equations for the $3n$ temperatures, T_i, T_{L_i}, and T_{R_i}, $i = 1, 2, 3, ..., n$, where n is the number of layers. These temperatures are determined using the Newton-Raphson iterative method. To formulate that solver, functions are defined using the heat balance and boundary conditions described earlier. Functions f_i^1, f_i^2, f_i^3, which will be set to zero for each i, are given in the equations that follow.

Exposed Left Side Balance (G.27)

$$f_i^1(T_{L_i}, T_{R_i}, T_i) = \begin{cases} T_{L_i} - T_{known} & i = 1 \\ T_{L_i} - T_{R_{i-1}} & c_i = 0 \\ \frac{k_i}{w_i} A_{i,L}(T_{L_i} - T_i) + \frac{k_i}{w_i} A_{L,R}(T_{L_i} - T_{R_i}) & \\ + \sum_{k=1}^{i-1} A_{L_i R_k} h_{i,k}(T_{L_i} - T_{R_k}) + \sum_{k=1}^{i-1} A_{L_i R_k} \frac{\sigma\left(T_{L_i}^4 - T_{R_k}^4\right)}{1/\epsilon_{L_i} + 1/\epsilon_{R_k} + 1} = 0 & 2 < i < n \end{cases}$$

Exposed Right Side Balance (G.28)

$$f_i^2(T_{L_i}, T_{R_i}, T_i) = \begin{cases} \frac{k_i}{w_i} A_{i-1,R}(T_{R_i} - T_{i-1}) + \frac{k_i}{w_i} A_{L,R}(T_{R_i} - T_{L_i}) + & \\ \sum_{k=i+1}^{n} A_{R_i L_k} h_{i,k}(T_{R_i} - T_{L_k}) + \sum_{k=i+1}^{n} A_{R_i L_k} \frac{\sigma\left(T_{R_i}^4 - T_{L_k}^4\right)}{1/\epsilon_{R_i} + 1/\epsilon_{L_k} + 1} & 1 \le i < n \\ T_{L_i} - T_{R_{i-1}} & c_i = 0 \\ \frac{k_i}{w_i} A_{i-1,R}(T_{R_i} - T_{i-1}) + \frac{k_i}{w_i} A_{L,R}(T_{R_i} - T_{L_i}) + A\sigma(\epsilon_{R_n} T_{R_n}^4 - \epsilon_f \epsilon_{R_n} f T_f^4) & i = n \end{cases}$$

(G.29)

Contact Balance (G.30)

$$f_i^3(T_{L_i}, T_{R_i}, T_i) = \begin{cases} \frac{k_i}{w_i} A_i(T_i - T_{i-1}) + \frac{k_i}{w_i} A_{i,L}(T_i - T_{L_i}) + & \\ \frac{k_{i+1}}{w_{i+1}} A_{i+1}(T_i - T_{i+1}) + \frac{k_{i+1}}{w_{i+1}} A_{i,R}(T_i - T_{R_{i+1}}) & 1 \le i < n \\ T_i - T_{L_{i+1}} \text{ and } T_{i-1} - T_{R_{i-1}} & c_i = 0 \\ T_i - T_{R_i} & i = n \end{cases}$$

(G.31)

In so doing, the simultaneous nonlinear equations may be written as

$$\begin{aligned} f_i^1(T_{L_i}, T_{R_i}, T_i) &= 0, \quad i = 1, 2, 3, ...n \\ f_i^2(T_{L_i}, T_{R_i}, T_i) &= 0, \quad i = 1, 2, 3, ...n \\ f_i^3(T_{L_i}, T_{R_i}, T_i) &= 0, \quad i = 1, 2, 3, ...n \end{aligned} \tag{G.32}$$

and the Newton-Raphson algorithm for this system may be written as follows. Let I denote the iteration number, then

$$\begin{aligned} T_{L_i}^{I+1} &= T_{L_i}^I + \delta_{L_i}^I, \quad i = 1, 2, 3, ...n - 1 \\ T_{R_i}^{I+1} &= T_{R_i}^I + \delta_{R_i}^I, \quad i = 1, 2, 3, ...n - 1 \\ T_i^{I+1} &= T_i^I + \delta_i^I, \quad i = 1, 2, 3, ...n - 1 \end{aligned} \tag{G.33}$$

The deltas are the solution to the following linear system:

$$\begin{bmatrix} J^{11} & J^{12} & J^{13} \\ J^{21} & J^{22} & J^{23} \\ J^{31} & J^{32} & J^{33} \end{bmatrix} \begin{bmatrix} \delta_{L_i}^{I+1} \\ \delta_{R_i}^{I+1} \\ \delta_i^{I+1} \end{bmatrix} = \begin{bmatrix} f^1 \\ f^2 \\ f^3 \end{bmatrix}_I \tag{G.34}$$

where the Jacobian entries are given by

$$\begin{array}{lll} J_{ij}^{11} = \frac{\partial f_j^1}{\partial T_{L_j}} & J_{ij}^{12} = \frac{\partial f_j^1}{\partial T_{R_j}} & J_{ij}^{13} = \frac{\partial f_j^1}{\partial T_j} \\ J_{ij}^{21} = \frac{\partial f_j^2}{\partial T_{L_j}} & J_{ij}^{22} = \frac{\partial f_j^2}{\partial T_{R_j}} & J_{ij}^{23} = \frac{\partial f_j^2}{\partial T_j} \\ J_{ij}^{31} = \frac{\partial f_j^3}{\partial T_{L_j}} & J_{ij}^{32} = \frac{\partial f_j^3}{\partial T_{R_j}} & J_{ij}^{33} = \frac{\partial f_j^3}{\partial T_j} \end{array} \tag{G.35}$$

These entries may be evaluated analytically using Equations G.20-G.22. To assist with notation, it is helpful to review and define the following to functions. The Kronecker delta, δ_{ij}, is unity if $i = j$ and zero otherwise. Second, the integer unit step function, $u_{i,j}$, is unity if $j \geq i$ and zero otherwise. The entries of the Jacobian will now be derived below.

First, to assist in the taking of partial derivatives, the functions are re-written with each term split apart and made separate. The following terms are defined:

$$\begin{aligned} F_{R_iL_k} &\equiv A_{R_iL_k} \frac{\sigma}{1/\epsilon_{R_i} + 1/\epsilon_{L_k} + 1} \\ F_{L_iR_k} &\equiv A_{R_iL_k} \frac{\sigma}{1/\epsilon_{L_i} + 1/\epsilon_{R_k} + 1} \\ G_{R_iL_k} &\equiv A_{R_iL_k} h_{i,k} \\ G_{L_iR_k} &\equiv A_{L_iR_k} h_{i,k} \end{aligned} \tag{G.36}$$

so that our nonlinear functions may be written as follows:

Exposed Left Side Balance (G.37)

$$f_i^1(T_{L_i}, T_{R_i}, T_i) = \begin{cases} \left(\frac{k_i}{w_i}(A_{i,L} + A_{l,R}) + \sum_{k=1}^{i-1} G_{L_iR_k}\right) T_{L_i} + \left(\sum_{k=1}^{i-1} F_{L_iR_k}\right) T_{L_i}^4 \\ -\left(\frac{k_i}{w_i} A_{L,R}\right) T_{R_i} - \sum_{k=1}^{i-1} G_{L_iR_k} T_{R_k} - \sum_{k=1}^{i-1} F_{L_iR_k} T_{R_k}^4 - \left(\frac{k_i}{w_i} A_{i,L}\right) T_i & 1 < i \leq n \\ \\ T_{L_i} - T_{R_{i-1}} & c_i = 0 \\ T_{L_i} - T_{known} & i = 1 \end{cases}$$

Exposed Right Side Balance (G.38)

$$f_i^2(T_{L_i}, T_{R_i}, T_i) = \begin{cases} -\sum_{k=i+1}^{n} G_{R_iL_k} T_{L_k} - \sum_{k=i+1}^{n} F_{R_iL_k} T_{L_k}^4 \\ -\left(\frac{k_i}{w_i} A_{L,R}\right) T_{L_i} - \left(\frac{k_i}{w_i}(A_{i-1,R} + A_{L,R}) + \sum_{k=i+1}^{n} G_{R_iL_k}\right) T_{R_i} \\ +\sum_{k=i+1}^{n} F_{R_iL_k} T_{R_i}^4 - \left(\frac{k_i}{w_i} A_{i-1,R}\right) T_{i-1} & 1 \leq i < n \\ \\ T_{R_i} - T_{L_{i+1}} & c_i = 0 \\ \\ \frac{k_i}{w_i}(A_{i-1,R} + A_{L,R}) T_{R_i} - \left(\frac{k_i}{w_i} A_{L,R}\right) T_{L_i} - \left(\frac{k_i}{w_i} A_{i-1,R}\right) T_{i-1}) \\ +A\sigma\epsilon_{R_n} T_{R_n}^4 - A\epsilon_f \epsilon_{R_n} f T_f^4 & i = n \end{cases}$$

Contact Balance (G.39)

$$f_i^3(T_{L_i}, T_{R_i}, T_i) = \begin{cases} -\left(\frac{k_i}{w_i}A_{i,L}\right)T_{L_i} - \left(\frac{k_{i+1}}{w_{i+1}}A_{i,R}\right)T_{R_{i+1}} + \left(\frac{k_i}{w_i}A_i + \frac{k_i}{w_i}A_{i,L} + \frac{k_{i+1}}{w_{i+1}}A_{i+1} + \frac{k_{i+1}}{w_{i+1}}A_{i,R}\right)T_i & \\ \quad -\left(\frac{k_i}{w_i}A_i\right)T_{i-1} - \left(\frac{k_{i+1}}{w_{i+1}}A_i\right)T_{i+1} & 1 \le i < n \\ T_i - T_{L_{i+1}} \text{ and } T_{i-1} - T_{R_{i-1}} & c_i = 0 \\ T_i - T_{R_i} & i = n \end{cases} \tag{G.40}$$

Using the functions expressed as above, the Jacobian can now be written as follows:

First row of blocks:

$$J_{ij}^{11} = \frac{\partial f_i^1}{\partial T_{L_j}} = \begin{cases} \left(\frac{k_i}{w_i}(A_{i,L} + A_{L,R}) + \sum_{k=1}^{i-1} G_{L_i,R_k}\right)\delta_{i,j} + 4\left(\sum_{k=1}^{i-1} F_{L_i,R_k}\right)T_{L_i}^3\delta_{i,j} & 1 < i \le n \\ \delta_{i,j} & c_i = 0 \\ \delta_{i,j} & i = 1 \end{cases} \tag{G.41}$$

$$J_{ij}^{12} = \frac{\partial f_i^1}{\partial T_{R_j}} = \begin{cases} -\left(\frac{k_i}{w_i}A_{L,R}\right)\delta_{i,j} - G_{L_i,R_j}(1-u_{i,j}) - (4F_{L_i,R_j})T_{R_j}^3(1-u_{i,j}) & 1 < i \le n \\ \delta_{i,j-1} & c_i = 0 \\ 0 & i = 1 \end{cases} \tag{G.42}$$

$$J_{ij}^{13} = \frac{\partial f_i^1}{\partial T_j} = \begin{cases} -\frac{k_i}{w_i}A_{i,L}\delta_{i,j} & 1 < i \le n \\ 0 & i = 1 \end{cases} \tag{G.43}$$

Second row of blocks:

$$J_{ij}^{21} = \frac{\partial f_i^2}{\partial T_{L_j}} = \begin{cases} -(G_{R_i,_j})u_{i,j-1} - (4F_{R_i,L_j})T_{L_j}^3 u_{i.j-1} - \left(\frac{k_i}{w_i}A_{L,R}\right)\delta_{i,j} & 1 < i < n \\ \delta_{i,j} & c_i = 0 \\ -\left(\frac{k_i}{w_i}A_{L,R}\right)\delta_{i,j} & i = n \end{cases} \tag{G.44}$$

$$J_{ij}^{22} = \frac{\partial f_i^2}{\partial T_{R_j}} = \begin{cases} \left(\left(\frac{k_i}{w_i}(A_{i-1,R} + A_{L,R}\right) + \sum_{k=i+1}^{n} G_{R_i,L_k}\right)\delta_{i,j} + 4\left(\sum_{k=i+1}^{n} F_{R_i,L_k}\right)T_{R_j}^3\delta_{i,j} & 1 < i \le n \\ \delta_{i,j+1} & c_i = 0 \\ \frac{k_i}{w_i}(A_{i-1,R} + A_{L,R})\delta_{i,j} + 4A\sigma\epsilon_{R_j}T_{R_j}^3\delta_{i,j} & i = n \end{cases} \tag{G.45}$$

$$J_{ij}^{23} = \frac{\partial f_i^2}{\partial T_j} = \begin{cases} -\frac{k_i}{w_i}A_{i-1,R}\delta_{i-1,j} & 1 \le i < n \\ -\frac{k_i}{w_i}A_{i-1,R}\delta_{i-1,j} & i = 1 \end{cases} \tag{G.46}$$

Third row of blocks:

$$J_{ij}^{31} = \frac{\partial f_i^3}{\partial T_{L_j}} = \begin{cases} -\frac{k_i}{w_i} A_{i,L} \delta_{i,j} & 1 \leq i < n \\ 0 & i = n \\ -\delta_{i,j-1} & c_i = 0 \end{cases} \tag{G.47}$$

$$J_{ij}^{32} = \frac{\partial f_i^3}{\partial T_{R_j}} = \begin{cases} -\frac{k_{i+1}}{w_{i+1}} A_{i,R} \delta_{i,j-1} & 1 \leq i < n \\ -\delta_{i,j-1} & i = n \text{ or if } c_i = 0 \end{cases} \tag{G.48}$$

$$J_{ij}^{33} = \frac{\partial f_i^3}{\partial T_j} = \begin{cases} \frac{k_i}{w_i}(A_i + A_{i,L})\delta_{i,j} + \frac{k_{i+1}}{w_{i+1}}(A_{i+1} + A_{i,R})\delta_{i,j} - \frac{k_i}{w_i} A_i \delta_{i,j+1} - \frac{k_{i+1}}{w_{i+1}} A_{i+1} \delta_{i,j-1} & 1 \leq i < n \\ \delta_{i,j} \text{ and } \delta_{i,j-1} & c_i = 0 \\ \delta_{i,j} & i = n \end{cases} \tag{G.49}$$

The above expressions for the Jacobian are cumbersome from a programming standpoint. A more helpful representation is as follows: First row of blocks:

$$J_{ij}^{11} = \frac{\partial f_i^1}{\partial T_{L_j}} = \begin{cases} \text{Diagonal entry: } \left(\frac{k_i}{w_i}(A_{i,L} + A_{L,R}) + \sum_{k=1}^{i-1} G_{L_i,R_k}\right) + 4\left(\sum_{k=1}^{i-1} F_{L_i,R_k}\right) T_{L_i}^3 & 1 < i \leq n \\ \text{Diagonal entry:} 1 & c_i = 0 \\ \text{Diagonal entry:} 1 & i = 1 \end{cases} \tag{G.50}$$

$$J_{ij}^{12} = \frac{\partial f_i^1}{\partial T_{R_j}} = \begin{cases} \text{Diagonal entry: } -\left(\frac{k_i}{w_i} A_{L,R}\right) \text{ Before the diagonal: } -G_{L_i,R_j} - 4F_{L_i,R_j} T_{R_j}^3 & 1 < i \leq n \\ \text{Diagonal entry: } -1 & c_i = 0 \\ \text{Diagonal entry: } 0 & i = 1 \end{cases} \tag{G.51}$$

$$J_{ij}^{13} = \frac{\partial f_i^1}{\partial T_j} = \begin{cases} \text{Diagonal entry: } -\frac{k_i}{w_i} A_{i,L} & 1 < i \leq n \\ 0 & i = 1 \end{cases} \tag{G.52}$$

Second row of blocks:

$$J_{ij}^{21} = \frac{\partial f_i^2}{\partial T_{L_j}} = \begin{cases} \text{Diagonal entry: } -\left(\frac{k_i}{w_i} A_{L,R}\right) \text{ After the diagonal: } -(G_{R_i,L_j}) - 4F_{R_i,L_j} T_{L_j}^3 & 1 \leq i < n \\ \text{After the diagonal: } -1 & c_i = 0 \\ \text{Diagonal entry: } -\left(\frac{k_i}{w_i} A_{L,R}\right) & i = n \end{cases} \tag{G.53}$$

$$J_{ij}^{22} = \frac{\partial f_i^2}{\partial T_{R_j}} = \begin{cases} \text{Diagonal entry: } \frac{k_i}{w_i}\left(A_{i-1,R} + A_{L,R} + \sum_{k=i+1}^{n} G_{R_i,L_k}\right) + 4\left(\sum_{k=i+1}^{n} F_{R_i,L_k}\right) T_{R_j}^3 & 1 \leq i < n \\ \text{Diagonal entry: } 1 & c_i = 0 \\ \text{Diagonal entry: } \frac{k_i}{w_i}(A_{i-1,R} + A_{L,R}) + 4A\sigma\epsilon_{R_j} T_{R_j}^3 & i = n \end{cases} \tag{G.54}$$

$$J_{ij}^{23} = \frac{\partial f_i^2}{\partial T_j} = \begin{cases} \text{One entry before the diagonal: } -\frac{k_i}{w_i} A_{i-1,R} & 1 \le i < n \\ \text{One entry before the diagonal: } -\frac{k_i}{w_i} A_{i-1,R} & i = n \end{cases} \tag{G.55}$$

Third row of blocks:

$$J_{ij}^{31} = \frac{\partial f_i^3}{\partial T_{L_j}} = \begin{cases} \text{Diagonal entry: } -\frac{k_i}{w_i} A_{i,L} & 1 \le i < n \\ 0 & i = n \\ \text{Diagonal entry: } -1 & c_{i-1} = 0 \end{cases} \tag{G.56}$$

$$J_{ij}^{32} = \frac{\partial f_i^3}{\partial T_{R_j}} = \begin{cases} \text{One after the diagonal: } -\frac{k_{i+1}}{w_{i+1}} A_{i,R} & 1 \le i < n \\ \text{Diagonal entry: } -1 & i = n \\ \text{Diagonal entry: } -1 & \text{if } c_{i-1} = 0 \end{cases} \tag{G.57}$$

$$J_{ij}^{33} = \frac{\partial f_i^3}{\partial T_j} = \begin{cases} \text{Diagonal: } \frac{k_i}{w_i}(A_i + A_{i,L}) + \frac{k_{i+1}}{w_{i+1}}(A_{i+1} + A_{i,R}) & 1 \le i < n \\ \text{Diagonal-1 } -\frac{k_i}{w_i} A_i & 1 \le i < n \\ \text{Diagonal+1: } -\frac{k_{i+1}}{w_{i+1}} A_{i+1} & 1 \le i < n \\ \text{Diagonal: } 1 & \text{if } i = n, c_i = 0, \text{ or } c_{i-1} = 0 \end{cases} \tag{G.58}$$

Appendix H

Derivation of the Volumetric Expansion Equation

The volume of the tank increases for two reasons: (1) Internal pressure, the effect of which is modeled using Hooke's Law for elastic strain, and (2) Linear thermal expansion. In representing these two causes of expansion, we also must consider their effects in two directions: (1) Radial expansion, or in other words, expansion of the circumference of the tank, and (2) Expansion axially along the length of the tank. Thus, combining these ideas, there are a total of four aspects to consider, which we will do in turn, below.

To compute the elastic radial strain, we consider stretching in the circumferential direction, where the new circumference, C_e, in terms of the original circumference $C_{original}$ is $C_e = C_{original}(1 + \epsilon_c)$ where ϵ_c is given by Equation 14.10. Substituting $C = 2\pi r$ for circumference, we obtain $r_e = r_{original}(1 + \epsilon_c)$ as the new radius due to elastic stretching. Stretching in the axial direction, along the length, L, of the tank is, similarly, $L_e = L_{original}(1 + \epsilon_a)$.

To compute the thermal radial strain, we consider thermal expansion of the circumference. Using Equation 14.5 for the ratio of the hot to the cool length, the new circumference due to thermal expansion is $C_T = C_{original}R_T(T)$, which means that $r_T = r_{original}R_T(T)$. Likewise, thermal strain along the length produces the new length $L_T = L_{original}R_T(T)$.

Thus we have derived the equations for the four aspects mentioned at the beginning of the appendix. They are summarized in Table H.1. To derive the equation for the total volumetric expansion, we consider the elastic and

	Elastic Strain (Hooke's Law)	Thermal STrain
Radial (Circumferential)	$r_e = r_{original}(1 + \epsilon_c)$	$r_T = r_{original}R_T(T)$
Longitudinally (Axially)	$L_e = L_{original}(1 + \epsilon_a)$	$L_T = L_{original}R_T(T)$

Table H.1: Radial and lognitudinal strain relationships

thermal processes *sequentially*. In other words, to compute the radius $r_{combined}$ and length $L_{combined}$ due to the combined effects, we combine the changes in sequence, as,

$$\begin{aligned} r_{combined} &= \text{Thermal Process}\,(\text{Elastic Process}\,(r_{originial})) \\ &= \text{Thermal Process}\,(r_{original}(1 + \epsilon_c)) \\ &= r_{original}(1 + \epsilon_c)R_T(T) \end{aligned} \tag{H.1}$$

$$
\begin{aligned}
L_{combined} &= \text{Thermal Process}\left(\text{Elastic Process}\left(L_{originial}\right)\right) \\
&= \text{Thermal Process}\left(\left(L_{original}\left(1+\epsilon_a\right)\right)\right. \\
&= L_{original}(1+\epsilon_a)R_T(T)
\end{aligned}
\tag{H.2}
$$

Using those results, the new volume of the tank is computed as follows:

$$
\begin{aligned}
V_{combined} &= \pi\left(r_{combined}\right)^2\left(L_{combined}\right) \\
&= \pi\left(r_{original}(1+\epsilon_c)R_T(T)\right)^2\left(L_{original}(1+\epsilon_a)R_T(T)\right) \\
&= V_{original}(1+\epsilon_c)^2(1+\epsilon_a)R_T(T)^3)
\end{aligned}
\tag{H.3}
$$

Upon substituting for $R_T(T)$ from Equation 14.5 into the above equation, we obtain the desired result of Equation 14.12.